GEOLOGICAL SURVEY CIRCULAR 753

Short Papers of the U.S. Geological Survey Uranium-Thorium Symposium, 1977

Short Papers of the U.S. Geological Survey Uranium-Thorium Symposium, 1977

Edited by John A. Campbell

GEOLOGICAL SURVEY CIRCULAR 753

Papers presented April 27-28, 1977,
at the Colorado School of Mines, Golden

United States Department of the Interior
CECIL D. ANDRUS, *Secretary*

Geological Survey
V. E. McKelvey, *Director*

First printing 1977

Second printing 1977

Library of Congress catalog-card No. 77-600012

Free on application to Branch of Distribution, U.S. Geological Survey, 1200 South Eads Street, Arlington, VA 22202

PREFACE

This circular contains expanded abstracts for the technical papers presented at the 1977 Uranium and Thorium Research and Resources Conference, sponsored by the Branch of Uranium and Thorium Resources, U.S. Geological Survey. This Conference was held April 27 and 28, 1977, at the Colorado School of Mines, Golden. This was the second conference sponsored by the Branch--the first was held in December of 1975.

Readers interested in additional information about a paper presented at the meeting should contact the author directly. U.S. Geological Survey authors stationed in Denver can be reached by writing to Box 25046, Denver Federal Center, Denver, Colorado 80225. Authors stationed in Reston, Virginia, can be reached by writing to the U.S. Geological Survey, National Center, 12201 Sunrise Valley Drive, Reston, Virginia 22092. Current addresses for other authors appear at the beginning of their papers.

Any use of trade names and trademarks in this publication is for descriptive purposes only and does not constitute endorsement by the U.S. Geological Survey.

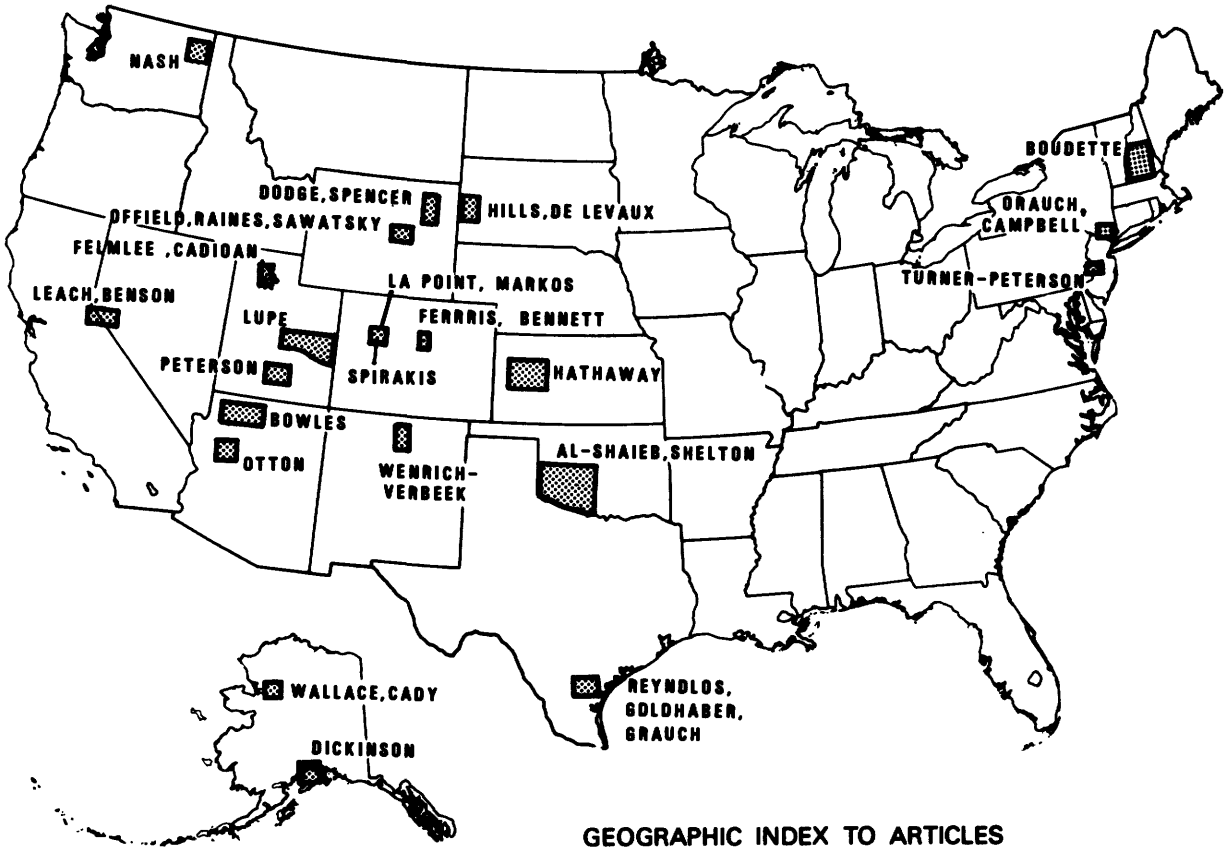

GEOGRAPHIC INDEX TO ARTICLES

CONTENTS

ABBREVIATIONS USED IN THIS CIRCULAR

Å----------angstroms
a----------chemical activity (relative)
atm----------atmosphere (pressure)
cal/mol deg----------calories per mole-degree
cm----------centimeters
cm/yr----------centimeters per year
cps----------counts per second
dc----------direct current
$\Delta G_f°$----------Gibbs free energy (of formation of minerals from the elements)
$\Delta H_f°$----------Enthalpy (of formation of minerals from the elements)
Eh----------oxidation-reduction potential
eTh----------equivalent thorium
eU----------equivalent uranium
ft^3/s----------cubic feet per second
g/cm^3----------grams per cubic centimeter
g/min----------grams per minute
GVW----------gross vehicle weight
γ----------gamma
IP----------induced polarization
kcal/mol----------kilocalories per mole
keV----------kilolectronvolts
kg----------kilograms
km----------kilometers
km^2----------square kilometers
km^3----------cubic kilometers
kV----------kilovolts
L_α----------alpha radiation from L energy level
ℓ/min----------liters per minute
m----------meters
m^3----------cubic meters
m/km----------meters per kilometer
m^3/s----------cubic meters per second
mA----------milliamperes
MeV----------megaelectronvolts
mm----------millimeters
mm^2----------square millimeters
mrad----------milliradians
m.y.----------million years
μm----------micrometers (microns)
μg/ℓ----------micrograms per liter
μμg/ℓ----------micromicrograms per liter
nm----------nanometers
ohm-m----------ohm-meters
pCi/ℓ----------picocuries per liter

P_{CO_2}----------partial pressure of CO_2
pH----------hydrogen ion activity
ppb----------parts per billion
ppm----------parts per million
S^o----------Entropy (of formation of minerals from the elements)

s----------seconds
θ----------Bragg angle
vlf----------very low frequency
vs----------versus
yr----------years

A GEOLOGIC FOUNDATION FOR URANIUM RESOURCE ASSESSMENT, TRIASSIC CHINLE FORMATION, SOUTHEAST UTAH

By Robert Lupe, U.S. Geological Survey, Denver, Colo.

Lupe (1976) has described the spatial relationship between depositional environments and uranium mineralization in the Chinle Formation in the San Rafael Swell-Canyonlands area. A similar spatial relationship exists between rock texture and uranium, because texture is determined by sedimentary processes which are characteristic of certain depositional environments. This relationship between rock properties and uranium observed at the outcrop was extended into the subsurface using textural data derived from logs of petroleum test wells to form the geologic basis for a resource assessment of unexplored areas (fig. 1).

Judging from the setting of known uranium deposits, areas with intermediate sandstone-mudstone ratios seem to be most favorable for uranium deposits (fig. 1). For purposes of assessment, favorable ground in the Chinle, which covers a third of the study area, was subdivided into 50 km^2 cells

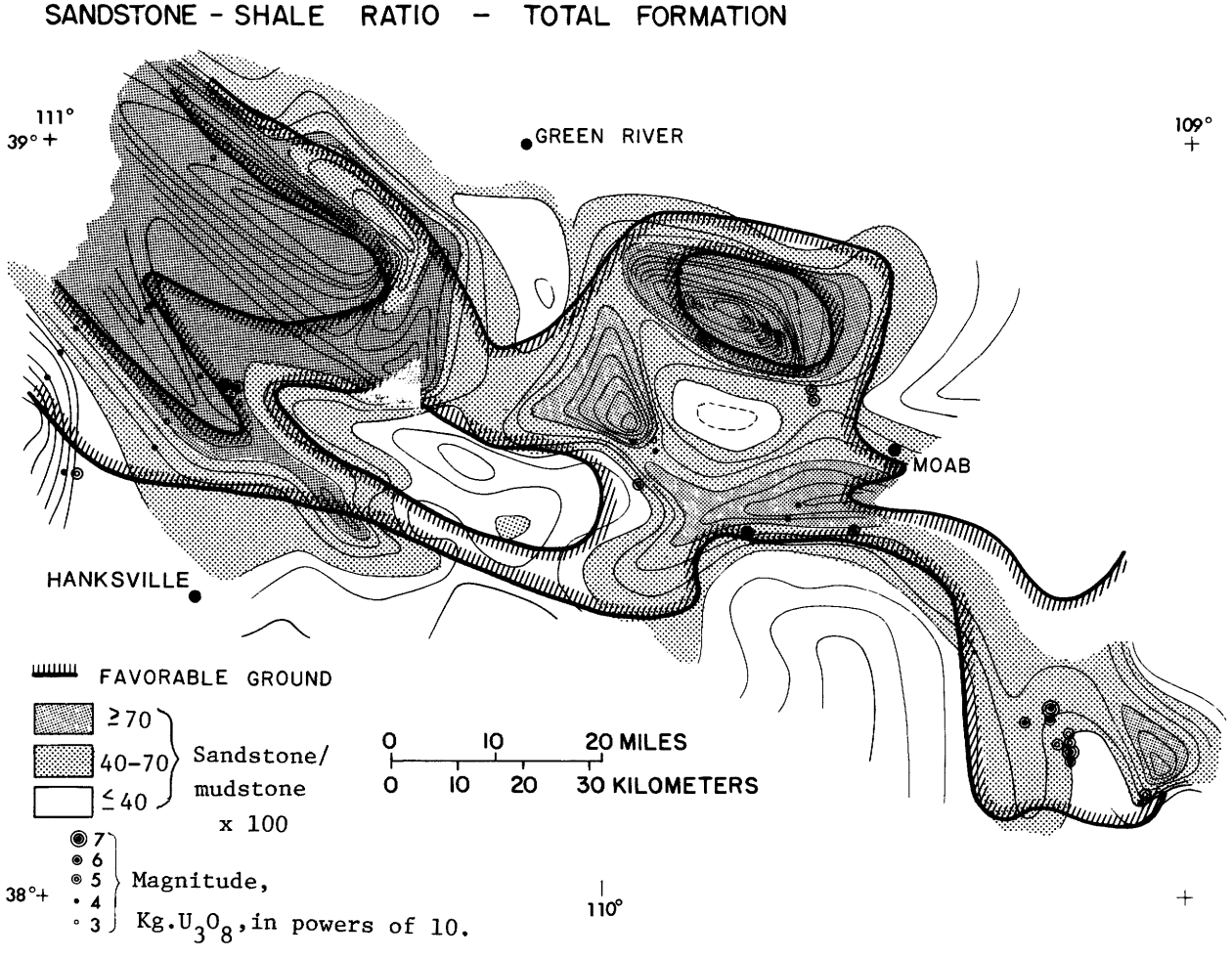

Figure 1.--Sandstone/mudstone ratio map from measured surface sections and logs of petroleum test wells of the Chinle Formation, southeast Utah, showing significant uranium deposits and favorable ground. The distribution of favorable ground is the comparison of known deposits to a composite of this map and a sandstone isopach map (not shown).

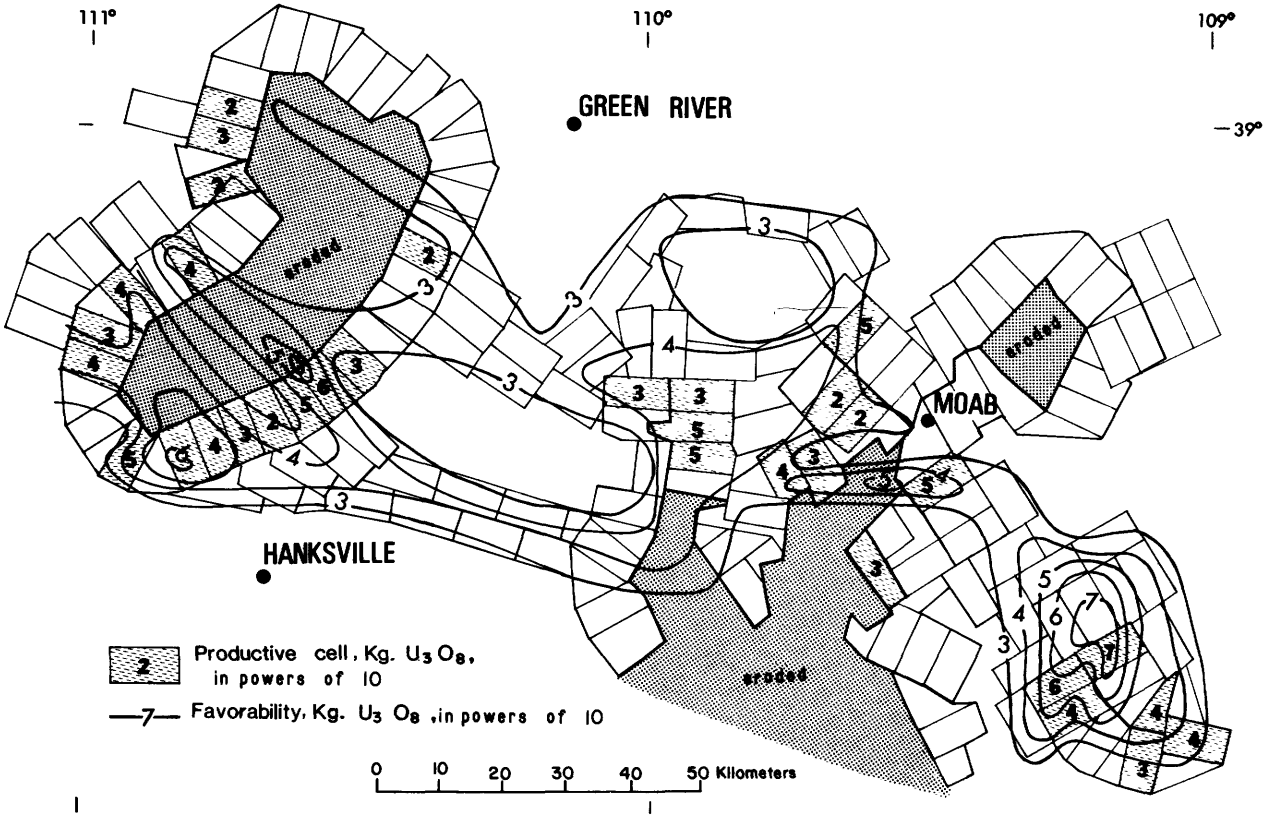

Figure 2.--Favorable and productive ground was subdivided into cells. These 50-km^2 cells include mineralized areas plus barren ground around a deposit. The cell was used in the assessment to compare areas of unexplored ground to productive ground. The distribution of speculative resources for the contour method is contoured from the distribution of favorable ground and from the distribution of known deposits from figure 1.

(fig. 2). These cells center on areas of known mineralization and include the surrounding barren ground which was explored as the result of the uranium discovery. The same size cells were also established in unexplored areas, and in explored but unproductive areas. It was decided arbitrarily that the cells should be 50 km^2 (5 km by 10 km extending lengthwise from the outcrop into the subsurface), but the areas explored around known deposits in the Chinle in the study area were typically about this size (fig. 2).

Ideally, the true value for <u>total</u> uranium in explored areas should be the data base for an assessment of adjacent, unexplored areas, but that value may never be known. Therefore, this assessment, which used available production data, will reflect only the volumes and grades of uranium that have been produced. Production values for explored cells are shown on figure 2.

After subdividing favorable ground into cells, two different methods of assessment were used. In the first method, the equal volume method, it is assumed that unexplored areas contain deposits similar to those discovered in adjacent and geologically similar areas. Assessed resources are simply the ratio between the total area of unexplored but favorable cells and the total area of productive cells, multiplied by production. The ratio of unexplored, favorable ground to productive ground is about 2.25 (3,800 km^2/1,700 km^2), and approximately 30x10^6 kg U_3O_8 have been produced in the study area. Hence, 68x10^6 kg U_3O_8 of a similar volume and grade to that produced is assessed for the area. If a better value for the amount of uranium in explored areas became known, then the amount of assessed resources could be multiplied by the ratio between the new value and the old to reach a more accurate assessment figure. Similarly, a change in cell size would change the ratio of the areas of favorable and productive ground.

The second assessment method, the contour method, is similar to the equal volume method but does not assume that unexplored areas contain deposits similar to those discovered; areas far from known deposits are credited with less uranium, because the assessment becomes more uncertain with increased distance from known deposits (figs. 1 and 2). By the contour method, the value of each individual cell is determined by multiplying the values of the intersecting contours by the fraction of the cell they intersect. For example, if a cell has half its area within the 10^3kgU_3O_8 contour, plus a fourth each in the 10^4- and 10^5-kg-U_3O_8

contours, then the cell contains $10^3/2+10^4/4+10^5/4=$ 28,000 kg U_3O_8 within its 50 km^2 area (fig. 2). The total resource value for the study area, the total of the values for all cells, is $(1x10^7)+(3x10^6)+(7.5x10^5)+(21.5x10^4)+(41.5x10^3)$ = approximately $14x10^6$ kg U_3O_8. However, the production data used for individual deposits is out of date. Production data for the entire area is current, so therefore, a better assessment value can be obtained by adjusting the old assessment value by the ratio between new and old production data: $(14x10^6)$ $(30x10^6/13x10^6)$ = $32x10^6$ kg U_3O_8.

The geographic distribution of favorable ground can be related to the distribution of other geologic features, such as regional structure (no relationship), potential source rocks in the Chinle (positive relationship), and subsurface gamma-ray anomalies (positive relationship).

Lupe, Robert, 1976, Depositional environments as a guide to uranium mineralization in the Chinle Formation, San Rafael Swell, Utah: U.S. Geol. Survey Jour. Research, v. 5, p. 365-372.

URANIUM MINERALIZATION DURING EARLY BURIAL, NEWARK BASIN, PENNSYLVANIA-NEW JERSEY

By C. E. Turner-Peterson, U.S. Geological Survey, Denver, Colo.

Sedimentation in the Triassic-Jurassic Newark basin was the result of infilling of a rift basin formed prior to continental breakup. Asymmetrical development of facies resulted from differential tectonism in an internally-drained lake basin. The Stockton Formation, which crops out along the southern margin, consists of conglomerate, gray fine-grained sandstone, red siltstone, and red mudstone. The Lockatong Formation, which crops out in the central part of the basin, contains analcimic black mudstone and carbonate rocks. The Brunswick Formation, which crops out along the northern margin of the basin, is composed predominantly of red siltstone and mudstone, and local conglomerate.

The Lockatong Formation has a lacustrine origin, as documented by Van Houten (1962). The presence of carbonate rocks, black mudstone, sedimentary analcime, fish remains, and conchostracans suggests that a perennial alkaline lake existed in the basin. The Stockton and Brunswick Formations, long considered fluvial, are here considered largely marginal lacustrine deposits, based on facies relations, sedimentary structures, and a newly found fossil.

Laterally coalescing fans of conglomerate, derived from a crystalline highland to the south, compose the base of the Stockton Formation. Basinward from the southern margin, the next facies consists of thick beds of gray, fine-grained, flat-bedded, well-sorted sandstone of the Stockton, interpreted to be nearshore lacustrine in origin. A conspicuous lack of trough crossbeds, foresets, ripples, and other typical current features indicates that there was no fluvial plain between the aprons of coarse material on the fans and the fine-grained sandstone in the lake. Fine-grained detritus settled out of suspension farther from shore to form the red siltstone and burrowed red mudstone facies of the Stockton. Black mudstone included in the Lockatong Formation was deposited in the central euxinic part of the lake. Locally the red, fine-grained facies of the Stockton is absent and the offshore black mudstone is interbedded with the nearshore lacustrine sandstone. Thus, facies distribution along the southern border reflects a fan-to-lake transition with development of thick, well-sorted nearshore sandstone beds.

Facies development along the northern border was notably different. The fans in the Brunswick Formation are not coalesced, are restricted in areal extent, and are dominated by debris flow units. An abrupt fan-to-lake transition, without development of a nearshore sandstone, is indicated by interfingering of fanglomerate with green and black mudstone, conchostracan-bearing red mudstone, and mollusk-bearing limestone in the Brunswick Formation.

The differences in the facies along the two margins of the basin, as reflected in the Stockton and Brunswick Formations, are explained by the tectonic model proposed for the basin. Geophysical data suggest that en echelon normal faults occur near the northern border with their downthrown sides towards the basin (Sumner, written commun., 1975). Faulting is also present along the southern border but sedimentary overlap is more common. The tectonic differences that characterize the two borders directly affected facies distribution in the basin. The development of a nearshore lacustrine sandstone facies in the Stockton may be attributed to a gentle slope of the basin floor along the southern margin which permitted sorting of detritus delivered to the basin. In contrast, the interfingering of low-energy lake beds and coarse debris-flow units in the Brunswick Formation can be attributed to poor sorting on a steep slope,

maintained by recurrent faulting, along the northern margin of the basin. A similar situation was documented in Death Valley (Denny, 1965), where a playa, flanked on the east and west by fans, occupies a graben. Renewed faulting along the east side causes greater tilting and subsidence along that margin. The west side fans, in response, have been extended and the playas have encroached upon the more restricted fans on the east side.

Uranium mineralization in the Newark basin occurred in the offshore lacustrine black mudstones of the Lockatong Formation and the nearshore lacustrine sandstones of the Stockton Formation. Mineralization occurred during or shortly after deposition of the host rock, as indicated by geochemical considerations discussed below.

Two agents (humic acids and aqueous sulfide) capable of fixing uranium were forming in the offshore black muds at the time of deposition. The bottom sediments of the central part of the lake were anaerobic, as indicated by the black color of the mudstones and the presence of pyrite. Ferroan dolomite in the offshore mudstone facies also indicates anoxic conditions because ferrous ions substitute for magnesium in dolomite only in reducing conditions. Sedimentary analcime indicates a high pH, perhaps as high as 9.4, in the pore waters of the black muds. Humates are soluble in basic solutions and thus the solubilization of humic acids was favored in the pore fluids of the black muds. Simultaneously, bacterial anaerobic respiration resulted in the reduction of sulfate to bisulfide within the bottom sediments. Uranium was fixed near the sediment-water interface in the black muds, resulting in widespread medium-grade (0.01-0.02 percent U_3O_8) uranium deposits in the Lockatong.

Mineralization in the nearshore sandstone beds of the Stockton occurred shortly after deposition. The proximity of mineralized sandstone to black mudstone units suggests that the black mudstones played an important role in uranium mineralization. It is proposed that the reducing agents generated within the black muds (humic acids and aqueous sulfide) were expelled during compaction into the adjacent, more permeable nearshore sands, providing the reductants necessary for uranium fixation in those sands. Uranyl ions were carried into the basin by ground water from uranium-rich crystalline rocks south of the basin. Recent studies (McBride and Pfannkuch, 1975) on ground water movement on the periphery of modern lakes demonstrate that seepage into a lake occurs largely in the nearshore zone. In a similar manner, uranium-bearing ground water passed into the nearshore sands and then upward into the lake. In this manner, large amounts of uranium-bearing ground water may have passed through the nearshore sands, where reductants expelled from the black muds would have caused the uranium to precipitate, resulting in localized mineralization (as much as 1.28 percent U_3O_8) in the Stockton.

If the reductants were provided by expulsion of fluids from the compacting black muds, as is proposed here, certain time constraints are imposed on the model. The generation of aqueous sulfide in sediments is greatest at shallow depths, restricting its availability as a reductant to early burial stages. Further limitations are imposed on the depth and timing of fluid expulsion, because clays compact readily during early burial and expel most of the pore fluids at that time. Thus, compaction-induced lateral movement of the fluids containing aqueous sulfide and humic acids from the black muds into the adjacent, more permeable nearshore sands, and the resulting uranium mineralization, occurred during early burial.

The model proposed here for uranium mineralization in the Newark basin has several important implications: (1) black mudstones associated with uranium deposits in the Newark basin played an active geochemical role during mineralization, and (2) mineralization in the Stockton Formation occurred shortly after deposition of the host sandstone because agents necessary for fixing uranium were generated in the pore fluids only during early burial.

Denny, C. S., 1965, Alluvial fans in the Death Valley region, California and Nevada: U.S. Geol. Survey Prof. Paper 466, 62 p.

McBride, M. S., and Pfannkuch, H. O., 1975, The distribution of seepage within lakebeds: U.S. Geol. Survey Jour. Research, v. 3, no. 5, p. 505-512.

Van Houten, F. B., 1962, Cyclic sedimentation and the origin analcime-rich Upper Triassic Lockatong Formation, west-central New Jersey and adjacent Pennsylvania: Am. Jour. Sci., v. 260, no. 8, p. 561-576.

SURFACE GEOPHYSICAL METHODS APPLIED TO URANIUM EXPLORATION IN CRYSTALLINE TERRANES

By Vincent J. Flanigan, U.S. Geological Survey, Denver, Colo.

Complementary geophysical methods are demonstrated to be valuable in identification of areas favorable for the deposition of uranium in crystalline terranes. Geophysical surveys conducted in eastern Washington State and Colorado have aided in mapping lithologic units and structures where exposures are poor. The Swartzwalder Mine area, Jefferson County, Colo., was selected as a survey test area. This test area included a segment of the major north-west trending fault system known as the Rogers Fault West. Included in the test area is a contact between a hornblende gneiss and a mica-schist unit both of the Precambrian X Idaho Springs Formation (fig. 1). Within the mica schist there are about 6 m of alternating layers of magnetite and quartz (Young, oral commun., 1977).

The purpose of the geophysical survey was to identify the electrical and magnetic properties of the lithologic units and to delineate the geophysical expression of the Rogers Fault crossing the test area. The entire test area is covered with a thin veneer of overburden making surface geologic mapping difficult. At the Schwartzwalder mine, uranium minerals are being mined from a system of faults and fractures which lie between two branches of the Rogers fault system. In the mine area, the two Rogers faults (east and west) are about a kilometer apart. While it is not possible to detect uranium mineralization at depth using surface geophysical methods, the ability to identify favorable areas for mineralization warrants the inclusion of geophysical surveys in a uranium exploration program.

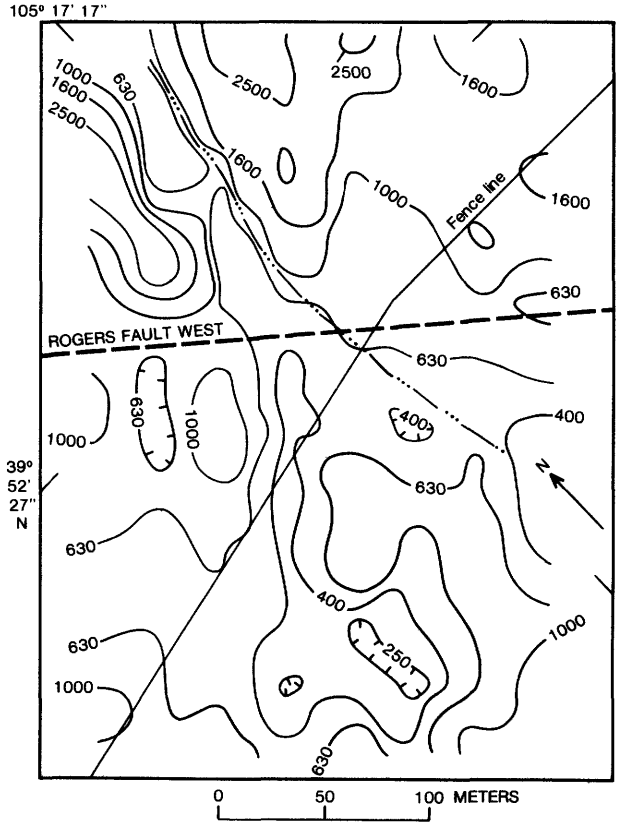

Figure 1

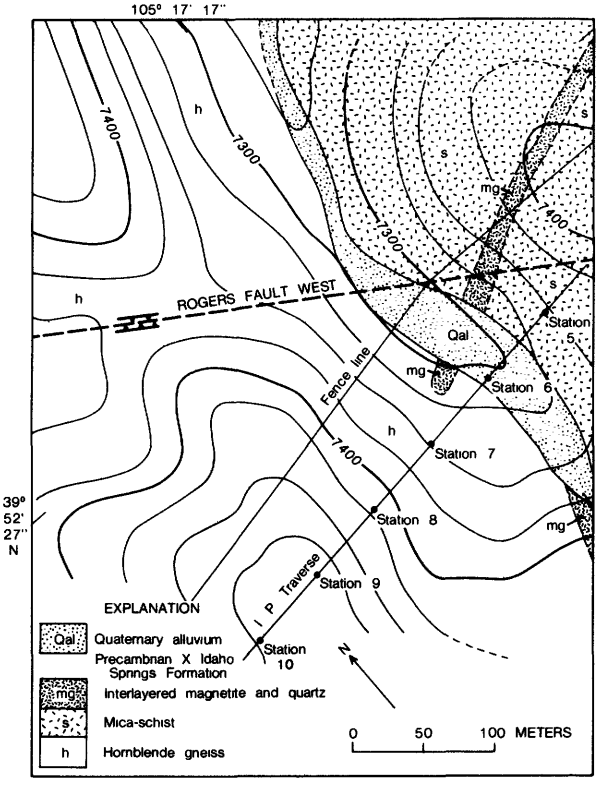

Figure 2

The test area is 275x265 m in extent and measurements were made on a 30.5 m grid across the area. Three methods were used to determine the electrical and magnetic nature of the rocks in the test area. Turam and VLF (very low frequency) electromagnetic methods measured the electrical character of the rocks. The magnetic character of the rocks was measured using a proton precession magnetometer. In addition, a single IP (induced polarization) profile was made across the contacts and structures delineated by the electromagnetic methods.

The electromagnetic methods indicated that the hornblende gneiss has an apparent resistivity of 1000 ohm-m or less (fig. 2) and the mica schist with the interlayered magnetite and quartz has apparent resistivities of from 1000 to 2500 ohm-m. The contact between the two units can readily be seen from the electromagnetic data. A relief of 12,000 gamma in the mica schist indicates concentrations of magnetite and also suggests the location of the contact between the two major rock types (fig. 3). The location of the Rogers Fault West is seen as a linear magnetic low, and has an associated conductive zone of less than 630 ohm-m. A second conductive zone was detected about 150 m south of the Rogers fault zone. The source of this anomaly is not readily apparent. The IP traverse crossing this area confirms the conductive nature of the area, and indicates a relatively good polarization characteristic in the conductive zone, suggesting possible sulfides in the near-surface rocks. Although there is no firm relationship between sulfide mineralization (mostly pyrite) and uranium mineralization, the geophysical data do indicate areas where more detailed study might be made.

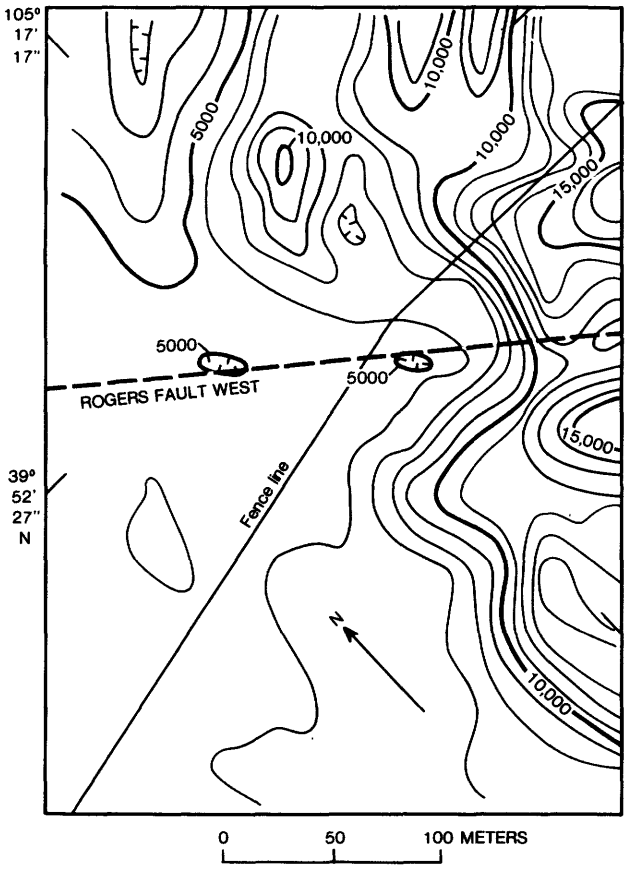

Figure 3

GEOPHYSICAL AND PETROLOGIC STUDIES OF RADIOACTIVE CONTACT ZONES OF PYROXENITE DIKES IN NEPHELINE SYENITE OF THE EKIEK CREEK PLUTON, WESTERN ALASKA

By Alan R. Wallace and John W. Cady,
U.S. Geological Survey, Denver, Colo.

A ground geophysical, petrographic, and petrophysical study was made of a subsilicic composite pluton, the Ekiek Creek Complex of Miller (1972), in western Alaska to determine the sources of coincident total-count gamma-ray and aeromagnetic anomalies detected in aerial surveys. This pluton is related to a series of subsilicic intrusive stocks in western Alaska and the eastern Siberian peninsula (Miller, 1972), (fig. 1). Airborne radiometric studies of several of the stocks in Alaska indicate uranium mineralization, and ground surveys have shown low-grade uranium concentrations of as much as 92 ppm (Jones, 1976). Owing to the lack of outcrops, the morphology of these stocks must be delineated by geophysical methods.

The project included data collection in the 3x5 km study area, and petrographic and petrophysical analyses of representative samples. Field geophysics involved nine major east-west traverses, as well as a number of shorter crossing traverses, and totaled 35 line km of magnetic, VLF, and four-channel gamma-ray spectrometer measurements. Petrophysical work on the samples included measurements of remanent magnetism and magnetic susceptibility, density, and electrical resistivity. Detailed petrographic studies of

representative samples also were made.

The Ekiek Creek pluton is a composite stock of Cretaceous age which intruded Lower Cretaceous silicic stocks and volcanic rocks. It includes two major silica-undersaturated rock types, fine-grained pyroxenite and medium-grained nepheline syenite. Field relationships between the two are anomalous. The pyroxenite occurs as broad tabular bodies in the syenite, but contact zones show veins of syenite through pyroxenite, and syenite along joints in pyroxenite, suggesting that the syenite intruded the pyroxenite. Extensive iron oxide alteration was noted along the contact zones, but no ore minerals were observed.

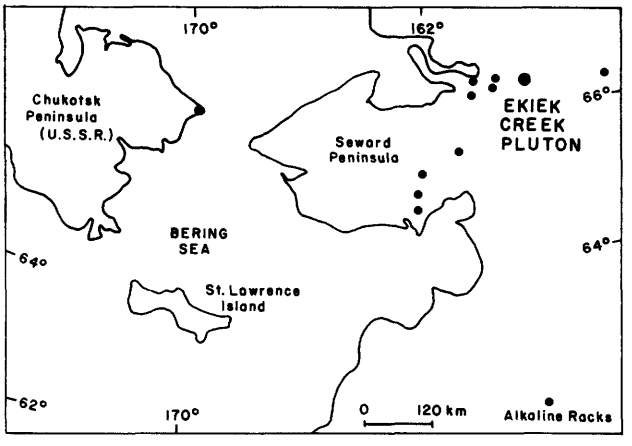

Figure 1

Petrographic studies of the samples collected in the field show a metamorphosed contact zone in addition to unaltered pyroxenite and nepheline syenite. The felsic rocks contain major orthoclase and nepheline, and varietal biotite, aegerine, and sphene. Melanite, a titanium-rich andradite garnet, occurs in variable amounts as deep-brown euhedral crystals of seemingly igneous origin. Zeolites, sericite, and cancrinite are common alteration products. The felsic rocks grade texturally from fine-grained hypidiomorphic-granular rocks to coarse porphyries containing orthoclase phenocrysts. The felsic rocks contain less than 15 percent mafic minerals, not including melanite, and orthoclase is much more common than nepheline.

The pyroxenites are fine to medium grained in thin section, and are composed of predominant aegerine-augite and biotite, and minor orthoclase, nepheline, sphene, and zeolites. Melanite, significantly, is absent. Flow textures are present in a few of the samples.

In contact zones poikiloblastic mafic minerals commonly contain inclusions of fine-grained melanite and orthoclase. The orthoclase and garnet become more common near the syenite, and euhedral garnets along the contact are poikiloblastic with inclusions of aegerine-augite. Microscopic contact relations between the pyroxenite and syenite show the syenite transecting preexisting flow structures in the pyroxenite.

Although many of the contact relations between the two major rock types suggest that the syenite, as the younger rock, intruded the pyroxenite, the tabular pyroxenite in the syenite points to the pyroxenite being the youngest rock. The increasing predominance of garnet and orthoclase in the pyroxenite near the contact indicates an interaction between the two rock types. It does not seem likely that the syenite, with a relatively low solidus temperature, could ionically diffuse through the pyroxenite to produce the garnet and orthoclase. The reverse situation is more probable, with the pyroxenite assimilating the components of the syenite along the contact. The pyroxenite intruded the felsic crystalline mush, with some assimilation, and, owing to its higher solidus temperature, crystallized in the mush. Cooling produced shrinkage cracks into which the felsic mush was drawn, forming what now appear to be dikes of syenite in pyroxenite.

As of this writing, the ground magnetometer, VLF, and gamma-ray data await position-recovery, and, in the case of magnetic data, smoothing before they can be contoured. Samples collected at about 45 rubble-crop exposures yield a generalized geologic map. However, a much more detailed geological map should result when geophysical contour maps become available.

Figure 2 shows ground magnetic, VLF, and gamma-ray profiles collected on an east-west traverse across the

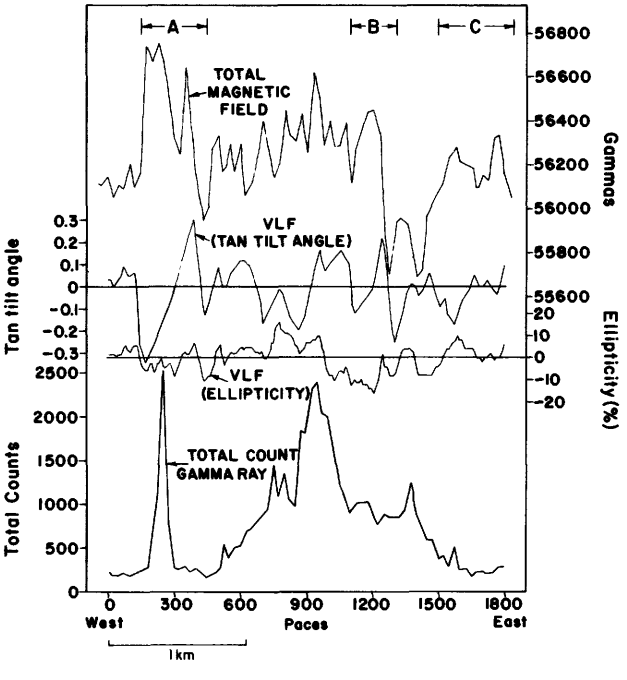

Figure 2

pluton. Magnetic highs labeled A and B coincide with zones of high conductivity, indicated by the "tangent tilt angle" VLF profile.

Magnetic and VLF anomalies A and B coincide with occurrences of pyroxenite. Anomaly B was traced in detail and found to be continuous for 500 m south and 1,600 m north of the east-west traverse. It is believed to mark a north-south-striking tabular body of pyroxenite at least 2,100 m long. Magnetic and VLF anomalies labeled A also occur on several east-west profiles, suggesting the presence of a second north-south tabular body, but the anomalies were not traced with the detail of anomaly B. Anomaly C did not show a clear VLF expression. Its appearance on several profiles suggests a possible third north-south-trending tabular body. Remanent magnetism and susceptibility measurements of samples show that the pyroxenite is more magnetic than the nepheline syenite.

The good correlation between the magnetic and VLF anomalies may occur because the ground is permanently frozen. Under ordinary temperature conditions VLF measurements are dominated by ionic conduction in water filled fractures. In frozen ground, however, ice-filled fractures would be non-conductive, and the VLF technique may be sensitive to changes in lithology.

The gamma-ray spectrometer traverses show zones of highest radioactivity along contacts between pyroxenite and nepheline syenite. Total counts measured over the contacts are 6 to 10 times those of the background over the muskeg, and 1.5 to 2.5 times those measured over the rubble-crops of the pluton as a whole. Iron-oxide staining, perhaps indicating hydrothermal alteration, is prominent along the contact zones. Detailed profiling by gamma-ray spectrometer shows that iron oxide-stained rocks are more radioactive than average, but the highest readings were obtained over a sharp, unoxidized contact of pyroxenite against nepheline syenite.

On a scale of kilometers, aeromagnetic highs of the Ekiek Creek pluton and of other alkalic plutons north of the Selawik Hills correlate with radioactivity anomalies. On a scale of 10 to 100 m, radioactivity anomalies correlate with contact zones between pyroxenite and nepheline syenite. The pyroxenite is distinguished by magnetic and VLF conductivity highs. Thus magnetic and electrical measurements, on either scale, may be tools for locating possible uranium mineralization.

Jones, B. K., 1976, Uranium and thorium in granitic and alkaline rocks in western Alaska: Master's thesis, University of Alaska, 123 p.

Miller, T. P., 1972, Potassium-rich alkaline intrusive rocks of western Alaska: Geol. Soc. America Bull., v. 83, p. 2111-2128.

A THEORY FOR THE ORIGIN OF THE RIFLE-GARFIELD VANADIUM-URANIUM DEPOSIT

By C. S. Spirakis, U.S. Geological Survey, Denver, Colo.

The Rifle-Garfield vanadium-uranium deposit, located in Garfield County, Colo., has been described in detail by Fischer (1960). The deposit occurs in eolian sandstones of Triassic and Jurassic age, and displays a distinct zonation of authigenic minerals, a feature whose origin has not been adequately explained in earlier works. In sequence, these zones are a 0.7-m-thick chromium-mica zone; a 0.1- to 0.6-cm-thick zone of galena and clausthalite in solid solution; a 1.3- to 2.5-cm-thick barren zone; and a zone of low-valent vanadium and uranium minerals, which is generally about 2 m thick but may be as much as 9 m thick. This latter zone is dominated by very fine-grained mixed-layered vanadium mica-montmorillonite, vanadiferous chlorite, and the vanadium mica, roscoelite. Each zone forms a curved surface, which may be traced for about 3 km in its long dimension and a few hundred m in its short dimension.

In the vicinity of the ore deposit, the upper meter or so of the underlying Chinle Formation is bleached. This altered zone is characterized by a slight loss of total iron and a partial reduction of ferric iron. According to Fischer (1960), the localization of this bleaching around the deposit suggests a genetic link between the alteration and the formation of the ore deposit.

Fischer (1960) considered reactions at an interface between two solutions to be the most logical explanation for the formation of the deposit, but he realized it was difficult to explain how the interface could be maintained for a long enough time for the ore to develop. Also, an interface by itself does not explain the origin of the zones or the alteration. The zonation, the alteration, and the long-lived interface could all be effects of semipermeable membranes.

The membrane properties of layers of clay minerals appear to result from the interactions of dissolved species with the negatively charged sites on the surfaces of clay platelets (Hanshaw, 1962). An important consequence of these interactions is that most ions and molecules diffuse more slowly in a membrane than in an open solution. Thus, these dissolved species diffuse away from a membrane faster than they do through it; hence, concentration gradients across a semipermeable membrane can be maintained and solutions of differing properties can be kept separate.

Another effect of a semipermeable membrane is the generation of pH changes on both sides of a membrane. One mechanism for generating pH changes with a membrane is described by Hartman (1947). As he points out, when an ion diffuses through a membrane, an ion of like charge must diffuse through in the opposite direction, or one of opposite charge must diffuse through in the same direction in order to maintain charge balance. When the diffusion of the hydrogen ion through the membrane is involved in maintaining charge balance, a pH change results.

A second mechanism for generating pH changes across a semipermeable membrane concerns the diffusion of H_2CO_3 through the membrane. Because H_2CO_3 is uncharged, it has little interaction with a membrane and diffuses through faster than other carbonate species. This relatively rapid diffusion of H_2CO_3 from a high-carbonate solution on one side of a membrane into a low-carbonate solution on the opposite side of the membrane, causes a disequilibrium among the carbonate species on both sides of the membrane. On the high-carbonate side, H^+ and HCO_3 associate to replace the lost H_2CO_3. In the process, H^+ is removed from the solution and the pH is raised. As more H_2CO_3 forms, it in turn diffuses through the membrane. On the low-carbonate side of the membrane, excess H_2CO_3 dissociates to H^+ and HCO_3 and thereby decreases the pH.

In the case of the Rifle-Garfield deposit, the vanadium-uranium zone of the ore is a potential semipermeable membrane. Hanshaw (1962) showed that montmorillonite (which forms a major part of the vanadium-uranium zone) can act as an effective membrane, thus supporting the possibility that the vanadium-uranium zone can function as a semipermeable membrane. It is assumed here that the interface at which the ore precipitated was between a carbonate solution and a sulfate solution. This assumption is supported by the abundance of carbonate- and sulfate-dominated ground waters at shallow to moderate depths; by the work of Hostetler and Garrels (1962), which suggests that the mineralizing solutions of the Colorado Plateau were carbonate-rich; and by the presence of galena in the deposit. The significance of the galena lies in the incompatibility of lead with sulfur in most ground-water solutions (Anderson, 1975). This incompatibility suggests that they were transported in different solutions; I believe one of these was a sulfate solution containing some H_2S, and the other was a carbonate solution that transported lead along with uranium, vanadium, and selenium. It is also assumed that the sulfate solution had a lower Eh and pH than the carbonate solution. At the interface, the lower Eh and pH of the sulfate solution caused uranium and vanadium to precipitate. Once a sufficiently dense layer of vanadium silicates formed, it began to function as a semipermeable membrane.

The vanadium-silicate membrane kept the two solutions separate and maintained the position of the solution interface while the ore grew. Diffusion of H_2CO_3 from the carbonate side to the sulfate side of the membrane created higher pH conditions on the carbonate side and lower pH conditions on the sulfate side. As HCO_3 diffused from the carbonate side to the sulfate side of the membrane, H^+ diffused through in the same direction in order to maintain charge balance. This diffusion of H^+ further increased the pH difference across the membrane.

On the sulfate side, where the pH, Eh, and carbonate content were lower, conditions were right for the precipitation of more vanadium and uranium minerals. Thus the vanadium-uranium zone grew by addition onto its sulfate side. On the carbonate side, the high pH generated by the membrane increased the solubility of vanadium and uranium and inhibited their precipitation in a region adjacent to that side of the membrane. That is the region now represented by the barren zone.

Diffusion of hydroxyl ions and H_2S away from the membrane established a pH gradient and a gradient in the H_2S concentration on the carbonate side of the membrane. As lead and selenium diffused into the higher pH and higher H_2S concentration near the membrane, they precipitated as galena and clausthalite, thus forming the galena-clausthalite zone.

It is suggested that silica, required for the precipitation of the chromium mica, was derived from the corroded quartz grains of the vanadium-uranium zone. The high pH near the membrane increased the solubility of silica and prevented the precipitation of the chromium mica in the barren zone. Farther from the membrane, the pH decreased and the chromium mica formed.

As the vanadium-uranium zone grew, chemical conditions within it changed. Leakage of the carbonate solution into the zone (which had formed on the sulfate side of the interface) slightly raised the pH, Eh, and carbonate content of the older parts of the zone. The position of the older parts of the vanadium-uranium zone was such that the pH in the older parts was increased by the membrane effects of the younger parts of the zone. The increased pH, Eh, and carbonate content of the older parts of the membrane had little effect on the very stable vanadium silicates; uraninite, however, was remobilized by these new conditions. The remobilized uraninite diffused farther toward the sulfate side where it reprecipitated and formed the observed zone of uranium enrichment on the edge of the

vanadium-uranium zone.

The acidic conditions generated on the sulfate side of the membrane may account for the alteration of the Chinle in that both the solubility of iron and the stability of ferrous compounds relative to ferric compounds increase in a more acidic environment.

The theory presented above, which involves diffusion through a semipermeable membrane that precipitated at a carbonatesulfate solution interface, provides a means of maintaining the interface despite mixing due to diffusion or flow, explains the possible origin of all of the observed zones, accounts for the alteration and its genetic link to the ore, and provides a reductant by the diffusion of H_2S from the sulfate solution.

Anderson, G. M., 1975, Precipitation of Mississippi Valley-type ores: Econ. Geology, v. 70, no. 5, p. 937-943.

Fischer, R. P., 1960, Vanadium-uranium deposits of the Rifle Creek area, Garfield County, Colorado: U.S. Geol. Survey Bull. 1101, 52 p. [1961].

Hanshaw, B. B., 1962, Membrane properties of compacted clays: Unpub. PhD. thesis, Harvard University, 113 p.

Hartman, R. J., 1947, Colloid chemistry, 2d ed.: Boston, Houghton Miffin Co., 604 p.

Hostetler, P. B., and Garrels, R. M., 1962, Transportation and precipitation of vanadium and uranium at low temperatures, with special reference to sandstone-type uranium deposits: Econ. Geology, v. 57, no. 2, p. 137-167.

A NEW STRUCTURAL MODEL FOR HUMIC MATERIAL WHICH SHOWS SITES FOR ATTACHMENT OF OXIDIZED URANIUM SPECIES

By J. K. Jennings and J. S. Leventhal
U.S. Geological Survey, Denver, Colo.

The literature has many references to structureless uranium-organic associations. The organic material usually associated with the uranium ore is unsoluble, but it is commonly believed that this material was originally a humic-acid type. Humic acids are the soluble products of inorganic and biological degradation of plant material. Several structural representations of humic acids based on experimental chemical studies have been presented in the literature in the past. Unfortunately, these models are deficient, but as a result of physical and chemical studies in the last 10 years can now be brought up to date. Humic acids have the approximate elemental chemical composition of 56 percent carbon, 34 percent oxygen, 6 percent hydrogen, 3 percent nitrogen, and 1 percent sulfur. There are numerous ways these elements can be combined, depending on the source, age, environment of deposition, and preservation of the humic material. One of the simplest chemical formulas which can be written (C_{150} O_{60} H_{180} N_6 S) gives a molecular weight of approximately 3,200, which is well within the normal molecular weight range of humic acids (1,000 to 10,000).

The elements oxygen, hydrogen, nitrogen, and sulfur in humic acids are usually present as functional groups such as acid, COOH; hydroxyl, OH; phenolic hydroxyl, C_6H_5OH; amino, NH_2; ketone, C=O; ester, COOR; ether, COC; and sulfhydryl, SH. Many of these groups can be positively or negatively charged (depending on the pH) or can share electrons (nitrogen, oxygen, and sulfur). By these mechanisms they can form ion-exchange and (or) chelate sites. These sites can interact with soluble oxidized uranium species such as UO_2^{+2}, $UO_2(CO_3)_2 \cdot H_2O^2$, and $UO_2(OH)^{+1}$. Figure 1 shows a structural model of humic acid with the above sites; they are shown with positive or negative charges that would be available over the whole pH range of 4 to 10. It is important to realize that real humic acids are each different in size and shape, and that they are three dimensional having external protrusions and internal voids. Our model is simplified, but we believe it is the most correct presented to date, especially in reference to interaction with uranium.

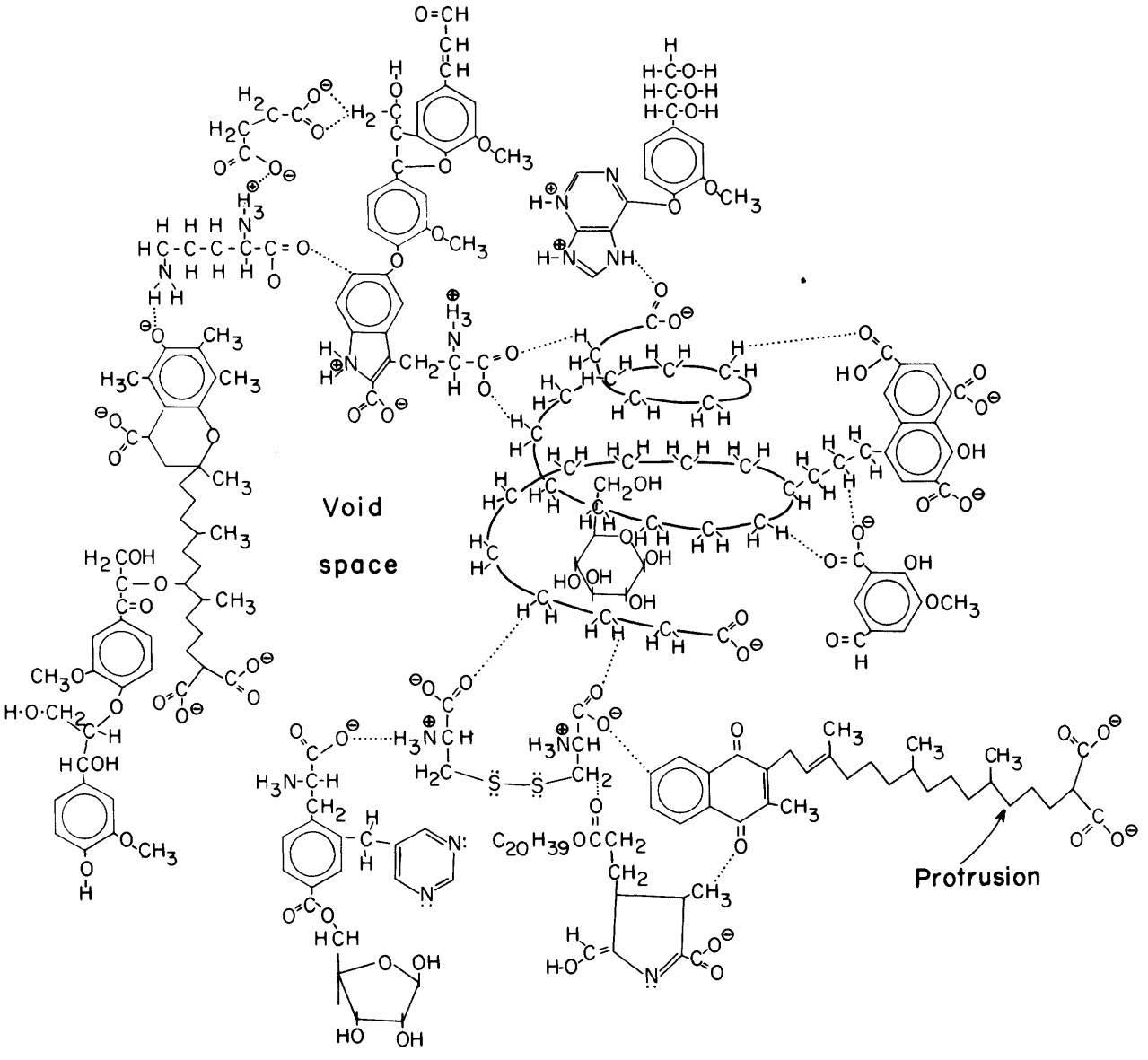

Figure 1.--Structural model of a humic acid having a molecular weight of approximately 5,000. The approximate chemical formula is $C_{249}O_{82}H_{320}N_{13}S_2$. The circled + and - and the : (on nitrogen and sulfur) show possible sites of uranium interaction.

NON-LINEAR COMPLEX RESISTIVITY FOR THE CHARACTERIZATION OF SEDIMENTARY URANIUM DEPOSITS

By Gary R. Olhoeft, U.S. Geological Survey, Denver, Colo.

Measurement of variations in physical and chemical properties by mapping changes in the electrical resistivity of the ground is a well known technique whereby a known electrical current is used to stimulate the ground while the resultant voltage generated is separately measured. The ratio of the voltage to the current times a geometric constant is then the observed resistivity. If the measurement is done at dc (zero frequency), only one number is obtained, the dc resistivity. At non-zero frequencies, however, the resistivity is a complex quantity and the resultant terms are usually expressed as the real part of the complex resistivity ("real resistivity") and the phase angle between the applied current and the measured voltage. For measurements at several frequencies, there are further parameters such as the percent frequency effect (PFE) which is a measure of the variation of the real resistivity with frequency.

In all of these techniques, it is assumed that the resistivity is a linear function of voltage and a linear reciprocal function of current, in which case we say that the system is linear and obeys Ohm's law. Thus, if we plot current vs voltage at dc the result is a straight line for a linear resistivity material. If the frequency is non-zero and there is a significant phase angle, a plot of current vs voltage will result in an ellipse (with limits of a straight line for 0 mrad (milliradians) phase angle and a circle for 1570.8 mrad phase angle). If the system has any non-linear components, the resultant plot will appear as a distorted line, ellipse or circle. The non-linear complex resistivity measurements described here are the result of driving a pure sine wave current into a sample, and studying the resultant voltage response for harmonic distortion.

Most unaltered materials, such as basalt or quartz sand, have extremely high resistivities when dry and low resistivities when in contact with water; in both cases the response is linear. This is due to the fact that the rock-water interaction in these materials is not very chemically active. In contrast, materials such as sulfides, clays, and zeolites are extremely chemically active at the water-rock interface either through direct oxidation-reduction reactions or through adsorption-desorption reactions (such as in the cation exchange process). The currents which result while these reactions are proceeding cause non-linear responses in such materials.

At very low current densities, when little chemical action is occurring, these materials may be linear. With increasing current density, chemical activity increases and the system becomes non-linear. The nature of the observed non-linearity is a direct function of the type of chemical reaction. Also, as the frequency of the applied current is varied, the non-linear response changes character and eventually disappears as the driving current begins to exceed the rate of the chemical reaction.

Detailed laboratory work has been proceeding on a series of very carefully acquired, handled, and prepared natural and synthetic materials which are respresentative of sedimentary uranium deposits. Strong differences have been observed between the linear response of quartz sand and the two most common types of non-linear response due to oxidation-reduction reactions (as occurring in sulfides) and due to adsorption-desorption reactions (as in the cation exchange process in clays and zeolites). Although the dry sulfide minerals may have non-linear responses due to their semiconducting nature, all of the observed non-linear responses reported here are due to reactions at the rock-water interface.

A single non-linear response for a typical sulfide such as pyrite is very complicated due to the occurrence of several different reactions. There is a hierarchy in the sequence of reaction as the current is increased and then decreased. This hierarchy allows observance of specific individual reactions. Each reaction occurs at a specific rate and is influenced by the chemical environment (such as the pH, Eh, and so on of the water). Further, some reactions are reversible while others are not. By observing the characteristic non-linear response of a sample as a function of frequency and interpreting that as the presence or absence, rate, and relative magnitude of various chemical reactions it thus becomes possible to identify several types of material (clay vs sulfide, for example), sorbable ions in solution, and to place limits on the oxidation state of the minerals as well as the Eh and pH of the ground water.

The laboratory work has already demonstrated that distinctions may be made between clays, sulfides, shales, and graphites. Also, the relative oxidation state is observable.

Although non-linear complex resistivity is useful as a laboratory tool, it does not appear that it will be successfully applied as a surface exploration technique.

The problems of divergent and widely varying current densities are very great. As a downhole logging tool, however, it shows exceptional promise. This is especially true in areas where an in situ or solution mining process must be tailored to the specific ground water and mineral chemistry of a given site. As a logging tool, non-linear complex resistivity should then be able to delineate and characterize an orebody as to variations in pH and Eh (by observing the changes in various sulfide chemical reactions), as to relative concentrations of clays and sulfides, as to the availability and mobility of sorbable ions, and possibly as to variations in cation exchange capacity.

There is a considerable amount of detailed laboratory work which has yet to be performed. It has already been demonstrated that clays and sulfides have very different non-linear responses, but it has yet to be shown whether or not individual sulfides (pyrite vs chalcopyrite) may be discriminated or whether individual clays (kaolinite vs montmorillonite) may be discerned. It has been shown that the relative oxidation states of some materials are observable, but absolute calibrations should be possible.

Bockris, J. O., and Reddy, A. K. N., 1970, Modern electrochemistry, vols. 1 & 2: London, Plenum Press, 1432 p.

Fink, J. B., 1976, Electrochemical experiments on base metal sulfides, 52nd Annual Meeting of the Southwestern and Rocky Mountain Division of the AAAS, Tucson, Arizona: Preprint American Association for the Advancement of Science, 18 p.

Hall, S. H., 1975, A method of measuring rock electrode kinetics: Jour. Electroanal. Chem., v. 59, p. 323-333.

Katsube, T. J., Ahren, R. H., and Collett, L. S., 1973, Electrical non-linear phenomena in rocks: Geophysics, v. 38, p. 106-124.

Klein, J. D., 1976, A laboratory investigation of the non-linear impedance of mineral-electrolyte interfaces: M.Sc. thesis: Dept. of Geology and Geophysics, Univ. of Utah, Salt Lake City, Utah, 94 p.

TOTAL-FIELD MAGNETIC SURVEYING AS AN EXPLORATION TOOL FOR SEDIMENTARY URANIUM DEPOSITS

By Louis J. O'Connor and Bruce D. Smith,
U.S. Geological Survey, Denver, Colo.

Total-field magnetic surveying is a relatively simple and inexpensive geophysical exploration method. In order to test applications in the exploration for sedimentary uranium deposits, ground surveys have been conducted in several areas over known mineralization. Results indicate that magnetic surveying can detect subtle variations in the distribution of magnetic minerals in the sedimentary section. In many cases, these variations can be spatially related to uranium orebodies.

Induced magnetization is usually the primary source of magnetism in sedimentary rocks. The majority of magnetic anomalies are due to changes in the strength of the induced field caused by local variations in the quantity of magnetic minerals distributed in the rocks. The common magnetic minerals are Fe-Ti oxides, the most important being magnetite. Their distribution is controlled by the depositional processes of the sedimentary environment and by their possible alteration due to geochemical processes.

In the fluvial to transitional marine sandstones that most commonly host sedimentary uranium deposits, magnetic minerals can occur both as local concentrations associated with stream channels and as disseminated detrital grains. The mechanical deposition of these minerals is dependent upon the size, shape, and mass of the grain and the velocity and sorting capability of the environment. Adler (1973); Adams, Curtis, and Hafen (1975); and Reynolds (1975) have discussed how oxidizing and reducing conditions, related to the formation of sedimentary uranium deposits, can alter detrital magnetic minerals. Of particular interest in the application of magnetic surveying techniques is the reported partial to complete destruction of magnetic minerals in the vicinity of some sedimentary uranium deposits and the correlation of low magnetic susceptibility with uranium (Ellis and others, 1968).

The ability of magnetic mapping to detect anomalies associated with sedimentary uranium deposits is dependent upon the contrast of magnetic properties (if any) of mineralized rocks with surrounding rocks and upon the size and depth of that zone of contrast. Increasing depth will decrease the size of an anomaly associated with a given source and increase the possibility of it being obscured by other magnetic sources. This factor limits the usefulness of surface magnetic methods in exploring for deeper uranium deposits. However, even when no anomalies can be directly

associated with fronts, valuable geologic information such as the location of channel sands and changes in facies can be inferred from magnetic data. This information could prove useful in indirectly guiding exploration.

Due to the relatively small quantities of magnetic minerals in sedimentary rocks, magnetic anomalies are typically small. In order to accurately detect these anomalies, two magnetometers with 1/4-gamma sensitivity were used in our surveys. One magnetometer was used as a local base station to monitor diurnal variations of the geomagnetic field, while the other instrument was used for field surveying. As a compromise between rapid surveying and the need for adequate details, readings were usually taken at 30 m intervals. If changes in magnetic levels across short distances were recognized in the field, intermediate readings were taken to fill in the details of the anomaly. The time correlation of base and field readings allowed the accurate removal of diurnal variations. Regional variations related to basement anomalies and to the spatial variation of the earth's field were removed by the subtraction of low order polynomial trend surfaces from the data. The residual fields represent the effect of local sources in the sedimentary section.

Two surveys were conducted in northern Colorado over roll fronts in the Upper Cretaceous Laramie Formation (fig. 1, area 1). One survey was made on exposed Laramie with a roll front occurring in a sand unit approximately 15 m below the surface. A strong correlation was found between a sharp 15-gamma negative anomaly and the mineralized zone. This anomaly probably results from the relative depletion of magnetic minerals in the vicinity of the roll front.

A second survey was made where approximately 45 m of the White River Formation (Oligocene) unconformably overlies the Laramie. Here mineralization occurs in the Laramie about 75 m below the surface. No magnetic anomalies could be directly associated with the ore. The lack of any distinctive magnetic signature may be due to the greater depth to the deposit, or to the absence of those conditions that produced the relatively low magnetic values in the previous case. Trends in the magnetic map do show a similarity to trends in the isopach of the ore sand. This may be the result of the concentration of magnetic minerals in the area of greatest sand deposition. Although not a direct guide to uranium, the ability to map trends in the thickness of the ore sand could still be useful where uranium mineralization can be related to such variations.

Two surveys were also conducted in the Powder River Basin. One survey in the central portion of the basin was directed at uranium deposits 45-50 m deep in the Eocene Wasatch Formation (fig. 1, area 2). A small negative anomaly correlates with the oxidized side of the zone of mineralization (fig. 2). The other area surveyed (fig. 1, area 3) has uranium mineralization in the Fort Union (Paleocene) and Wasatch Formations, ranging from near surface to deeper than 150 m. Here the magnetic pattern is complex, reflecting perhaps both the local complexity of the geologic units and their alteration history, and uranium deposits are not marked by any consistent magnetic signatures.

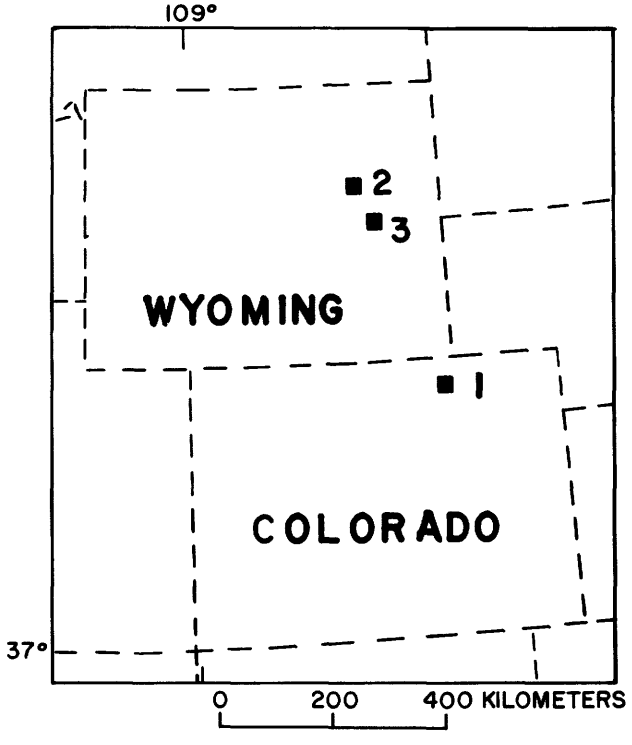

Figure 1.--The location of study areas. Numbers indicate survey areas discussed in text.

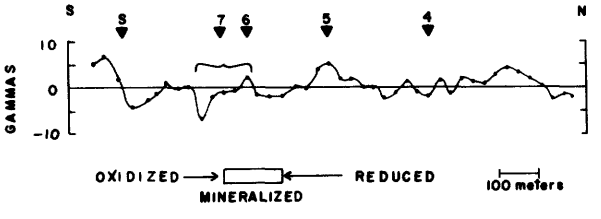

Figure 2.--Second residual magnetic profile, drillholes, and generalized relations of uranium ore in area 2. Mineralization is at a depth of approximately 50 m. Bracket indicates area of magnetic anomaly.

The depth, size, and magnetic properties of mineralization and the influence of local geologic features are controlling factors on the magnetic patterns observed in surface surveys. Despite the complexities introduced by these local factors, the method, which involves only one or two people and commercially available instruments, is rapid

and inexpensive and promises to be a useful exploration tool for sedimentary uranium deposits.

Adams, S. S., Curtis, H. S., and Hafen, P. L., 1975, Alteration of detrital magnetite-ilmenite in continental sandstones of the Morrison Formation, New Mexico, in Uranium exploration methods: Internat. Atomic Energy Agency, Vienna, p. 219-253.

Adler, H. H., 1973, Exploration for uranium in sandstones--geochemical, remanant magnetic, and sulfur isotope applications, in Uranium exploration methods: Internat. Atomic Energy Agency, Vienna, p. 155-166.

Ellis, J. R., Austin, S. R., and Droullard, R. F., 1968, Magnetic susceptibility and geochemical relationships as uranium prospecting guides: U.S. Atomic Energy Comm. R.I.D., rept. 4, G.J.O. Grand Junction, Colo., 21 p.

Reynolds, R. L., 1975, Alteration of iron-titanium oxide minerals associated with uranium deposits in sandstones, in Craig, L. C., Brooks, R. A., and Patton, P. C., eds., Abstracts of the 1975 Uranium and Thorium Research and Resources Conference: U.S. Geol. Survey Open-File Rept. 75-595, p. 38-39.

ORIGIN OF URANIUM IN THE MIDDLE PRECAMBRIAN ESTES CONGLOMERATE, EASTERN BLACK HILLS, SOUTH DAKOTA--INFERENCES FROM LEAD ISOTOPES

By F. Allan Hills and Maryse H. Delevaux,
U.S. Geological Survey, Denver, Colo.

The middle Precambrian (or Precambrian X) Estes Conglomerate, which crops out approximately 23 km northwest of Rapid City, South Dakota, in Lawrence, Meade, and Pennington Counties, contains beds of well-sorted quartz- and quartz-pebble conglomerate (oligomictic conglomerate), in which pyrite may form as much as 25 percent of the matrix. Commonly these beds are moderately radioactive (table 1) and locally they contain minor gold (table 2 and fig. 1).

The Estes Conglomerate lies unconformably upon the Benchmark Iron-formation (a banded quartz-taconite rock) and upon the Boxelder Creek Quartzite (Bayley, 1970) both of the Nemo Group. Most pebbles and larger clasts in the Estes apparently were derived from these two formations. In its northernmost exposures, at the head of Little Elk Canyon, the Estes may lie unconformably upon the lower Precambrian (or Precambrian W) Little Elk Granite, although outcrops are poor and the contact relations are not firmly established. Quartz pebbles predominate over quartzite pebbles in oligomictic beds in the Estes at this locality, suggesting that the granite, and quartz veins within the granite, may have been the source rock for these oligomictic beds.

Pyrite, gold, and radioactive minerals in oligomictic

Table 1.--Uranium and thorium concentrations in weathered rocks, calculated fresh-rock uranium concentrations, and $^{207}Pb/^{206}Pb$ ages of Estes Conglomerate

Sample No.	Weathered rock (Delayed neutron analyses)			Fresh-rock (calculated)		$^{207}Pb/^{206}Pb$
	U ppm	Th ppm	Th/U	U ppm	Th/U	Age in m.y.
BH-76-5b	41	164	4.0	66	2.48	1925
BH-76-13a	11	700	6.4	114	6.14	2150
BH-76-14a	36	188	5.2	104	1.81	2075
BH-76-19	21	173	8.2	77	2.25	2000
BH-76-26	11	110	10.0	44	2.30	2810

Table 2.--Gold content of samples of Estes Conglomerate containing ≥0.05 ppm Au[1]

Sample No.	Au (ppm)	Sample No.	Au (ppm)
BH-76-9b	0.16	BH-76-20a	0.08
BH-76-14a	0.06	BH-76-26	0.28
BH-76-14d	0.05	BH-76-28a	1.39
BH-76-14e	0.25	BH-76-28b	0.49
BH-76-19	0.06	BH-76-28c	0.37

[1]All samples reported by Hills (1977) were analyzed for Au. For the locations of barren samples, see his figures 2 and 5. Au determined by fire assay and atomic absorption by J. G. Crock, Joseph Haffty, and A. W. Haubert.

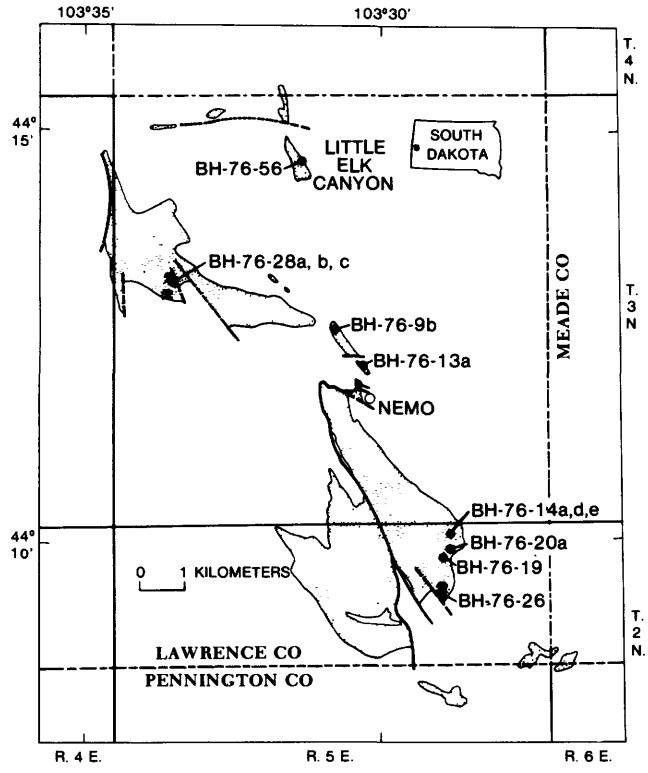

Figure 1.--Area of explosure of the Estes Conglomerate (stippled) with sample localities. (Geology adapted from Bayley, 1972).

beds of the Estes Conglomerate have been interpreted as heavy-mineral concentrates formed in placer deposits of early middle Precambrian age (Hills, 1977). However, the possibility that uranium was introduced into these conglomerates by more recent epigenetic processes cannot be ruled out on the basis of field and geochemical evidence. Intense weathering of outcrops, facilitated by oxidation of pyrite, would have eliminated any easily altered uranium minerals that originally were present, making mineralogical studies of samples from outcrop of little value in distinguishing between a syngenetic and an epigenetic origin for the uranium. The degree of weathering and oxidation of Estes Conglomerate appears to be greatest where the oligomictic beds originally contained the most pyrite (estimated from pyrite molds). Therefore, these same areas probably have the greatest potential for containing commercial-grade uranium.

Oxidation and leaching of the oligomictic conglomerates have obscured the answers to two important questions: (1) What process concentrated uranium in the Estes Conglomerate?; and (2) how much uranium is present below the zone of oxidation and leaching? Lead-isotope ratios from weathered samples provide tentative answers to these questions that may be useful in deciding whether a bore-hole program is warranted. According to the syngenetic or placer hypothesis, the uranium has resided in the oligomictic beds since the early middle Precambrian, whereas according to the epigenetic hypothesis, uranium was introduced at a relatively recent time. The $^{206}Pb/^{204}Pb$ and $^{207}Pb/^{204}Pb$ ratios should be higher than those for most ordinary rock lead if the syngenetic hypothesis is correct, and $^{207}Pb/^{206}Pb$ ages should be early or middle Precambrian.

The exact uranium content of the fresh rock cannot be determined from analyses of highly weathered samples because the uranium, as well as the lead and thorium, are depleted or enriched to some unknown extent in weathered samples. Nevertheless, if the age of a U-Th-Pb system is known or can be estimated from other data, the U/Th ratio responsible for producing the lead isotope system can be calculated with the following equation

$$\frac{^{238}U}{^{232}Th} = \left(\frac{^{206}Pb}{^{208}Pb}\right)_r \times \frac{(e^{\lambda' t} - 1)}{(e^{t\lambda} - 1)} \qquad (1)$$

where $(^{206}Pb/^{208}Pb)_r$ is radiogenic lead, t is the age of U-Th-Pb system, is the decay constant for ^{238}U, and is the decay constant for ^{232}Th. This equation is strictly true only where the U-Th-Pb system has remained closed until geologically recent times.

The $^{238}U/^{232}Th$ ratios determined by equation (1) are not sensitive to errors in the independently determined age (t); errors as great as 500 m.y. produce variations of less than 5 percent in $^{238}U/^{232}Th$, provided the lead is moderately radiogenic. However, the $^{238}U/^{232}Th$ ratio calculated may be in error because the degree of weathering and lead removal from uranium-rich phases may differ from that in thorium-rich phases.

The low solubility and low mobility of thorium in the weathering environment suggests that the fresh-rock uranium tenor can be estimated by using a chemical analysis for thorium in conjunction with the $^{238}U/^{232}Th$ ratio derived from equation (1). The effects of weathering (preferential loss of uranogenic lead, introduction of lead from nearby rocks, and mobility of thorium) and of Precambrian metamorphism (loss of lead) are most apt to cause underestimation of fresh-rock uranium, whereas loss of uranium early in the history of the sample (perhaps during metamorphism) would cause overestimation of fresh-rock uranium.

Five samples of weathered Estes Conglomerate (fig. 1) yield the following ranges of isotope ratios: $^{206}Pb/^{204}Pb$ from 38.65 to 92.02; $^{207}Pb/^{204}Pb$ from 19.57 to 25.18; and $^{208}Pb/^{204}Pb$ from 50.04 to 168.25. These ratios are higher than normal Precambrian rock leads and yield apparent $^{207}Pb/^{206}Pb$ ages that range from 1925 m.y. to 2810 m.y. (table 1).

Based on an assumed age of 2500 m.y. for the U-Th-Pb system and corresponding common lead ratios (Stacey and Kramers, 1975, Table 9), equation (1) yields apparent fresh-rock Th/U ratios that range from 1.8 to 6.1 and

fresh-rock uranium concentrations of as much as 114 ppm.

Geologic age, sedimentary characteristics, and the coherence of uranium, thorium, and gold in oligomictic beds of the Estes Conglomerate support an interpretation of uranium in the Estes as fossil placer deposits, similar in origin to uraniferous conglomerate in the Elliot Lake District of Ontario and the Witwatersrand of South Africa. By their antiquity, the $^{207}Pb/^{206}Pb$ ages support the syngenetic or fossil placer hypothesis and appear to rule out the recent-epigenetic hypothesis.

Although the semiquantitative estimates of fresh-rock uranium tenor, based on lead-isotope analyses of five samples, do not confirm that ore-grade rock is present, they indicate that as much as 90 percent of the uranium originally present has been leached from the conglomerate. This suggests that part of the uranium may be present in soluble minerals, such as uraninite, and that economic concentrations may occur in the Estes where sedimentologic conditions and source rock were favorable. The Estes Conglomerate, especially where it contains a high proportion of detritus from the Little Elk Granite, merits further examination by means of boreholes.

Bayley, R. W., 1970, Iron deposits of the Estes Creek area, Lawrence County, South Dakota, in Geological Survey research 1970: U.S. Geol. Survey Prof. Paper 700-B, p. B93-B101.

_____1972, Preliminary geologic map of the Nemo district, Black Hills, South Dakota: U.S. Geol. Survey Misc. Geol. Inv. Map I-712.

Hills, F. A., 1977, Uranium and thorium in the Middle Precambrian Estes Conglomerate, Nemo District, Lawrence County, South Dakota--A preliminary report: U.S. Geol. Survey Open-File Rept. 77-55, 27 p.

Stacey, J. S., and Kramers, J. D., 1975, Approximation of terrestrial lead isotope evolution by a two-stage model: Earth and Planetary Sci. Letters, v. 26, no. 2, p. 207-221.

THE ROLE OF BOREHOLE ELECTRICAL MEASUREMENTS IN URANIUM EXPLORATION

By Jeffrey Daniels and James Scott
U.S. Geological Survey, Denver, Colo.

The only borehole electrical resistivity-related measurement that is commonly used in uranium exploration is the single-point resistance log. This measurement is used exclusively for stratigraphic correlation and, as such, is a valuable and inexpensive exploration tool. However, single-point measurements do not provide quantitative information concerning the physical or lithologic properties of the rocks.

Resistivity and induced polarization (IP) logs are also useful for stratigraphic correlation, and in addition they can provide information concerning the physical characteristics of rocks. Quantitative characterization of lithologic conditions by use of these logs can be a useful indicator of favorable environments for uranium occurrence.

Figure 1 shows the single-point resistance and resistivity logs in an ore zone and outside of the ore zone for a uranium deposit in the Powder River Basin. The ore deposition is characterized by a high calcite cement content at the bottom of the ore sand, a depletion of calcite cement in the middle of the ore sand, and an increase in calcite cement at the top of the ore sand (off top of fig. 1). This is clearly illustrated by the resistivity logs in figure 1. However, the single-point resistance logs do not clearly show the difference (in spite of the fact that the recording sensitivity is much higher for the resistance logs). Although calcite cement near the bottom of the ore zone is indicated on the single-point resistance log, the log also shows spikes such as the one at a depth of 53 meters that are caused by variations in borehole diameter rather than lithology.

The primary advantage of using quantitative resistivity and IP logs, is the ability to use them for detecting anomalous concentrations of non-radioactive minerals associated with uranium mineralization. Figure 2 shows the correlation that was found between resistivity values and clay content in the ore sand of a south Texas uranium deposit. This figure indicates that, for this deposit, the total clay content of the sand can be estimated directly from the resistivity logs. This can be important in areas where the clay content varies in different parts of the roll front.

IP measurements respond to the presence of certain clay minerals (particularly montmorillonite) and sulfides such as pyrite. Since the amounts of montmorillonite and pyrite vary across a uranium geochemical front, IP measurements can be

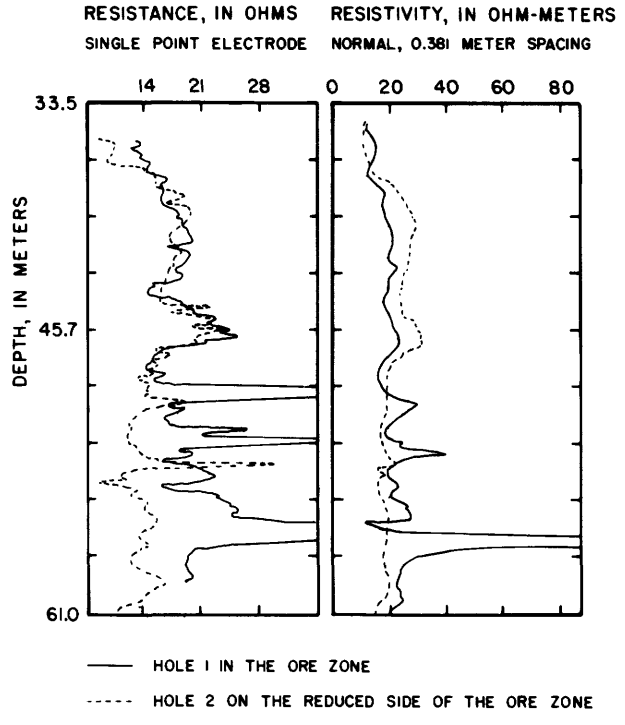

Figure 1.--Comparison of single-point resistance and resistivity logs in the ore zone (hole 1) and outside of the ore zone (hole 2).

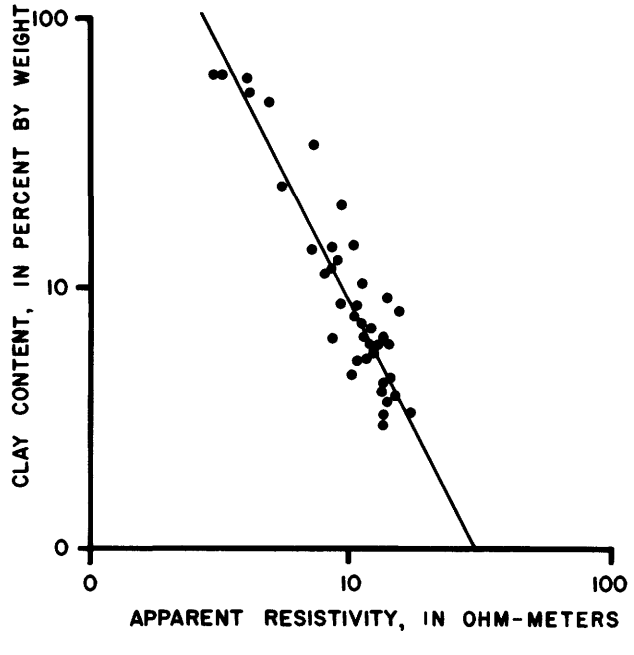

Figure 2.--Correlation between resistivity and total clay content for samples taken from the ore sand across a south Texas uranium deposit.

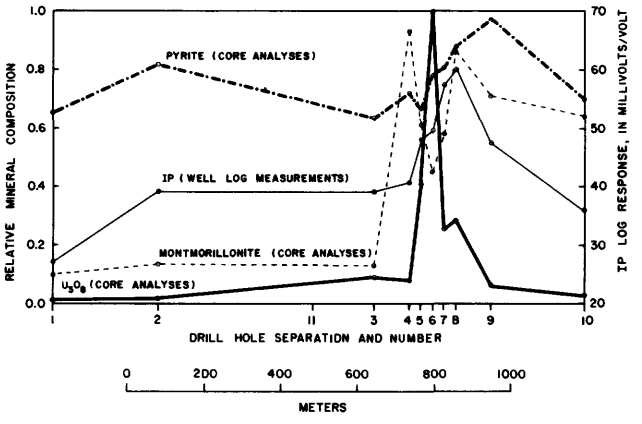

Figure 3.--Relationship between induced polarization log pyrite content, and montmorillonite content across a uranium deposit in south Texas.

used to locate the relative position of the uranium deposit with respect to a group of drill holes. Figure 3 shows the variation in pyrite, montmorillonite and IP response across a uranium deposit in south Texas. An increase in the montmorillonite and pyrite content correlates with an increase in the induced polarization response on the well logs.

Hole-to-hole measurements can make use of the quantitative response of well logging tools and can be used to minimize the number of drill holes necessary to locate on orebody. The electrical current source is placed in one drill hole and the electrical potential difference is placed in a hole at a large distance from the source hole. Potential difference measurements are made between bipole and electrodes, at discrete positions in the receiver hole. These resistivity and IP measurements give an indication of lithologic variations that exist between the boreholes.

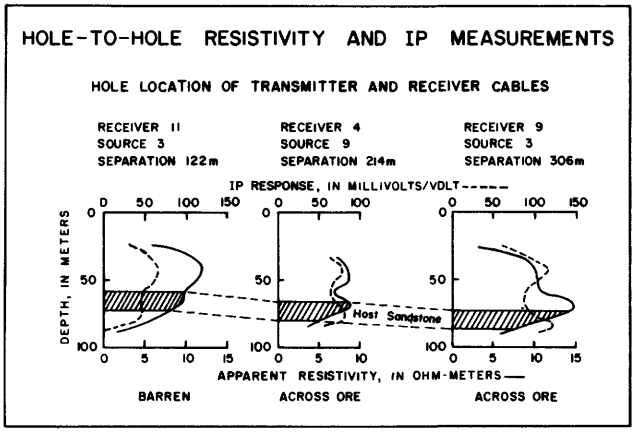

Figure 4.--Resistivity and induced polarization measurements across a uranium roll-type deposit in south Texas.

Interpretation of these measurements can eliminate unnecessary drilling and speed up the evaluation of marginal properties.

Examples of hole-to-hole measurements across two roll-type uranium deposits are illustrated in figures 4 and 5. The measurements shown in figure 4 are from the same property in south Texas as the data shown in figure 3. The hole-to-hole measurements across the ore zone show an IP anomaly that is believed to be caused by an increase in pyrite and montmorillonite near the center of the deposit. The resistivity data are not significantly anomalous across the ore zone.

The hole-to-hole data for the Powder River Basin property (fig. 5) reflect a different lithologic setting. The resistivity shows an anomalous high value across the center that is caused by an increase in calcite cement at the oxidized-reduced geochemical interface of the roll front. The IP high on the reduced side of the roll front is probably caused by relatively higher sulfide and (or) montmorillonite content on the reduced side of the ore zone.

The preceding examples show how the use of quantitative types of well logging information can lead to a better understanding of the uranium environment and can ultimately yield savings of both time and money. It should be cautioned that as geologic characteristics change for each geographic area, borehole responses will also change from area to area.

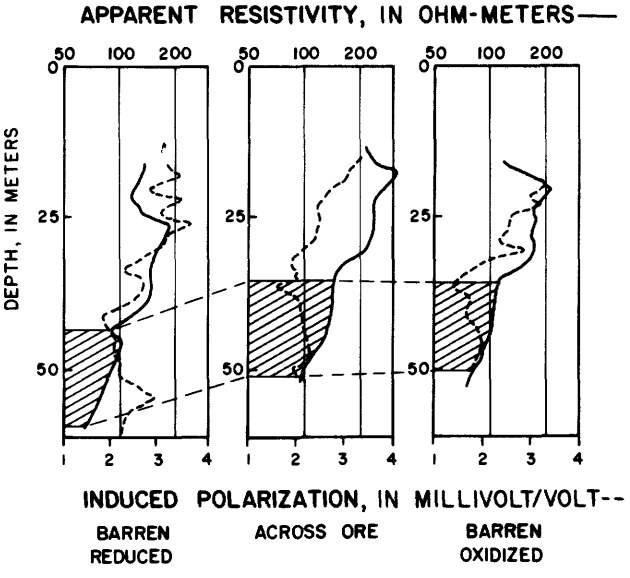

Figure 5.--Resistivity and induced polarization measurements across a uranium roll-type deposit in the Powder River Basin, Wyoming.

HOW TO PLAN AN AERIAL GAMMA-RAY SURVEY

By J. A. Pitkin and J. S. Duval
U.S. Geological Survey, Denver, Colo.

A number of parameters require consideration when an aerial gamma-ray survey is being planned. Some of the parameters to be considered are: the type of data to be obtained (gross-count or spectrometric), the ground interval between flight lines, the nominal survey flight altitude, and the detector volume to be used. Other factors not here discussed include instrumentation to be used, advance planning for flight operations, and scheme for data reduction.

The initial decision is whether the survey obtains gross-count or spectrometric data. The amount of money available is one consideration, as spectrometric surveys are more expensive than gross-count surveys by a factor of 3 or more. The goal of the survey is another factor to be considered. Gross count data provide aid for geologic mapping, but are less suitable for mineral exploration. Spectrometric data separate the contributions of the components--K, U, and Th--of the gross-count data, thereby providing more information and reducing the amount of ground follow-up required.

Target dimensions can be used to specify the desired flight line spacing and survey altitude, but other factors of a practical nature must also be considered. Coarse (>3 km) line spacing can suffice for detection of broad, regional anomalies. Fine (<3 km) line spacing is needed to detect localized anomalies or to provide aid for detailed geologic mapping. Low topographic relief in sedimentary basins may permit decreasing the flight altitude while greater topographic relief in crystalline areas may necessitate increasing the flight altitude. However, target detectability or ground resolution decreases as the altitude increases, and the percentage of a survey area covered

decreases with decreasing altitude. Furthermore, gamma-rays are absorbed in air exponentially as the air column increases in thickness, which means that the observed count rate decreases and statistical error increases as the flight altitude increases.

The parameters controlling aerial gamma-ray surveying interact in a complex manner. A graph and a table are included to enable easier understanding of this interaction and to provide means by which surveys can be designed. Figure 1 shows the expected corrected count rate per liter of detector as a function of altitude above ground for specific radioelement concentrations and can be used to estimate corrected count rates provided by a given crystal volume. For example, at an altitude of 122 m and with a volume of 13.6 liters, the count rates are 24.1 cps (counts per second) for 1 percent K, 4.4 cps for 1 ppm eU_1, 11.9 cps for 1 ppm eU_2, and 1.4 cps for 1 ppm eTh. eU_1 uses only the 1.76-MeV photopeak, while eU_2 is a sum of the 1.12- and 1.76-MeV photopeaks. The e for equivalent prefix is used because of the potential for disequilibrium in the U and Th decay series.

Table 1 complements figure 1 by showing how count rate error increases as detector volume decreases. Note the large error in U count rate caused by using only the 1.76-MeV photopeak. Both the figure and the table, while based upon different concentrations, were compiled with data that were normalized to 122 m and had corrections applied for Compton scattering, airborne bismuth-214, cosmic radiation and aircraft background radiation. Other graphs (not included) illustrate the percentage of area covered by an aerial survey for several flight altitudes as a function of flight-line spacing, the estimated ground resolution as a function of detector altitude, and the expected gross count rate per liter of detector as a function of altitude for two rock types.

All of these graphs and tables, together with a knowledge of the survey objectives, the type of terrain to be surveyed, and the available funds can be used to objectively select the survey parameters.

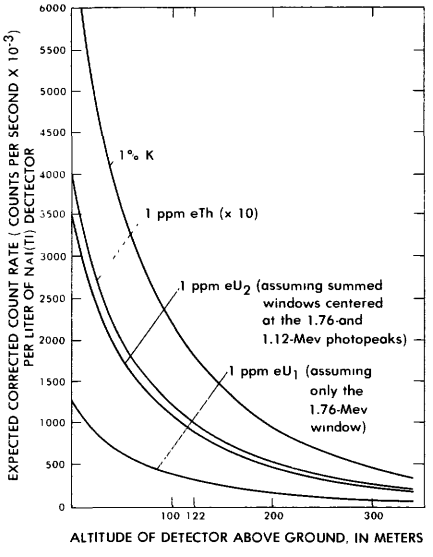

Figure 1

Table 1.--Corrected count rates for K, $^1U_1$, $^2U_2$, and Th showing estimated errors for three detector volumes

[Constant ground concentrations are 1.1 percent K, 1.7 ppm eU, and 4.5 ppm eTh. All data normalized to 122 m flight altitude]

Detector volume, in liters	K, cps	K error, percent	$^1U_1$, cps	U_1 error, percent	$^2U_2$, cps	U_2 error, percent	Th, cps	Th error, percent
54.5	106 ±20.2	±19	28±14.6	±52.2	84 ±21.6	±25.7	25 ±7.8	±31.2
27.3	53.1±13.4	±25.2	14±10.6	±75.7	42.3±17.8	±42	12.5±5.4	±43.2
13.6	26.5± 9.1	±34.3	7± 8.1	±115.7	21.2±12.8	±60.4	6.2±3.7	±59.7

[1]assuming only the 1.76-MeV windows.

[2]assuming summed windows centered at the 1.12- and 1.76-MeV photopeaks.

COMPOSITE IMAGES OF RADIOMETRIC DATA FROM SOUTH TEXAS AND WYOMING

By J. S. Duval, J. A. Pitkin, and D. L. Macke
U.S. Geological Survey, Denver, Colo.

Aerial radiometric measurements of the apparent surface concentrations of potassium (K), uranium (eU), and thorium (eTh) are usually presented as stacked flight-line profiles or, where line spacing permits, as contour maps. In either presentation, an interpreter must examine the profiles or maps individually and must then synthesize the data to produce a map related to geology or potential uranium mineralization. Even with the aid of a computer and the use of statistical techniques, such a synthesis is a difficult and subjective task.

A technique developed by the U.S. Geological Survey can be used to produce a single composite representation which synthesizes three components of the data (either K, eU, and eTh, or eU/eTh, eU/K, and eTh/K). The contour maps, in the form of equally spaced grid points, are converted to gray-tone images in which each grid point becomes a picture element (pixel) and the density of the gray tones is proportional to the magnitude of the count rates. Each of the three components is assigned one of the primary colors (magenta, cyan, or yellow) and a transparent color copy of each component is made using the Diazo process. Overlaying the resulting color images produces a composite, false-color image that is a visual synthesis of the three components.

Composite color images have been produced using data from aerial surveys flown in an area around Freer, Tex. and in Converse County, Wyo. Figure 1A shows radiometric units determined from the composite image of the radioelements K, eU, and eTh using the data from an aerial gamma-ray survey near Freer, Texas (Schulz, 1975a); the figure also shows the geology and faults of the area (adapted from the Crystal City and Laredo Atlas Sheets of the Texas Bureau of Economic Geology, Austin, Tex.), and locations of known uranium mineralization. Each radiometric unit appears on the composite image as a relatively uniform, distinctive color or combination of colors. The radiometric units show good agreement with the mapped geology: units A and B correlate with the Oakville Sandstone, unit E with the Goliad Sand, units C and D with the Catahoula Tuff, units G and J with the Frio Clay, and units H and I with the Jackson Group. Unit M may correspond to some of the terrace deposits along the Nueces River, although the bulk of the mapped alluvium has the same radiometric character as does much of the Catahoula Tuff. The remaining radiometric units, F, K, L, N, and O, show up as subtle color variations, the specific colors being determined by the lithologic unit within which the areas lie. Of these five units, F and N show correlations with areas of known uranium mineralization. One hypothesis that might explain some of these subtle color variations is that they reflect differences in the geochemical character of the ground due to the presence of gases eminating from buried petroleum deposits. If this hypothesis is true, these areas can be interpreted as locations with a favorable environment for uranium deposition, because the petrolic gases act as reductants that precipitate uranium from the ground waters.

Figure 1B shows radiometric units determined from the composite image of the radioelements K, eU, and eTh using the data from an aerial gamma-ray survey in Converse County, Wyo. (Schulz, 1975b); in addition, the figure shows geology (adapted from Sharp and Gibbons, 1964), and locations of uranium mines. Each radiometric unit corresponds to a relatively uniform, distinctive color or combination of colors. The radiometric units show poor agreement with the mapped geology. Unit E correlates with eolian sand that is easily identified on standard aerial photographs. Unit F correlates with the water course of the Dry Fork of the Cheyenne River. Our tentative interpretation of the remaining radiometric units is that units A, B, C, D, and K represent distinctive lithologies or soils, and that units G, H, I, J, and L represent alteration zones, although much of unit I reflects the presence of open-pit mines. We suggest that locations where units I and J occur are likely targets for uranium exploration.

Schulz, K. A., 1975a, Airborne gamma-ray spectrometry and aeromagnetic survey of the Freer area in Duval, Live Oak, McMullen, and Webb Counties, Texas: U.S. Geol. Survey Open-File Rept. 75-294, 5 p.

_____1975b, Airborne gamma-ray spectrometry and aeromagnetic survey of part of the southern Powder River Basin in Converse County, Wyoming: U.S. Geol. Survey Open-File Rept. 75-661, 6 p.

Sharp, W. N., and Gibbons, A. B., 1964, Geology and uranium deposits of the southern part of the Powder River Basin, Wyoming: U.S. Geol. Survey Bull. 1147-D, 60 p.

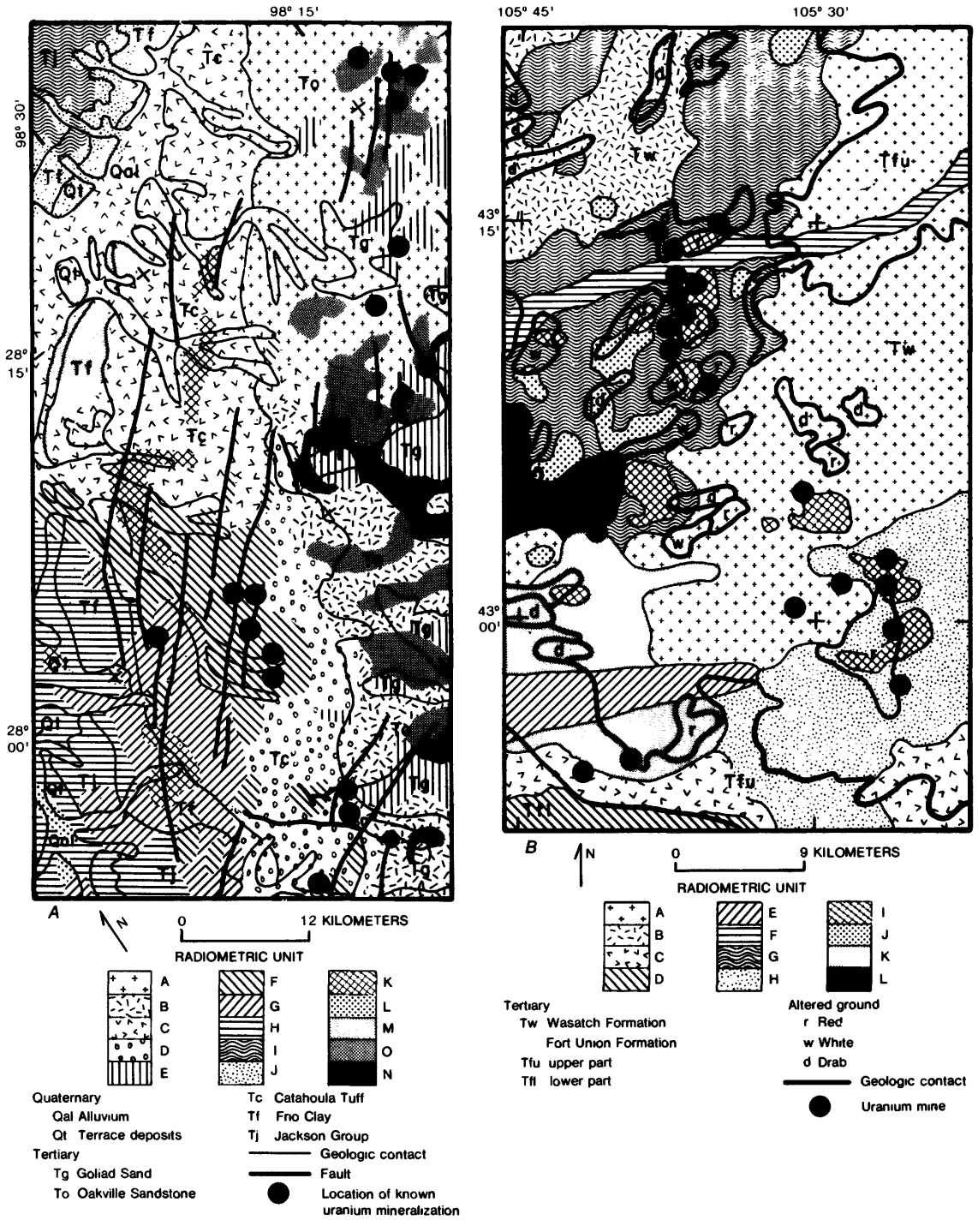

Figure 1.--Map of radiometric units determined from composite image of radioelements K, eU, and eTh for aerial gamma-ray surveys near (A) Freer, Tex., and (B) Converse County, Wyo. The geology and faults of A were adapted from the Crystal City and Laredo Atlas Sheets of the Texas Bureau of Economic Geology, Austin, Tex. The geology of B was adapted from Sharp and Gibbons (1964).

TWO-MICA GRANITE AND URANIUM POTENTIAL IN THE NORTHERN APPALACHIAN OROGEN OF NEW ENGLAND

By Eugene L. Boudette, U.S. Geological Survey, Reston, Va.

Northern Appalachian rocks make up a dissected northeastward-plunging orogenic system. Roots of the orogen are manifested by rocks of the infrastructure in southern New England. The present erosion surface intersects rocks of progressively higher crustal levels northeastward, reaching the suprastructure in Maine. Rocks of the orogen are buttressed to the west by the Precambrian rocks of the Grenville Series of the Adirondacks and contain discrete Precambrian terrains interspersed with predominantly Paleozoic rocks. The rocks may be subdivided into eugeosynclinal and miogeosynclinal successions and ascribed to major tectono-stratigraphic zones for purposes of long-range correlation.

At least two zone boundaries in the orogen can be interpreted to coincide with plate or intraplate sutures. An Early Ordovician orogenic culmination is documented by a Middle Ordovician unconformity. Orogenic events (older than Early Silurian) are traditionally ascribed to the Taconian. Events assigned to the Taconian vary in time from place to place, and a trampoline model can, in fact, be invoked in which the orogen was restless between (at least) the Early Cambrian and Carboniferous in both longitudinal and lateral anisotropic disharmonic motion.

The end of the Taconian is interpreted to be signalled by the closing of an island arc against the continental Appalachians in Late Ordovician to Early Silurian time. The sedimentologic and plutonic geochronologic record indicates that initial interplate collision probably occurred in Early to Middle Silurian time and was completed probably after the Late Mississippian, a period which spans at least 80 m.y. and includes the entire Acadian orogeny.

Plate collisions caused the deformation in the Appalachian orogen. It was during an orogenic culmination that two-mica granite (Gauthier, 1973, 1974) was generated, probably by extraction from rocks called here informally migmatite which is exposed near the town of Massabesic in southeastern New Hampshire and in eastern Massachusetts. This migmatite was produced from the partial melting, during metamorphism, of eugeosynclinal detrital or volcanic rocks found west of the interplate suture. These rocks are part of the segment welded onto the ancestral Appalachians after the Taconian.

Eugeosynclinal deposition probably continued until emplacement of the synkinematic plutons during the Acadian. Plutonism probably coincided with emplacement of a hot mantle slice beneath the geosynclinal assemblage. This slice also provided the heat for the Acadian metamorphism. This mantle material reacted, in part, with crustal host rock, was mobilized into sheets (Nielson and others, 1976), and crystallized into a gabbro-quartz monzonite intrusive suite of Early Devonian age.

Subsequent to the emplacement of the gabbro-quartz monzonite suite, westwardly transported allochthons were stacked on site on thrust faults in the suprastructure. At the same time, two-mica granite was extracted from the migmatite by anatexis. The mobilized two-mica granite moved westward in sheets in association with the allochthons, possibly, in part, coring nappes. The two-mica granite composes a second intrusive suite and was assigned to the Devonian Concord Granite (Billings, 1956).

The Concord Granite crops out in three belts in New Hampshire, presumably in the infrastructure. The belts apparently coincide with antiformal flexures in allochthons which expose partial to complete sections of two-mica granite at least 1 km thick. The easternmost (Milford) belt closely parallels and appears to grade into the migmatite to the east wherein it is interpreted to be rooted. The Central (Swenson) belt probably represents outliers of the same sheet (or sheets) making up the Milford belt. Granite in the Milford and Swenson belts is an excellent quarrystone. In these belts it is more massive than the foliated granite in the western Lake Sunapee belt.

The two-mica granite contains uranium minerals exposed in two parallel roadcuts along Interstate Route 89 (I-89) in New London, N. H., and the Lake Sunapee belt, reported first by William Bateman (oral commun., 1968) during the cutting of the highway grade. The mineralized pluton is everywhere strongly jointed and is intensely sheared at a few places. The pluton has a moderate systematic foliation probably formed partly by flowage and partly by inherited relic foliation in screens dragged parallel to flowage. The foliation geometry suggests that the pluton is a subhorizontal sheet that has been antiformally arched along a north-south axis. This sheet probably was more than a kilometer thick in its central zone. Preliminary ground-gamma radiometry by W. A. Bothner (oral commun., 1976) shows that the mineralized zone in the I-89 roadcuts can probably be traced both northwest and southeast to the borders of the pluton. The proposed trend of the Boston-Ottawa geophysical lineament, a regional topographic photolinear, and the mineralized zone are all parallel.

Oxidized uranium minerals in a zone more than 4 m thick are exposed in the I-89 cut. This occurrence of secondary uranyl-phosphate minerals resembles that of the Daybreak

mine near Spokane, Wash. Uranium minerals in the Lake Sunapee deposit occur mainly in fractures, local fault gouge, and biotitic schlieren. The granite is somewhat more fractured than correlative rock north and south on regional strike, but not conspicuously so. In the nearly 10 years since the mineralization was exposed by roadcuts and the water table was lowered, more than 90 percent of the yellow uranium minerals have been leached away by vadose ground water. The top of the original water table is believed to have fluctuated within the mineralized zone. It is possible that the uranium minerals have reprecipitated at the lowered (reestablished) water table.

Two-mica granite is recognized for its metallogenic specialization in tin, tungsten, beryllium, lithium, fluorine, and uranium. Uranium production in France and in the Iberian peninsula is from Variscan or Hercynian-age two-mica granites. Concord Granite can be compared with the uranium-producing granites of the Massif Central of France and fits the evolving international model for two-mica granites based upon an apparent anatectic origin, emplacement during an orthotectonic event, and probable requisite preconcentration of uranium in its parent rock, thought to be the migmatite.

Anomalous radioactivity is associated with the migmatite. The radioactivity pattern may partly be related to sulfide- magnetite-quartz-uraninite(?) veins and pegmatites which apparently also contain uranium oxides. The oxidized uranium deposit at Lake Sunapee obviously involves a secondary concentration of uranium. It is presently unknown if the oxidized uranium minerals were derived from orthomagmatic veins as in Massabesic area of New Hampshire and in Massachusetts and the Massif Central of France or younger hydrothermal veins as proposed by Page (in press) or a broadly disseminated source.

It is significant that carbonate-rich lamprophyre dikes are associated with the Concord Granite, especially as seen in the mineralized rock at Lake Sunapee. Carbonate lamprophyre emplacement in Variscan granites is concurrent with uraniferous vein emplacement and transformation of parts of the granite to episyenite, and the mobility of the uranium is related to carbonate complexing (Poty and others, 1974). Exploration on this basis should be focused on episyenite and lamprophyre zones, especially in the upper zones of the Concord sheets.

Application of the Variscan model to the Concord Granite requires that all three outcrop belts as well as the migmatite be considered potential ore terrane. Facies of the Concord Granite also intrude the migmatite in a situation interpreted to be auto-intrusion.

Gauthier, J.-C., 1973, Évolution granitique, dévelopment des granites à deux micas et géochimie des alcalins dans la Marche orientale (Massif Central Francais), L'evolution granitique: Sci. Terre, v. 18, no. 4, p. 317-352.

_____1974, Évolution granitique, dévelopment des granites à deux micas et geochimie des alcalins dans la Marche orientale (Massif Central Francais), Geochimie des alcalins rares: Sci. Terre, v. 19, no. 2, p. 119-151.

Nielson, D. L., Clark, R. G., Lyons, J. B., Englund, E. J., and Borns, D. J., 1976, Gravity models and mode of emplacement of the New Hampshire plutonic series, in Lyons, P. C., and Brownlow, A. H., eds., Studies in New England geology: Geol. Soc. America Mem. 146, p. 301-318.

Page, L. R., (in press), Guides to prospecting for uranium and thorium in New Hampshire and adjacent areas: New Hampshire Dept. Resources and Econ. Devel. Bull.

Poty, B. P., Leroy, Jacques, and Cuney, Michel, 1974, Les inclusions fluids dans les minerais des gisements d'uranium intragranitiques du Limousin et du Forez (Massif Central, France), in Formation of uranium ore deposits: Internat. Atomic Energy Agency Proc. Ser. No. STI/PUB/374, p. 569-582 [includes English summ.].

GROUND-WATER FLOW AND THE SHAPE OF URANIUM ROLL DEPOSITS

By C. Gerald Warren, U.S. Geological Survey, Denver, Colo.

In this study the characteristics of ground-water flow were related to the shape of the oxidation front of sandstone-type orebodies. An understanding of this relationship provides a tool for studying the ground-water flow during the time that a deposit was forming. Many ground-water flow patterns were evaluated to find the associated shape of the oxidation front. The type of ground-water flow that produced shapes similar to those found in actual deposits is postulated to represent the actual flow of ground water as the deposits formed.

The oxidized tongue associated with a roll-type uranium orebody was created by oxidants reacting with the pyrite and other ore components. The rate at which the oxidized tongue advanced was controlled by the rate at which the oxidants were delivered to the oxidation front. Although all oxidants were delivered by ground water there were two separate and distinct processes involved: (1) oxidants were transported by the moving ground water, (2) oxidants were moved by diffusion from regions of high concentration to regions of low concentration.

These delivery processes were described by a differential equation and solved by computer analysis. The results were displayed on microfilm in a graphical form resembling the shape of a roll front of an actual orebody. A movie showing the development of an oxidation front and uranium orebody was obtained by recording successive computer-generated representations of the roll front.

In the movie, a bulge or roll develops in the oxidation front within the zone of maximum flow in the aquifer. Although parts of the orebody may lag behind in the less permeable zones of the aquifer, they are slowly destroyed by oxidants that are delivered by the diffusion process. In a simple homogeneous aquifer system the shape of the roll gradually achieves maturity and its dimensions are a function of the ratio between flow velocity and diffusion. For example, an average ground-water velocity of 2×10^{5} cm/s (6.3 m/yr) and an oxidant diffusion coefficient of 2×10^{5} cm^2/s will produce a C-shaped oxidation front with a profile about twice as wide as the height of the aquifer.

ECONOMIC IMPLICATIONS OF A NEW HYPOTHESIS OF ORIGIN OF URANIUM- AND COPPER-BEARING BRECCIA PIPES, GRAND CANYON, ARIZONA

By C. G. Bowles, U.S. Geological Survey, Denver, Colo.

Uranium and copper ores have been mined in the Grand Canyon from breccia pipes developed within Mississippian to Permian formations, including the Redwall Limestone (Mississippian), Supai Group (Pennsylvanian and Lower Permian), and Hermit Shale (Lower Permian); weak mineralization occurs as well in the upper part of pipes within the Lower Permian Coconino Sandstone, Toroweap Formation, and Kaibab Limestone. Some breccia pipes formed during Mesozoic time, but collapse may have begun as early as Late Permian time. Other pipes apparently were formed during erosion of the Grand Canyon and may be no older than middle to late Cenozoic. Recurrent collapse has also occurred in the older breccia pipes.

The breccia pipes in the Grand Canyon are generally believed to be either cryptovolcanic structures or collapse structures formed by solution of limestone by hydrothermal waters. Copper and uranium deposits in these structures are attributed to hydrothermal mineralizing solutions. This view is derived from studies of the Orphan mine by Gabelman and Boyer (1958); Kerr (1958); Kofford (1969); Gornitz and Kerr (1970). Isotopic studies by Miller and Kulp (1963) and Adler (1963), and fluid-inclusion geothermometry by Gornitz (1969) suggest that the temperature during mineralization of the Orphan pipe may have been less than 100°C.

The following hypothesis proposes that formation of the breccia pipes and primary mineralization resulted from low-temperature hypogene solutions that consisted either dominantly or entirely of artesian ground water. However, secondary enrichment by either supergene or mesogene (mingled descending and ascending) solutions concentrated the metals in medium- to high-grade orebodies. This hypothesis rejects a cryptovolcanic origin for the structures. Emphasis is placed upon the hydrologic system believed to dominate the development and mineralization of most breccia pipes. Canyon cycles of erosion strongly influenced or controlled secondary enrichment.

The typical mineralized pipe developed in four stages: (1) initial solution and collapse in the Redwall Limestone; (2) stoping into the overlying Supai Group and alteration by bleaching and carbonate cementation; (3) continued stoping and primary mineralization, consisting predominantly of pyrite, chalcocite, and uraninite; and (4) secondary enrichment.

Limestone solution and collapse within the Redwall Limestone began during the Mesozoic when northeastward tilting of the Colorado Plateau and the bevelling of Paleozoic strata southwest of the area now occupied by the Mogollon Rim permitted ground water to recharge the Redwall. Artesian pressure initiated an upward flow of ground water along fractures in the limestone. The ground water, containing dissolved carbon dioxide and saturated with calcium and magnesium bicarbonate is postulated to have

migrated upwards from the dolomitic Whitmore Wash and Thunder Springs Members of the Redwall Limestone. Upon entering the calcitic Mooney Falls Member the water is believed to have mixed with other ground water that was saturated with calcium bicarbonate but which contained a smaller concentration of dissolved carbon dioxide. The mixing of waters having differing concentrations of dissolved solids and gases caused disequilibrium and undersaturation with respect to calcium carbonate (Bögli, 1964) and dissolution within the Mooney Falls Member. The water continued upwards into the overlying Horseshoe Mesa Member, which previously had been made highly transmissive during development of the pre-Pennsylvanian karst surface. Limestone solution in the upper Redwall formed chimneys filled with collapse breccia.

During stage 2 dissolution of the Redwall Limestone continued, and upward stoping extended the collapse structure into the Supai. Accompanying alteration consisted of bleaching and carbonate cementation of the breccia and adjacent red beds. Collapse stoping in the Supai eventually intersected aquifers that had lower artesian pressures than were present in either the Redwall or the pipe, and aquifers in the Supai were thus recharged by the artesian water.

Ground water from the Redwall Limestone contained reductants, probably dissoved hydrogen sulfide (H_2S), bisulfide (HS^1) and and sulfide (S^2) ions, as well as organic carbon released from the dissolved limestone. Dissolved carbon dioxide and hydrogen sulfide were released from solution as the pressure of the water ascending in the pipe structure decreased. Release of dissolved carbon dioxide caused both the precipitation of calcite cement and an increase in the sulfide and bisulfide ion activity. Reducing solutions moved through the brecciated red beds and into the sandstone aquifers; iron was reduced and pyrite was precipitated. Where the reductants were not as abundant, oxidation of the dissolved sulfides formed an acidic solution that attacked and removed hematite, thus bleaching the breccia and the enclosing sandstone host rocks. Beyond the limits of bleaching a purplish-red halo of iron and manganese oxides formed around some bleached zones.

Primary mineralization of the pipe marked the beginning of stage 3. As more aquifers in the Supai were penetrated by stoping and recharged by artesian flow, the pressure within the pipe decreased. Ground water carrying high-valence copper and uranium ions then entered the pipe from the lower sandstone aquifers of the Supai. Mixing of the ground water in the pipe with ground water from aquifers in the Supai caused iron, copper, and uranium ions to be reduced, and pyrite, chalcocite, and uraninite were precipitated in the pipe above the point of recharge by aquifers in the Supai. Iron was available in relatively large amounts in the ground water, and pyrite was readily precipitated.

The commencement of Grand Canyon erosion initiated stage 4, in which secondary enrichment of uranium and copper in a supergene or mesogene environment was accompanied by renewed collapse in the breccia pipe. Beginning in Miocene time oxygenated vadose and ground water leached uranium and sulfide deposits within the breccia pipe, decemented breccia fragments, pipe-fill sediments, and adjacent sandstone host rocks, and dissolved limestone in adjacent beds. This decementation caused renewed collapse, slump, and redistribution of detrital material in the pipe. Within the zone of oxidation minerals were formed from high-valence copper and uranium, but farther below the water table secondary chalcocite and uraninite were precipitated in a reducing environment. The reductants may have been the primary sulfide minerals or the sulfide ions in artesian water that flowed from the breccia pipe into aquifers in the Supai and eventually discharged as springs into the Colorado River drainage.

The secondary enrichment process appears to be related mainly to the development of an extensive erosion surface known as the Esplanade. This surface formed in the Grand Canyon during middle to late Miocene or early Pliocene time. All known uranium and copper orebodies occur below the level of this ancient valley surface or below less extensive surfaces that formed in the eastern Grand Canyon during the same period of time.

Damming of the Colorado River by lava flows in the western part of the canyon during late Pliocene(?) and middle Pleistocene time may have contributed to supergene development of ores by reestablishing water tables at and below the Esplanade surface. Possibly the volcanic activity released hydrogen sulfide to the ground water to provide favorable conditions for ore deposition and enrichment. The economic significance, however, is speculative pending further studies.

The above hypothesis for the origin of uranium and copper-bearing breccia pipes in the Grand Canyon suggests that the best ore potential is limited to large breccia pipes that stoped through the upper part of the Supai Group into overlying formations. In these pipes primary mineralization during stage 3, followed by enrichment during stage 4, was most likely to form an ore deposit below the Esplanade surface. A greater enrichment and a more restricted vertical distribution of ore should be expected in pipes in areas where the Esplanade surface is especially well developed. Secondary enrichment probably decreases laterally away from the Colorado River. Copper and uranium deposits are more likely to be preserved in pipes downdip from the canyon where there has been little recharge of the Paleozoic aquifers since Miocene time.

Adler, H. H., 1963, Concepts of genesis of sandstone-type uranium ore deposits: Econ. Geology, v. 58, no. 6, p. 839-852.

Bögli, A., 1964, Corrosion par melange des eaux: Internat. Jour. Speleology, v. 1, pt. 1-2, p. 61-70.

Gabelman, J. W., and Boyer, W. H., 1958, Relation of uranium deposits to feeder structures, associated alteration and mineral zones, in Volume 2, Survey of raw material resources: Second United Nations Internat. Conf. on Peaceful Uses of Atomic Energy, Geneva 1958, Proc., p. 338-350.

Gornitz, V. M., 1969, Mineralization, alteration, and mechanism of emplacement, Orphan ore deposit, Grand Canyon, Arizona: Columbia Univ. Ph.D. thesis.

Gornitz, V. M., and Kerr, P. F., 1970, Uranium mineralization and alteration, Orphan mine, Grand Canyon, Arizona: Econ. Geology, v. 65, no. 7, p. 751-768.

Hamblin, W. K., 1969, Late Cenozoic lava flows in the Grand Canyon of the Colorado River, Arizona, in Geology and natural history of the Grand Canyon region: Four Corners Geol. Soc. Field Conf., 5th, Powell Centennial River Expedition, [Durango, Colo.] 1969, p. 41-60.

Kerr, P. F., 1958, Criteria of hydrothermal emplacement in [Colorado] Plateau uranium strata: Internat. Conf. on Peaceful uses of Atomic Energy, 2d, Geneva 1958, Proc., v. 2, p. 330-334.

Kofford, M. E., 1969, The Orphan mine, in Geology and natural history of the Grand Canyon region: Four Corners Geol. Soc. Field Conf., 5th, Powell Centennial River Expidition, [Durango, Colo.] 1969, p. 190-194.

Miller, D. S., and Kulp, J. L., 1963, Isotopic evidence on the origin of the Colorado Plateau uranium ores: Geol. Soc. America Bull., v. 74, no. 5, p. 609-629.

COMPUTER-ENHANCED IMAGES AND GEOLOGIC STUDIES, SOUTHERN POWDER RIVER BASIN, WYOMING

By T. W. Offield, G. L. Raines, and D. L. Sawatzky
U.S. Geological Survey, Denver, Colo.

Different surface geologic materials of interest in uranium exploration show varying reflectance characteristics and vegetation assemblages in computer-enhanced Landsat images of the southern Powder River Basin. Well-drained (sandy, coarse-grained) and poorly drained (clayey, fine-grained) soils are distinguished by conspicuous vegetation differences; a major vegetation change marks the line drawn by some mappers for the somewhat disputed contact of the Fort Union (Paleocene) and Wasatch (Eocene) Formations. Within the area underlain by generally coarse-grained sandstones of the Wasatch, numerous areas have vegetation like that of the Fort Union, suggesting the presence of inliers of the Fort Union or finer grained facies in the Wasatch. An intermediate vegetation and soil combination near the town of Bill, shown by subtle spectral contrast in a color-enhanced image of a single ratio of Landsat bands 5 and 6 (fig. 1), marks an area mapped by Sharp and Gibbons (1964) as a claystone-siltstone border facies of the Wasatch near the contact with the Fort Union.

Color enhancement of images produced from single ratios is achieved by compositing three color films each of which represents contrast stretches of three different segments of the image gray scale. This and other enhancements of the band 4 to band 5 ratio image, especially when combined with enhanced versions of other band-ratio images, permit reasonably good discrimination of exposed hematite-stained materials in altered ground associated with uranium roll-front mineralization (fig. 2). The described vegetation differences and red altered ground are not discernible in available high-altitude, color-infrared photographs. Field and laboratory measurements of spectral reflectance show that absorption bands characteristic of ferric iron are obvious in spectra of altered rocks and their overlying residual soils but are absent or minimal in spectra of unaltered materials. This is the basis of the detection of red altered ground using Landsat data. The field spectra show that bands not available on Landsat but available in aircraft scanners should permit better discrimination of hematite-stained, altered materials and possibly of calcite-cemented materials associated with uranium roll-fronts.

The Wasatch-Fort Union contact is conspicuous in nighttime thermal-infrared images available for a very short segment of the contact. A thermal boundary matches the contact shown on one of two geologic maps that depict the contact differently. Some of the thermal contrast relates to topographic changes with which the contact coincides in places, but where the contact departs from the topographic line so does the thermal boundary.

Enhanced Landsat images show many linear topographic elements 2 to 25 km long (fig. 3) and so regularly developed that they are inferred to represent geologic structure. Azimuth-frequency maxima occur at N. 75° E., N. 45° W., and N. 30° W. Northwest-trending lineaments are dominant on the east side of the basin and northeast-trending lineaments are dominant on the west side. The Box Creek-Monument Hill

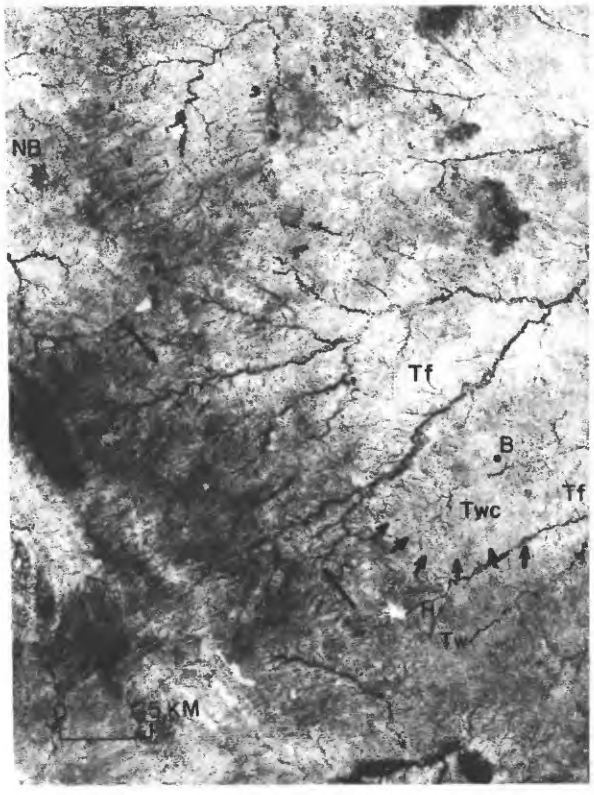

Figure 1.--Black-and-white copy of color-enhanced image of Landsat-band ratio 5/6. Tf, Fort Union Formation; Tw, Wasatch Formation; Twc, claystone facies of Wasatch (Sharp and Gibbons, 1964); small arrows mark approximate claystone-sandstone facies of Wasatch contact; long arrows mark major lineament. H, Highland mine; B, Bill; NB, North Pumpkin Butte. North approximately at top of image.

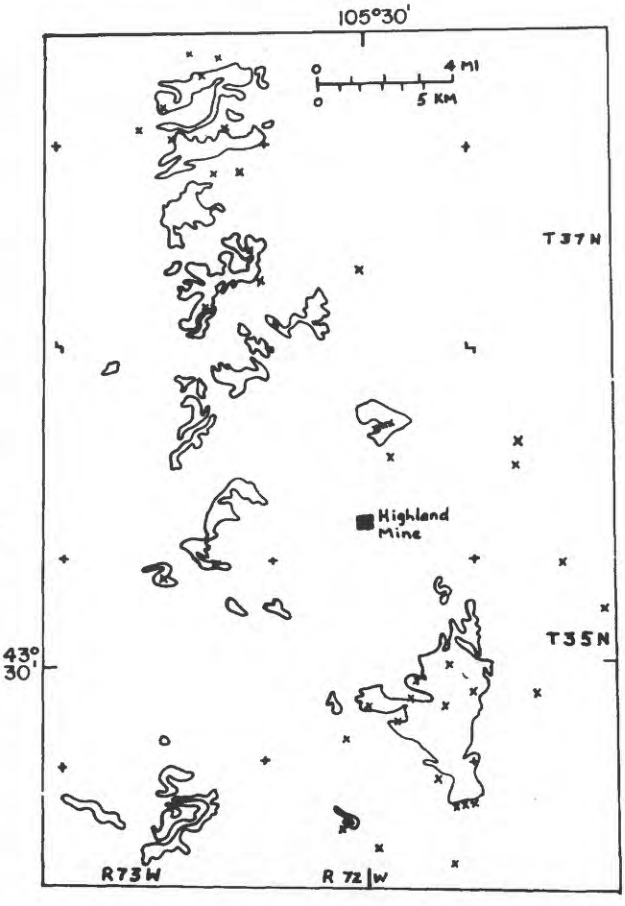

Figure 2.--Map outlining areas of red altered ground (from Sharp and Gibbons, 1964); x, distinctive iron discoloration seen in color-ratio composite image.

uranium area is located at the boundary of the two lineament domains. Lineaments in this uranium area match the northwest trend of subsurface folds and ore-sand, isopachs mapped at the Highland mine by Langen and Kidwell (1973). A color-enhanced image of a Landsat band 5 to band 6 ratio reveals a NNW-trending lineament marked by changes in vegetation and stream-course patterns (fig. 1). Alluviation in stream courses crossing the lineament suggests that downwarping has affected stream gradients. The line is

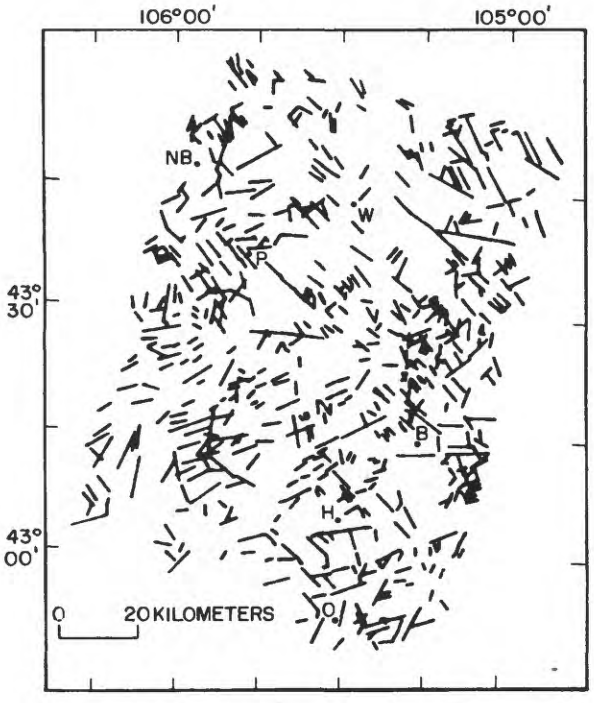

Figure 3.--Map showing lineaments defined in Landsat images. O, Orpha, H, Highland mine; B, Bill; P, Pine Tree; NB, North Pumpkin Butte.

suspected of marking a subtle, relatively young structural sag parallel to and west of a postulated positive fold axis (Sharp and Gibbons, 1964). Uranium occurrences are scattered in a narrow belt west of this newly defined lineament, but the line marks the west limit of economic mineralization discovered so far. Limited well-water chemical data (Hodson and others, 1973) indicate a change in dominant type of dissolved solids from calcium bicarbonate west of the lineament to sodium sulfate or sodium bicarbonate in the uranium district east of the lineament. The lineament directly overlies a major downwarp axis defined from subsurface data (E. S. Santos, written commun., 1976). We offer the hypothesis that a structural sag impeded the flow of uranium-bearing solutions and promoted major uranium deposition just east of the structure.

Hodson, W. G., Pearl, R. H., and Druse, S. A., 1973, Water resources of the Powder River Basin and adjacent areas, northeastern Wyoming: U.S. Geol. Survey Hydrol. Inv. Atlas HA-465.

Langen, R. E., and Kidwell, A. L., 1973, Geology and geochemistry of the Highland uranium deposit, Converse County, Wyoming: Wyoming Geol. Assoc. Earth Sci. Bull., v. 6, no. 4, p. 41-48.

Sharp, W. N., and Gibbons, A. B., 1964, Geology and uranium deposits of the southern part of the Powder River Basin, Wyoming: U.S. Geol. Survey Bull. 1147-D, 60 p.

CHARACTERIZATION OF FINE-GRAINED BLACK URANIUM ORES BY TRANSMISSION ELECTRON MICROSCOPY

By Gordon L. Nord, Jr., U.S. Geological Survey, Reston, Va.

Mineralogical and geochemical investigations of primary uranium minerals (uraninite and coffinite) and of the mechanisms by which these phases oxidize to the yellow uranyl minerals have been greatly hampered by the fine-grained nature of the primary crystalline phases and the black amorphous colloidal nature of the products of the early oxidation steps. The high resolution (~2 Å) of the transmission electron microscope (TEM) provides an opportunity to study these phases directly (electron petrography). In addition, TEM with scanning capability (STEM) can obtain electron diffraction data and X-ray energy spectra from crystallites as small as 100 Å.

This technique has been used to study black organic material containing fine-grained coffinite ($U(SiO_4)_{1-x}(OH)_{4x}$) from the La Sal no. 2 mine, Mesa County, Colo. (the type locality, Stieff and others, 1956). The coffinite-bearing material was made into a 20-μm-thick doubly polished thin section. Part of the thin section was further thinned to electron transparency (1 μm) by argon ion milling. Another part was used by H. T. Evans, U.S. Geological Survey, for determining the lattice constants of tetragonal coffinite (a = 6.938(1) Å, c = 6.291(2) Å) with a focusing Guinier powder camera) (fluorite standard). Figure 1a is a scanning electron micrograph of the thin-section surface showing the coffinite (light) as elongated grains (1-2 μm wide, 10-15 μm long) filling collapsed plant-cell cavities in a carbonaceous matrix (dark). At higher magnification in the transmission electron microscope (fig. 1b), these grains

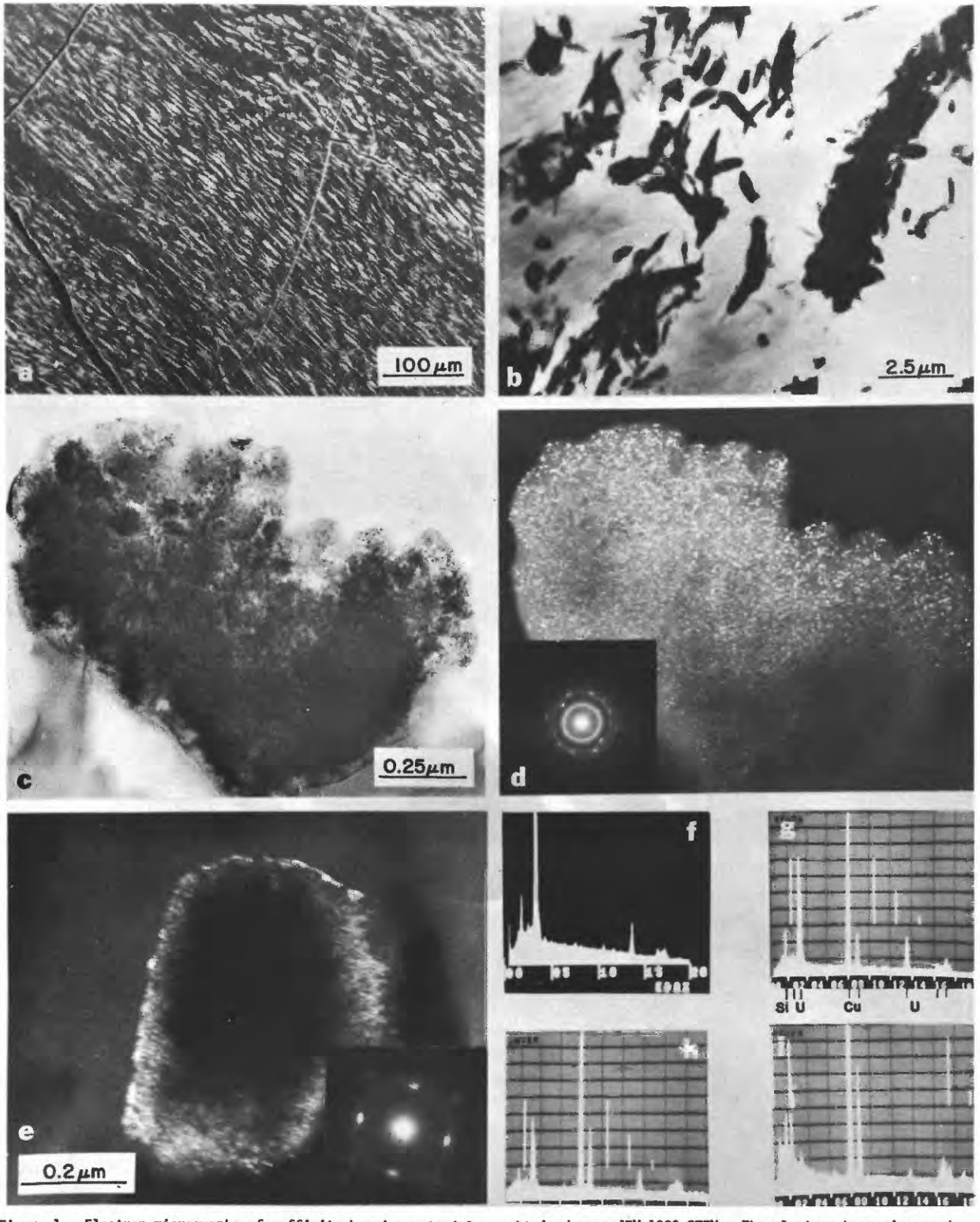

Figure 1.--Electron micrographs of coffinite-bearing material. a, SEM image; b, transmission electron micrograph; c and d, bright- and dark-field images, respectively, of same area; e, dark-field micrograph showing the (100) faces of another grain; f, typical spectra from the SEM (Si(K_α) and U(L and M) peaks. The spectra in g-i were obtained on a JEM 100C STEM. The electron beam size used for analysis is ~100 Å in diameter; therefore, a single crystal can be analyzed. g, from a coffinite single crystal; Cu peaks are from the sample holder. h, from an area high in uraninite; and i, from the carbonaceous matrix.

appeared as aggregates consisting of individual crystals ranging from 30 to 500 nm in size embedded in the more transparent carbonaceous matrix. The coffinite crystals were rounded, rather wheat-shaped, and elongated parallel to [001], and some had developed prism faces.

Figures 1c and 1d are bright-field and dark-field electron micrographs, respectively, of an irregularly shaped single crystal of coffinite. Covering the surfaces of the coffinite grains were 5- to 15-nm particles which produced diffraction rings in the selected area electron diffraction (SAED) pattern (fig. 1d, inset) overprinting the single-crystal diffraction spots of the coffinite grain. To obtain the dark-field micrograph in figure 1d, the electron beam was tilted, allowing only the first and most intense diffraction ring of the particles to contribute to the image; no single-crystal spots were allowed. The dark-field image therefore shows intensity only from the particles; the coffinite phase is dark. These particles were found covering all the coffinite grains observed, and were determined to be cubic and to have a unit cell edge of a = 5.46 Å (the cell edge was determined using both the coffinite and evaporated gold as a standard), which is consistent with an unoxidized uraninite.

The single-crystal patterns from coffinite are consistent with its tetragonal symmetry. Figure 1e shows a squarish grain with the c-axis parallel to the electron beam. The inset SAED pattern shows the intense 200 and 020 diffraction net in a square pattern. Note that the spots are broadened in an arc, which indicates the coffinite lattice is severely strained, perhaps becoming metamict.

Electron microprobe and qualitative X-ray energy-dispersive analyses in SEM (fig. 1f) and in a JEM 100C STEM (fig. 1g) all show the presence of only U and Si in the coffinite. In particular the elements Ca, Th, and Pb were found to be below detectability (∿0.1 weight percent) in the electron microprobe. Spectra taken in the part of the grain with the most abundant particle phase (uraninite) show a significantly smaller Si peak (fig. 1h). Figure 1i is a spectrum taken from the carbonaceous matrix; no crystalline material was nearby. Peaks indicating the presence of Na, S, and Si are strong; a U peak much smaller than the Si peak is also present. It should be reemphasized that no microcrystalline phase (>2-5 nm), such as quartz, was detected in the carbonaceous matrix. Nor was quartz detected with the coffinite by electron diffraction.

The small uraninite particles are interpreted as reaction products from the breakdown of coffinite; the silica exists as an amorphous phase associated with the coffinite and the matrix. Brodin and Sidorenko (1974) found similar particles of uraninite derived from coffinite which were more highly oxidized (a_0 = 5.37 Å) than the uraninite in this study (a_0 = 5.46 Å). They interpreted the uraninite as a reaction product formed during the transformation of coffinite to a metamict state. A thermal spike is probably the driving force for this reaction. Alternatively, the breakdown of coffinite to fine-grained uraninite plus silica may be a necessary step in the sequence by which coffinite oxidizes to the yellow uranyl minerals, reflecting the inability of the coffinite structure to accept the smaller hexavalent uranium atom and its charge-compensating defect.

Brodin, B. V., and Sidorenko, G. A., 1974, Radiogennye pseudomorfozy po koffinitu [Radiogenic pseudomorphs after coffinite]: Vses. Mineralog. Obshch Zapiski, v. 103, no. 4, p. 470-475.

Stieff, L. R., Stern, T. W., and Sherwood, A. M., 1956, Coffinite, a uranous silicate with hydroxyl substitution--a new mineral: Am. Mineralogist, v. 41, nos. 9-10, p. 675-688.

EXAMPLES OF URANIUM DISTRIBUTION GRAPHICS IN GEOLOGIC ROCK SPECIMENS ILLUSTRATED WITH THE RADIOLUXOGRAPH, INDUCED FISSION TRACKS, AND OTHER TRACKS METHODS

By J. R. Dooley, Jr., C. N. Conwell,[1] Pieter Berendsen,[2]
J. K. Otton, C. T. Pierson, W. D. Hoisington,[3]
D. A. Lindsey, and J. N. Rosholt,
U.S. Geological Survey, Denver, Colo.

Exploration for uranium and thorium has renewed interest in rapid and specific methods for locating and identifying the distribution of these elements in geologic materials. Fast photographic film along with the amplification provided by the Radioluxograph (Dooley, 1958; 1972) can provide autoradiographs which graphically illustrate the distribution of the uranium-series and thorium-series isotopes from sections of geologic specimens in a relatively short time. Radioluxographs of ore-grade material with as little as 1,000 ppm uranium can be made in a few minutes to a few hours. Detection of sub-ore-grade material containing as little as 10 ppm uranium and thorium can generally be made with the Radioluxograph in several days, but homogeneous distributions require somewhat longer autoradiographic exposure times. This method is best suited for a quick and inexpensive reconnaissance view of the uranium and thorium distribution on a "macro" scale.

Induced fission from a nuclear reactor or other high-flux source of neutrons can specifically detect uranium and, to a lesser extent, thorium from the fission tracks produced upon Lexan, mica, and other solid-state particle detectors (Fleischer and Price, 1963; Fleischer and others, 1965; 1975). After being properly developed by chemical etching the detector serves as a fission-track map which can be viewed under the microscope and compared with the specimen which produced the tracks. Samples that are over-irradiated produce a high concentration of tracks which is visible to the unaided eye, and is somewhat similar to an autoradiographic image. Most reactors can only accommodate sample sections less than 2.5 cm in diameter and are generally used to study low uranium concentrations because of the reactor's capacity to produce high neutron fluxes. Alpha decay from the naturally occurring radioisotopes and other induced nuclear reactions can be recorded on cellulose nitrate and used for "micro" autoradiography if exposure to light and other photographic effects can be avoided. Microscopic examination of alpha-particle tracks on these detectors and in nuclear photographic emulsions (Yagoda, 1949) are almost always required and give better resolution than other "macro" methods of autoradiography.

Radioluxographs were made of sawed rock sections and drill cores. Polished sections and uncovered thin sections can be used with induced fission tracks and other alpha track methods as well as with the Radioluxograph. Homogeneous distribution of 3 ppm uranium and 11 ppm thorium was found in a tektite with a Radioluxograph. Nonhomogeneous distributions of uranium and thorium are categorized into single accessory minerals; aggregates; concentrations along bedding, vein or fracture fillings; and mineral zoning localizations. High levels of single grain radioactivity dispersed within lower levels of homogeneous or nonhomogeneous radioactivity are best demonstrated with two autoradiographs of different exposure lengths. Semiquantitative determination of uranium can be made from comparing successive autoradiograph exposures of different time lengths or different neutron flux intensities and quantitative determinations can be made from track counting.

Dooley, J. R., Jr., 1958, The radioluxograph--a fast, simple type of autoradiograph: United Nations Internat. Conf. Peaceful Uses Atomic Energy, 2d, v. 3, Paper 1762, p. 550-553.

_____1972, The high-speed radioluxograph with single-scintillation sensitivity for autoradiography of geologic samples [abs.]: Internat. Conf. Nuclear Photography and Solid State Track Detectors, 8th, Proc., v. II, p. 453, Bucharest, Romania.

Fleischer, R. L., and Price, P. B., 1963, Tracks of charged particles in high polymers: Science, v. 140, no. 3572, p. 1221-1222.

Fleischer, R. L., Price, P. B., and Walker, R. M., 1965, Tracks of charged particles in solids: Science, v. 149, no. 3682, p. 383-393.

_____1975, Nuclear tracks in solids: Univ. Calif. Press, 605 p.

Yagoda, Herman, 1949, Radioactive measurements with nuclear emulsions: New York, John Wiley and Sons, Inc., 356 p.

[1] State of Alaska, Department of Natural Resources College Alaska.

[2] Kansas Geological Survey, Lawrence, Kansas.

[3] Dartmouth College, Hanover, New Hampshire.

SPECULATION ON THREE POSSIBLE MODES OF EMPLACEMENT OF URANIUM INTO DEPOSITS OF THE MIDNITE MINE, STEVENS COUNTY, WASHINGTON

By J. Thomas Nash, U.S. Geological Survey, Denver, Colo.

Oxidized and reduced uranium minerals that make up the Midnite uranium deposits are localized in metapelite and metacarbonate rocks of the Precambrian Y Togo Formation adjacent to a Cretaceous(?) porphyritic quartz monzonite pluton (Becraft and Weis, 1963; Nash and Lehrman, 1975). The present distribution of uranium minerals is interpreted to represent destruction and redistribution of earlier formed mineralized zones. Description of original (primary) uranium minerals and interpretation of their genesis is hampered by overprinting of later features and by a simple and nonspecific paragenesis that seems to have been repeated at several times. At least three modes of uranium emplacement, or combinations of them, seem possible.

One possibility is penesyngenetic accumulation of uranium in carbonaceous mud of the Togo Formation about 1300 m.y. ago. As a result of mapping and reinterpretation of the stratigraphy of the mine area it now appears that the Togo was deposited in a marine shelf environment as a sequence of impure carbonate sediments overlain by carbonaceous mud and sand. The lower metacarbonate rocks of the Togo, about 1,100 m of chiefly diopside hornfels and marble, are probably equivalent to the lower part of the Wallace Formation of the Belt Supergroup exposed about 180 km to the east. Apparently overlying the metacarbonate rocks is a sequence of graphitic metapelite about 1,000 m thick that contains 1-3 percent iron sulfides; the uranium deposits are in these rocks. This sedimentary sequence is similar to that of the Alligator Rivers region, Australia, described by Dodson and others (1974). The proposed syngenetic uranium enrichment during lower Paleozoic sedimentation. If uranium accumulated in carbonaceous mud of the Togo Formation along with pyrite, it would later have been mobilized during two periods of metamorphism and have migrated toward the pluton. This sequence of events should have left a record of anomalous uranium concentrations in equivalent strata outside of the mine area, and to my knowledge none has been observed. Moreover, petrologic features of the pluton suggest that it crystallized at high water pressure and released water into its wall rocks; I consider it unlikely that uranium could have migrated in the opposite direction.

A second possibility, which I favor, is hydrothermal emplacement of uranium by postmagmatic fluids evolved from the porphyritic quartz monzonite. Age and petrologic data support this hypothesis. Age determinations on plutonic rocks and a sample of pitchblende are approximately the same, about 100 m.y. (Becraft and Weis, 1963). The pluton is two-mica granite, has porphyritic texture, and contains zones of pegmatite and aplite-- features interpreted to indicate crystallization at relatively high water pressure and release of water after saturation. Also, fission-track maps of thin sections indicate that about 80 percent of the uranium in the pluton is associated with magnetite and very little is contained in refractory minerals such as zircon. On the basis of these observations I suggest the following sequence of events: during emplacement the magma became saturated with an aqueous phase, and this fluid was released along certain zones, some of which may have been established by preintrusion faults. The hydrothermal fluid possibly leached uranium from previously crystallized magnetite in the pluton and transported it into the contact aureole to create a zone of very low grade (0.0X percent) disseminated uranium mineralization. This process operated by diffusion, hence did not produce veins, and had a chemistry (low chlorine and sulfur) that precluded hydrogen metasomatic alteration typical of base-metal sulfide deposits. Subsequently, the low-grade protore was enriched to ore grade during middle to late Tertiary leaching and redistribution (Nash and Lehrman, 1975; Nash, 1975).

The third possibility, supergene emplacement, could have started in about the Oligocene, by which time the pluton had been exhumed. There is evidence for leaching of uranium in present-day weathering profiles in the pluton. Although freshest samples of the porphyritic quartz monzonite today contain about 16 ppm uranium (probably a minimum estimate of original content), a limiting parameter appears to be the amount of the pluton in a position suitable for leaching and ground-water transport into the deposits. I estimate that only 0.2 to 0.3 km^3 of the pluton could have been in the proper hydrologic position, and this volume of rock probably could not provide enough uranium unless there was extremely favorable conditions for leaching, transport, and deposition. However, the supergene process may have added uranium to rocks previously mineralized by Cretaceous metasomatism.

Becraft, G. E., and Weis, P. L., 1963, Geology and mineral deposits of the Turtle Lake quadrangle, Washington: U.S. Geol. Survey Bull. 1131, 73 p.

Dodson, R. G., Needham, R. S., Wilkes, P. G., Page, R. W., Smart, P. G., and Watchman, A. L., 1974, Uranium mineralization in the Rum Jungle-Alligator Rivers Province, Northern Territory, Australia, in Formation of uranium ore Territory, Internat. Atomic Energy Agency Proc. Ser., no. STI/PUB/374, p. 551-568.

Nash, J. T., 1975, Secondary enrichment of uranium at the Midnite mine, Washington, in Craig, L. C., Brooks, R. A., and Patton, P. C., eds., Abstracts for the 1975 Uranium and Thorium Research and Resources Conference: U.S. Geol. Survey Open-File Rept. 75-595, p. 32.

Nash, J. T., and Lehrman, N. J., 1975, Geology of the Midnite uranium mine, Stevens County, Washington--a preliminary report: U.S. Geol. Survey Open-File Rept. 75-402, 36 p.

CONCEPTUAL-MATHEMATICAL MODELS OF URANIUM ORE FORMATION IN SANDSTONE-TYPE DEPOSITS

By Joel S. Leventhal and Harry C. Granger
U.S. Geological Survey, Denver, Colo.

Relatively simple calculations allow estimates to be made of the time required to produce a sandstone-type ore deposit of a given size using reasonable assumptions for the removal of uranium from igneous source rocks, for uranium content of ground water, ground-water flow rate, uranium entrapment efficiency, and host-rock porosity and density.

Mass balance calculations indicate that removal of half the uranium from a relatively small volume of source rock (7.7×10^5 m^3) having a specific gravity of 2.6 and originally containing 10 ppm uranium would yield 10 metric tons of uranium--approximately equal to a deposit that contains 26,000 pounds U_3O_8. This amount is equivalent to that obtainable by weathering and leaching a 300 m x 300 m area of granite to a depth of 8.5 m or a 3 km x 3 km area of volcanic ash about 8.5 cm thick. The time required to remove uranium from such source rocks depends, in part, on their porosity and permeability which, in turn, are related to either the grain size of the ash or the degree of fracturing of granite, and, of course, the solubility of the uranium. The amount of weathering and rainfall and the infiltration of meteoric water into the ground-water system also need to be considered. It can be calculated that 10^9 m^3 of water containing 10 ppb uranium are needed to form a deposit that contains 10 metric tons of uranium. If the rainfall is 25 cm/yr, this amount of water would fall on the granite noted above in about 44,000 years and the ash in 440 years. These are minimum estimates because the uranium may not be removed in this time, and it is unlikely that all the rainwater would enter the ground-water system. If only 10 percent of the rainwater infiltrated the rock, the above time periods would be increased by a factor of 10.

Using several reasonable assumptions, a calculation can be made of the time required to form a roll-type deposit that averages 5 m wide across the roll front and which contains 10 metric tons of uranium. If this deposit averages 0.25 percent uranium, it contains about 4,000 metric tons of ore, and if this ore has a specific gravity of 2, it has a volume of about 2,000 m^3. The 10^9 m^3 of ore-bearing solution needed to supply 10 metric tons of uranium, assuming a uranium content of 10 ppb and 100 percent precipitation, is about 500,000 times the volume of the ore deposit.

The ore formed as the solution flowed through the 5-m-wide orebody. If the hydraulic gradient is 9.4 m/km and the host rock is a medium-grained sandstone having a permeability of 2 darcys, then the bulk water flow is 5.3 m/yr. That is about 5.3 m^3 of water flowing through a cross-sectional area of 1 m^2 in a year. This means that each year a volume of water about equal to the volume of ore percolates through the roll, and that it will take about 500,000 years to form the assumed 0.25 percent uranium orebody. If the ore solution were richer and contained as much as 50 ppb uranium, it then would take only about 100,000 years to form the same orebody.

A series of nomograms can be constructed in which known data can be used to determine variables and scientists can make their own estimates of the variables.

GEOLOGY OF URANIFEROUS TERTIARY ROCKS IN THE ARTILLERY PEAK-DATE CREEK BASIN, WEST-CENTRAL ARIZONA

By James K. Otton, U.S. Geological Survey,
Denver, Colo.

Uranium occurs in Tertiary rocks of the Artillery Peak-Date Creek basin 150 km northwest of Phoenix, Arizona. Although the original size and shape of the basin is unknown, it presently underlies an area 30 km wide that extends 80 km from the southern end of the McCracken Mountains southeast of an area of low hills near the intersection of U.S. Highway 93 and State Highway 71 (fig. 1).

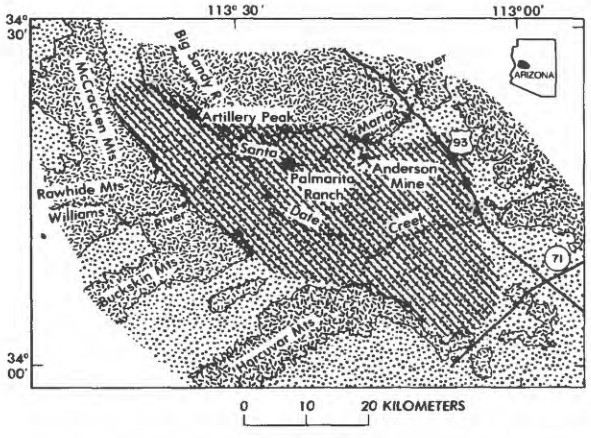

Figure 1.--Index and generalized geologic map of the Artillery Peak-Date Creek basin area. Pattern, outline of present basin; light stipple, Tertiary to Holocene basin fill; dark stipple, Precambrian and Mesozoic basement rocks.

Lasky and Webber (1944, 1949) first mapped and described Tertiary rocks in the Artillery Mountains manganese district in the western part of the basin. More recently, Shackelford (1976), J. S. Gassaway (written commun., 1972, 1976), I. Lucchita (oral commun., 1976) and the author have studied the rocks of the basin and adjacent areas.

The Tertiary rocks within the basin consist of Eocene(?) sedimentary and intermediate to mafic volcanic rocks belonging to the Artillery Formation named by Lasky and Webber (1944) who had assigned an Eocene(?) age to it and its probable lateral equivalents; lower Miocene silicic volcanic and tuffaceous sedimentary rocks; upper lower to middle Miocene(?) mafic to intermediate volcanic rocks, coarse clastic sedimentary rocks and tectonic breccias belonging to the Chapin Wash Formation named by Lasky and Webber (1944) who assigned a Pliocene(?) age to it; upper Miocene(?) basalt; and upper Miocene(?) to Holocene sedimentary rocks. Facies relations within these units are complex, unconformities are common, and no unit can be traced continuously throughout the basin.

The Eocene(?) rocks of the basin are best exposed at the northwestern end and along the northeastern margin of the basin. The rest of the basin is largely covered by the Holocene sedimentary rocks. The maximum thickness ot the Tertiary section is about 2,500 m near the confluence of the Big Sandy River and the Santa Maria River (J. S. Gassaway, written commun., 1977). One drill hole 8 km south of the Anderson mine encountered 1,700 m of Tertiary sedimentary and volcanic rocks.

The rocks of the basin are generally tilted to the south or southwest and have been cut by normal faults. The predominant faults have a northwesterly trend, although east-west and northeast-trending faults have also been observed. Movement on the northwest-trending faults seems to have been recurrent throughout most of the history of the basin. Greatest offsets occur in the upper part of the Artillery Formation of the eastern part of the basin. Offsets are progressively smaller in younger rocks. Low-angle normal(?) faulting, interpreted as gravity glide faulting with a probable source in the Rawhide Mountains (Shackelford, 1976), has occurred at least once in the western part of the basin during deposition of the Chapin Wash Formation and may also have occurred during deposition of the upper part of the Artillery Formation. The sedimentary rocks of the basin have also been gently folded periodically.

A thin sheet of arkose and arkosic conglomerate of Eocene(?) age was the first Tertiary sediment deposited in the basin. This arkose is the lowermost unit of the Artillery Formation, and is generally well preserved in the western part of the basin but in the eastern part it is exposed only in isolated patches unconformably overlain by younger rocks. At the type locality in the Artillery Mountains in the western part of the basin, the Artillery consists of fine-grained calcareous sandstone and siltstone, successively overlain by volcanic pebble conglomerate, limestone, metavolcanic breccia, and limestone and basalt. Although exposures are not continuous to the east, the calcareous siltstone and limestone of the Artillery appear to intertongue with sandstone which, in turn, intertongues with andesitic(?) flows and agglomerates and other volcanic rocks.

An age of 43.3 m.y. has been obtained for the basalt in the upper part of the formation near Artillery Peak (J. S. Gassaway, written commun., 1976).

Unconformably overlying the Artillery Formation are unnamed lower Miocene rocks. At the far western end of the basin these are silicic volcanics which have been dated at 17.1 m.y. (J. S. Gassaway, written commun., 1977). In the vicinity of Artillery Peak, the lower Miocene unit consists of tuffs interbedded with sandstone. Throughout its western exposures the unit is thin. North of the mouth of Date Creek and east of the Big Sandy River, the tuffs and relatively fine-grained fluvial rocks grade into a thick section of gray calcareous boulder to sandy conglomerate and tan sandy conglomerate and sandstone which, in turn, grades into a red-brown Fe- and Mn-rich sandy conglomerate and sandstone near Palmerita Ranch. East of Palmerita Ranch these rocks intertongue with tuffaceous mudstones and siltstones and other rocks which form the mineralized unit at the Anderson Mine.

Overlying this lower Miocene unit is the Chapin Wash Formation. West of the Big Sandy River, the formation consists of basalt, conglomerate, a massive megabreccia and manganiferous conglomerate and sandstone. The base of the Chapin Wash appears to have been intruded by andesitic bodies near the confluence of the Big Sandy and Santa Maria Rivers. East of the Big Sandy River, the megabreccia and manganiferous clastic facies are absent. The basalt at or near the base of the formation has been dated at 15.9 m.y. (J. S. Gassaway, written commun., 1976).

The younger basin-fill rocks overlying these three units include an upper Miocene(?) basalt that locally caps a few mesas in the western end of the basin; upper Miocene(?) to Holocene fanglomerate that is several hundred feet thick in the central and southeastern part of the basin, but apparently has been largely removed by erosion in the western part of the basin; and Holocene alluvium.

At the Anderson Mine in the eastern part of the basin, uranium occurs in silicified, tuffaceous, locally carbonaceous lacustrine mudstones, calcareous mudstones, and siltstones. These lacustrine and overlying fluvial rocks compose a unit that ranges in thickness from 60 to 120 m in surface exposures, and thickens considerably downdip to the south in the subsurface. This unit is here correlated with the unnamed lower Miocene silicic volcanic and tuffaceous sedimentary rocks in the western part of the basin.

Fossil plant material, consisting of thin beds of lignitic(?) material and silicified twigs, leaves, and roots, is abundant. Uranium occurs principally in thinly bedded siltstones rich in carbonaceous or silicified plant material. In many places these siltstones are highly stained by Fe- and Mn-oxides. Carnotite is the only uranium mineral yet recognized, and is probably secondary. The primary uranium phase has yet to be identified: in the mineralized carbonaceous rock it may be a urano-organic complex; and in the silicified rock it may be a urano-silica or urano-iron hydroxide complex.

Interbedded with the mineralized tuffaceous siltstones are unmineralized, thickly bedded, greenish-gray tuffaceous mudstones, white to light-gray tuffaceous calcareous mudstones with abundant calcareous microfossils, and sparse sandstone and siltstone. A thin conglomerate is observed locally at the base. The overlying fluvial rocks consist of upward coarsening gray to greenish-gray sandstones and sandy conglomerates. Virtually the entire unnamed lower Miocene unit is rich in tuffaceous material and is anomalous in uranium content.

Approximately 2 km west of Artillery Peak, uranium occurs in carbonaceous, calcareous siltstones and fine-grained sandstones immediately overlying the basal arkose of the Artillery Formation. The arkose overlies basement rocks which are rich in uranium and thorium in the Artillery Peak area.

Lasky, S. G., and Webber, B. N., 1944, Manganese deposits in the Artillery Mountains region, Mohave County, Arizona: U.S. Geol. Survey Bull. 936-R, p. 417-448.

_____1949, Manganese resources of the Artillery Mountains region, Mohave County, Arizona: U.S. Geol. Survey Bull. 961, 86 p.

Shackelford, T. J., 1976, Structural geology of the Rawhide Mountains, Mohave County, Arizona: Univ. Southern Calif. Ph.D. thesis, 176 p.

URANIUM ASSOCIATED WITH IRON-TITANIUM OXIDE MINERALS AND THEIR ALTERATION PRODUCTS IN A SOUTH TEXAS ROLL-TYPE DEPOSIT

By Richard L. Reynolds, Martin B. Goldhaber, and Richard I. Grauch,
U.S. Geological Survey, Denver, Colo.

Electron microprobe and petrographic studies have been conducted on a suite of ore-bearing samples from a roll-type uranium deposit in south Texas. Each sample from the nose and lower limb of the roll was separated into size fractions less than and greater than 44 m, and each size fraction was further subdivided by bromoform density separation into heavy and light mineral groups. Uranium in the light, fine-grained fraction appears to be predominantly associated with silicon, calcium, potassium, and aluminum. Uranium in the heavy fractions occurs primarily with titanium and iron, and to a lesser extent with sulfur, calcium, and silicon. Uranium was frequently observed in association with a TiO_2 phase that originates largely, if not exclusively, from the alteration of iron-titanium (Fe-Ti) oxide minerals. It is possible that some uranium occurs as a silicate (coffinite?).

The TiO_2 phase in the ore-bearing zones originated primarily by expulsion of Ti during the replacement of detrital Fe-Ti oxides (titanomagnetite and titanohematite) by iron sulfide (FeS_2) minerals (fig. 1). Uranium occurs in association with TiO_2 on the margins of relict Fe-Ti oxide grains in various stages of conversion to FeS_2. Where replacement is complete, uranium-bearing TiO_2 surrounds the

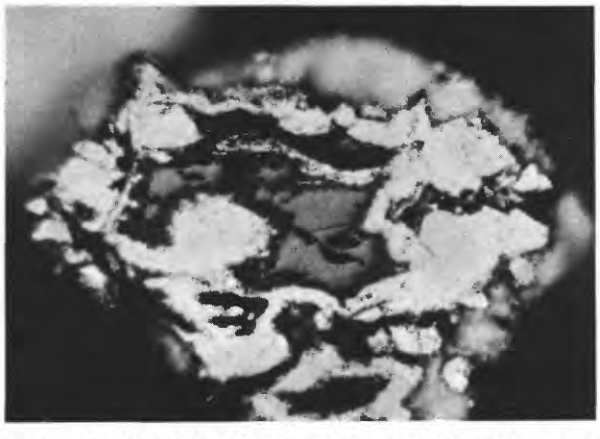

Figure 1.--Titanohematite (light gray) replaced by pyrite (white) along grain margins and fractures within grain. TiO_2 (hazy, white phase) forms partial rim around iron sulfide. Grain from reduced rock remote from ore. Length of field is 158 m. Grain viewed in oil under reflected light.

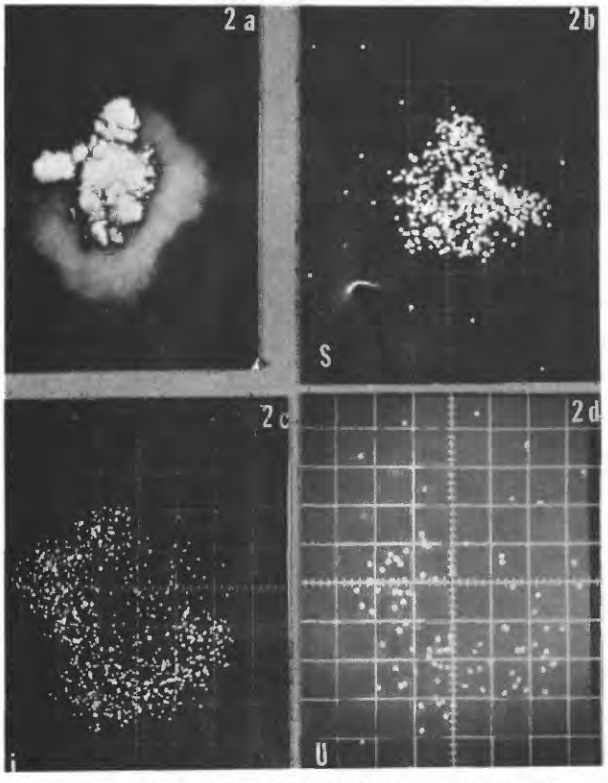

Figure 2.--Pyrite (bright white) partly surrounded by TiO_2 (hazy, white). Grain from mineralized rock at nose of uranium roll. Long dimension of grain is 29 m. (b) X-ray image of sulfur distribution of grain shown in a. Fe distribution (not shown) is identical. Note that X-ray map is mirror image of photomicrograph in this as in following diagrams. (c) X-ray image of titanium distribution. Corresponds to TiO_2 phase shown in a. (d) X-ray image of uranium distribution showing that the majority of uranium is coextensive with titanium.

sulfides (fig. 2). Uranium occurs not only in authigenic TiO_2 surrounding altered Fe-Ti oxides, but also in TiO_2, within the altered grains. Figure 3 illustrates a uraniferous TiO_2 phase that formed by the alteration of a detrital titanomagnetite. That this grain was originally titanomagnetite is indicated by ghosts of ilmenite lamellae along (111) crystallographic planes. Silicon in this grain

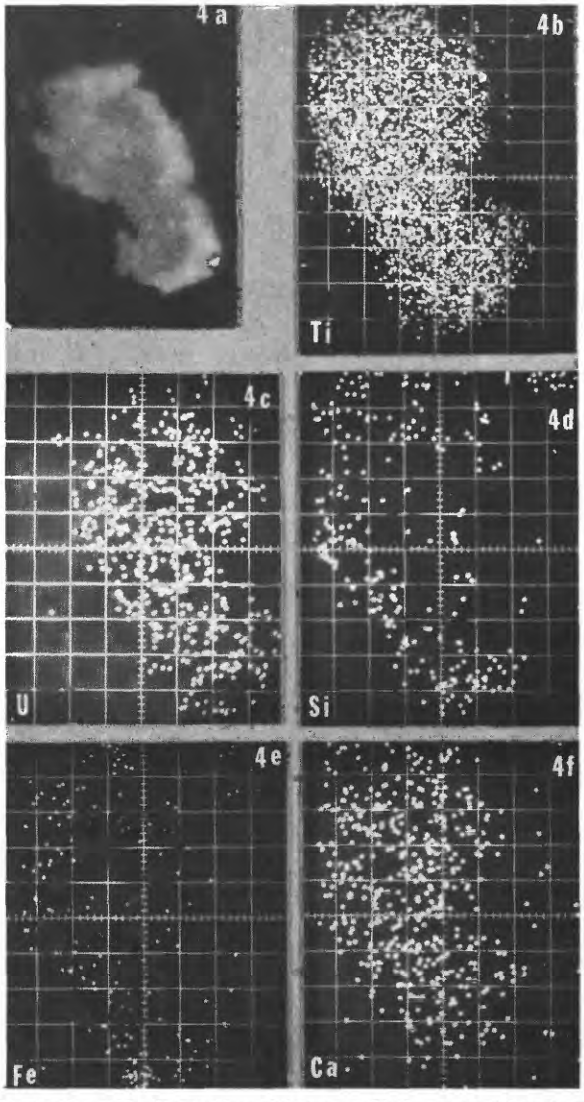

Figure 4.--TiO_2 (a) with small iron sulfide grain (white) at margin in lower right. Note zonation (light-gray rim partly surrounding darker gray interior) within TiO_2. Long dimension of grain is 72 m. X-ray images show distribution of titanium (b), uranium (c), silicon (d), iron (e), and calcium (f). Note that light-gray rim is enriched in silicon and iron, whereas uranium is evenly distributed throughout the grain. (Uranium X-ray image (c) is shifted to right.)

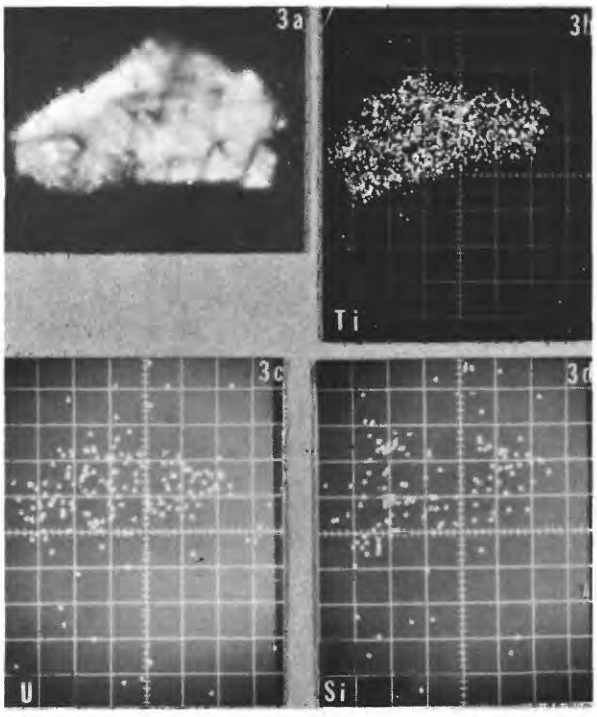

Figure 3.--TiO_2 (white areas in a) produced by alteration of titanomagnetite, with ghost ilmenite lamellae (dark gray) in trellis pattern. Long dimension of grain is 33 m) X-ray images show distribution of titanium (b), uranium (c), and silicon (d).

Figure 5.--Alteration of detrital titanohematite in mineralized rock. Mottled light-gray and black phases consist of abundant titanium, iron, and sulfur with minor uranium, is relict of the original detrital grain. Iron sulfide (white) occurs on margin of grain by replacement and overgrowth and along fractures within grain. Length of field is 390 m.

is largely coextensive with uranium, which indicates the possible presence of a uranium silicate. Silicon and uranium also occur together along part of the margin of the TiO_2 grain in figure 4. The interior of this grain, however, contains significant uranium but is much lower in silicon.

Alteration of Fe-Ti oxide minerals has not led in every case to the segregation of TiO_2 into a discrete phase. In some titanomagnetite and titanohematite grains in mineralized rock, we have observed other alteration phases (fig. 5), petrographically distinct from TiO_2, that contain abundant titanium, iron, and sulfur together with lesser amounts of uranium, silicon, and calcium.

Previous studies have established the association of uranium with titanium in hydrothermal vein and Precambrian quartz- pebble conglomerate uranium deposits (Ferris and Ruud, 1971; Roscoe, 1969). Our results demonstrate the affinity of uranium for titanium-bearing alteration products of Fe-Ti oxide minerals in a south Texas roll-type deposit.

Ferris, C. S., and Ruud, C. O., 1971, Brannerite--its occurrences and recognition by microprobe: Colorado School Mines Quart., v. 66, no. 4, p. 1-85.

Roscoe, S. M., 1969, Huronian rocks and uraniferous conglomerates in the Canadian Shield: Canada Geol. Survey Paper 68-40, 205 p.

URANIUM-LEAD APPARENT AGES OF URANIFEROUS SECONDARY SILICA AS A GUIDE FOR DESCRIBING URANIUM MOBILITY

By R. A. Zielinski, K. R. Ludwig, and D. A. Lindsey
U.S. Geological Survey, Denver, Colo.

The two case studies presented below illustrate the use of U-Pb isotope systematics to investigate the timing of migration of uraniferous silica saturated solutions. It is assumed that time of uranium mobilization is reflected in the U-Pb apparent ages of secondarily precipitated, uraniferous, cryptocrystalline silica. Apparent ages of secondary silica may be compared with ages of host rocks and nearby uranium deposits to further describe the timing of uranium migration in a particular area.

Case 1: Shirley Basin, Wyoming--Chalcedony veinlets occur in silicified tuffaceous siltstone and limestone beds near the base of the Oligocene White River Formation (NE 1/4 sec. 21, T. 28 N., R. 79 W.). The veinlets are present as gray translucent fracture fillings less than 5 cm wide (fig. 1A). The majority of veinlets closely parallel bedding although some small veinlets crosscut bedding at angles up to 90°. The silicified sequence of siltstone and limestone is as much as 14 m thick and represents a series of shallow lake sediments. This sequence covers an area of at least 8x3 km in the central Shirley Basin (Harshman, 1972) and overlies major uranium deposits in Eocene sandstones. Fission-track maps of the veinlet selected for dating revealed a homogeneous distribution of uranium. Silica saturation of ground water probably resulted from the downward percolation of ground water through glassy tuff of the overlying White River Formation. Silica gel and uranium coprecipitated from solution to produce the uraniferous veinlets.

One of these veinlets was crushed, and inclusion-free material was hand picked from it and washed with water prior to analysis. Uranium and lead concentrations in this material, determined by isotope dilution, were 242 ppm and 0.93 ppm, respectively. Apparent ages were slightly discordant: 18.8 0.3 m.y. for $^{206}Pb/^{238}U$, and 20.1 0.8 m.y. for $^{207}Pb/^{235}U$. The discordance results from either preferential loss of radioactive daughters of ^{238}U or the presence of an unrecognized component of inherited Precambrian lead. The maximum possible age of the veinlets is that of the host rock (32.4 2.6 m.y. zircon fission-track age by C. W. Naeser). Radiometric ages as young as 24 3 m.y. determined for nearby uranium deposits in the underlying sandstone (Ludwig, 1977) are compatible with the hypothesis that some uranium was derived from leaching of tuffs. Secondary silica and uranium ores which occur in the same host rock and are subjected to the same maximum age restrictions should provide tighter limits to the timing of uranium migration.

Case 2: Thomas Range, Utah--Uraniferous opal veinlets 1 cm wide occur in fractures in 38- to 39-m.y.-old rhyolitic ash-flow tuff at the Autunite No. 8 prospect (SW 1/4 sec. 10, T. 13 S., R. 11 W.) in the Thomas Range. The veinlets may have been deposited by hydrothermal activity related to nearby beryllium, fluorspar, and uranium mineralization. Mineralization in the Thomas Range accompanied or followed topaz rhyolite volcanism that began 21 m.y. ago and ended with extrusion of voluminous flows of

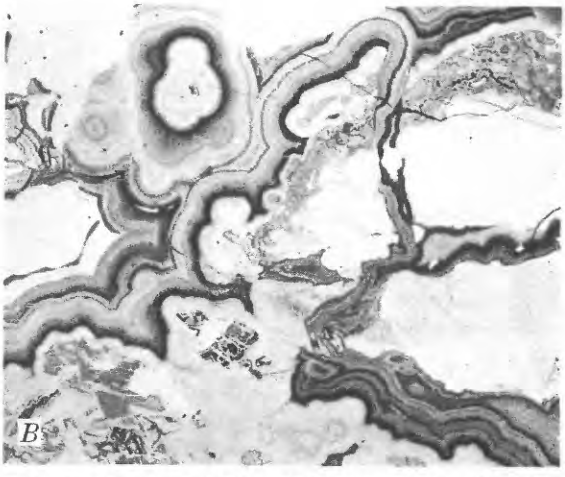

Figure 1.--A, Cryptocrystalline silica veinlets in silicified tuffaceous siltstone, White River Formation, Shirley Basin, Wyoming. B, Fission-track image of the uranium distribution in uraniferous opal veinlets, Autunite No. 8 prospect, Thomas Range, Utah. Area of view about 1 cm^2.

topaz rhyolite 6 to 7 m.y. ago (Lindsey, 1977). The areas of most intense mineralization occur in water-laid tuff associated with 21-m.y.-old rhyolite at Spor Mountain, but traces of mineralization are present in tuff interbedded with 6- to 7-m.y.-old rhyolites in the Thomas Range.

The opal veinlets in the Autunite No. 8 prospect were dated to obtain additional information concerning the age of mineralization and its relationship to volcanism in the Thomas Range. Fission-track maps (fig. 1B) revealed U distribution to be very homogeneous within concentric growth zones (500-1,000 ppm U). The analyzed opal fragments contained 1,220 ppm uranium and 0.88 ppm lead, and gave nearly concordant apparent ages of 3.5 m.y. The results support the hypothesis that some, and possibly all, of the beryllium-fluorspar-uranium mineralization occurred after the eruption of voluminous topaz rhyolite 6-7 m.y. ago.

Harshman, E. N., 1972, Geology and uranium deposits, Shirley Basin area, Wyoming: U.S. Geol. Survey Prof. Paper 745, 82 p.

Lindsey, D. A., 1977, Epithermal beryllium deposits in water-laid tuff, western Utah: Econ. Geology, v. 72, no. 2 (in press).

Ludwig, K. R., 1977, Uranium daughter migration and U/Pb isotope apparent ages of uranium ores, Shirley Basin, Wyoming: Econ. Geology (in press).

PRECAMBRIAN URANIUM ASSOCIATED WITH A METAMORPHOSED MASSIVE SULFIDE BODY--CAMP SMITH AREA, NEW YORK

By Richard I. Grauch and David L. Campbell
U.S. Geological Survey, Denver, Colo.

Precambrian uraninite is associated with a zoned massive sulfide body at the Phillips mine (Klemic and others, 1959) and, locally, in other zones along the contact between units of amphibolite gneiss and quartzo-feldspathic leucogneiss in the Camp Smith area, Putnam and Westchester Counties, New York.

The Camp Smith area is underlain by a complexly folded, interlayered sequence of metamorphosed (granulite facies) submarine volcanogenic, carbonate, pelitic rocks, and minor amounts of granitic and pegmatitic material. The three major rock units are amphibolite gneiss, quartz-feldspar-biotite leucogneiss, and quartz-feldspar-hornblende-(±biotite) leucogneiss. The amphibolite gneiss unit is variable in composition and appearance, ranging from massive dark-green amphibolite to banded hornblende-quartz-feldspar gneiss. Minor horizons of magnetite-rich amphibolite gneiss and scapolite-rich amphibolite gneiss are included in that unit. The biotite leucogneiss unit includes minor amounts of marble, graphitic calc-silicate gneiss, graphitic metachert, biotite-garnet-quartz-feldspar gneiss, and amphibole-pyroxene-garnet-graphite skarn. Compositional variations within the hornblende leucogneiss are minor and are reflected by variations from 1:0 to 1:1 in the ratio of hornblende to biotite. All three of the major rock units host small amounts of quartz-feldspar pegmatite and hornblende-quartz-feldspar-(±pyroxene) pegmatite.

Uraninite is found in four different host rocks: magnetite-rich and scapolite-rich layers in amphibolite gneiss; hornblende-pegmatite; and the outer, Cu-Ni-bearing zone of the massive sulfide body. Uraninite occurs in magnetite-rich layers as small euhedral to anhedral crystals, some of which are embayed by magnetite. In the scapolite-rich layers, uraninite occurs as minute inclusions in scapolite and hornblende. The magnetite-rich and scapolite-rich layers appear to be near the contact between light and dark colored gneisses. Hornblende pegmatites, interpreted as being anatectic in origin, are most abundant near that contact. The pegmatites contain uraninite as anhedral inclusions in hornblende and apatite, and as large (up to 1 cm) euhedral crystals; uraninite unit cells range from 5.460 to 5.480 A. In the massive sulfide body uraninite is apparently restricted to the Cu-Ni-bearing zone which in addition contains apatite, pyrrhotite, pyrite, chalcopyrite, marcosite, magnetite, and molybdenite. The core of the sulfide body is apparently massive pyrrhotite with little if any uraninite, pyrite, or chalcopyrite. The uraninite occurrences mentioned above have two features in common: association of uraninite with apatite and proximity to the lithologic break between melanocratic and leucocratic rocks. Minor concentrations of uranium are also found in small, presumably old, fractures near the lithologic break.

The association of high uranium concentrations with the contact between melanocratic and leucocratic rocks is also supported by geophysical work (manborne total field magnetic, E-mode VLF resistivity, and γ-ray spectrometric surveys). Geophysical measurements were made at 20 m intervals on lines 40 m apart over an area of about 400 by 800 m. The resulting contoured geophysical maps show some details not readily relatable relatable to known surface geology. Zones of sulfide mineralization often show some combination of high magnetic values, low resistivity, and high eU content (only the results from the uranium channel, eU, of the γ-ray spectrometer are considered). Proceeding across strike from northwest to southeast, we note the following, generalized, geophysical characteristics (fig. 1).

(1) A zone of high resistivity, low magnetic, and low eU values that probably contains little mineralization. Locally, however, there are low resistivity subzones that may be sulfide- or graphite-bearing.

(2) A narrow zone of low resistivity, high eU, and high magnetic values, that correlates with a uraniferous hornblende pegmatite.

(3) A zone of moderate-to-high resistivity, and moderate eU content that seems to typify the hornblende leucogneiss unit. The magnetic field in this zone is apparently uniform but its relative magnitude has not been evaluated.

(4) A zone that shows high resistivity and large variations in eU and magnetic values.

The close spatial association of uraninite, magnetite, and sulfides suggests an exploration target that should be readily identifiable through manborne and airborne geophysical techniques. Indeed, the Phillips mine area has been mapped as a major aeroradioactivity anomaly (Popenoe, 1966).

The massive sulfide body at the Phillips mine is apparently a strata-bound body located near the interface between mafic and felsic metavolcanogenic rocks. Some of the mafic and probably most of the felsic rocks were originally deposited as clastic sediments with variable amounts of pelitic and carbonate components. It is proposed that during deposition of the sediments some mechanism, possibly the

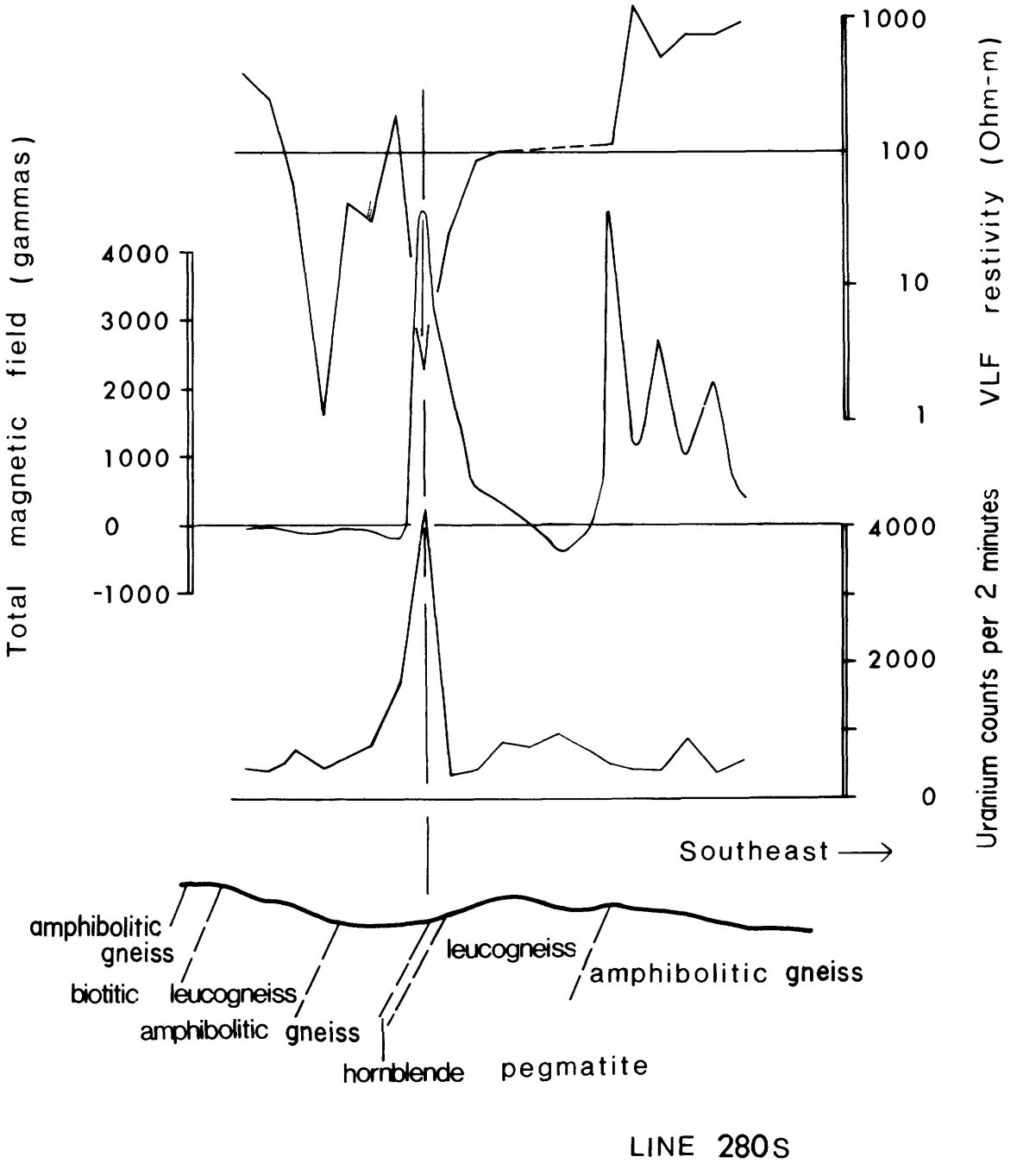

Figure 1.--Geological cross section and related geophysical expression of a portion of the Phillips mine area (geology modified from Klemic and others, 1959).

precipitation of apatite, caused widespread but low-grade concentration of uranium. This mechanism was presumably operative during the waning stages of massive sulfide formation and the beginning stage of magnetite deposition. During subsequent granulite facies metamorphism uraninite was formed. This hypothesis appears to explain the association

of uraninite with apatite and the proximity of uranium-bearing rocks to the contact between melanocratic and leucocratic units. Other uranium occurrences (Grauch and Zarinski, 1976) in the Hudson and Jersey Highlands may be explained by this model and seem to offer excellent targets for future exploration.

Grauch, R. I., and Zarinski, Katrin, 1976, Generalized descriptions of uranium-bearing veins, pegmatites, and disseminations in non-sedimentary rocks, eastern United States: U.S. Geol. Survey Open-File Rept. 76-582, 114 p.

Klemic, Harry, Eric, J. H., McNitt, J. R., and McKeown, F. A., 1959, Uranium in Phillips mine-Camp Smith area, Putnam and Westchester Counties, New York: U.S. Geol. Survey Bull. 1074-E, p. 165-199.

Popenoe, Peter, 1966, Aeroradioactivity and generalized geologic maps of parts of New York, Connecticut, Rhode Island, and Massachusetts: U.S. Geol. Survey Geophys. Inv. Map GP-359.

THE DISTRIBUTION OF URANIUM IN SEDIMENT SAMPLES AS DETERMINED BY MULTI-ELEMENT ANALYSIS

By John D. Tewhey
Earth Sciences Section
Lawrence Livermore Laboratory
Livermore, California 94550

A number of sediment samples collected from the Walker River, Winnemucca and Smoke Creek Basins, Nevada, as part of a National Uranium Resource Evaluation (NURE) program orientation study, were selected for detailed analysis in order to determine the nature of the uranium distribution in sediments from a semiarid environment. The results of this study suggest that an estimate of the leachable versus nonleachable uranium in samples studied can be made on the basis of certain geochemical indicators that are obtainable by means of multielement instrumental neutron activation analysis (INAA).

Sediment samples were split into seven size fractions ranging from 63 m to 2000 m and each fraction was subjected to a 30-element INAA (including uranium) to determine its bulk chemical characteristics. Each split was then subjected to a heavy-liquid separation to facilitate optical mineralogical analysis. Light fractions (3.19 g/cm^3) consisted primarily of quartz, feldspar and mica; heavy fractions (3.19 g/cm^3) commonly consisted of sphene, zircon, magnetite, hematite, epidote, augite, and hornblende. The contribution that each mineral made towards the total uranium content of the split was determined by using the average abundance of uranium in the mineral as given by Rogers and Adams (1972), or by analyzing representative mineral fragments from one of the larger size fractions by INAA. In the latter case, the contribution from leachable uranium was minimized by (1) keeping a small ratio of surface area to mass by choosing several large grains for analysis rather than many small ones, and (2) by washing the grains prior to analysis. For each size fraction, the difference between the total uranium in the sample and the sum of the contributions of the individual minerals was considered to represent the leachable uranium (fig. 1A). The amount of leachable uranium in the various size fractions determined by the procedure described above correlates reasonably well with the amount determined by acid-leaching experiments. The absolute amount of leachable uranium as analyzed by leaching experiments is always less than the amount calculated on the basis of INAA, but the relative amounts in the various size fractions and in different samples as determined by the two methods are correlative (fig. 1A and B).

Through analysis of the INAA data for eight samples, it has been found that the amount of leachable uranium in samples from the area studied can be correlated with certain geochemical parameters, such as Th/U ratios and Zr and La values. Sediment samples containing heavy resistate minerals often exhibit moderately high uranium concentrations and concomitant low values of leachable uranium. In general, heavy resistate minerals are characterized by having high Th/U ratios (Adams and Weaver, 1958). The resistates from the area studied are also characterized by moderately high concentrations of Zr and the rare earth elements. In figure 2, weighted Zr-La values (ppm Zr + 10 ppm La) are plotted against the Th/U ratio of fine- and coarse-grained size fractions of eight sediment samples. An indication of the percentage of leachable uranium with respect to the total uranium concentration, as determined by acid leaching experiments, is given for each sample. Note that samples with high percentages of leachable uranium (solid circles) tend to be characterized by low Th/U ratios and low Zr-La values, and those exhibiting low values of leachable uranium (open circles) tend to have higher Th/U ratios and Zr-La

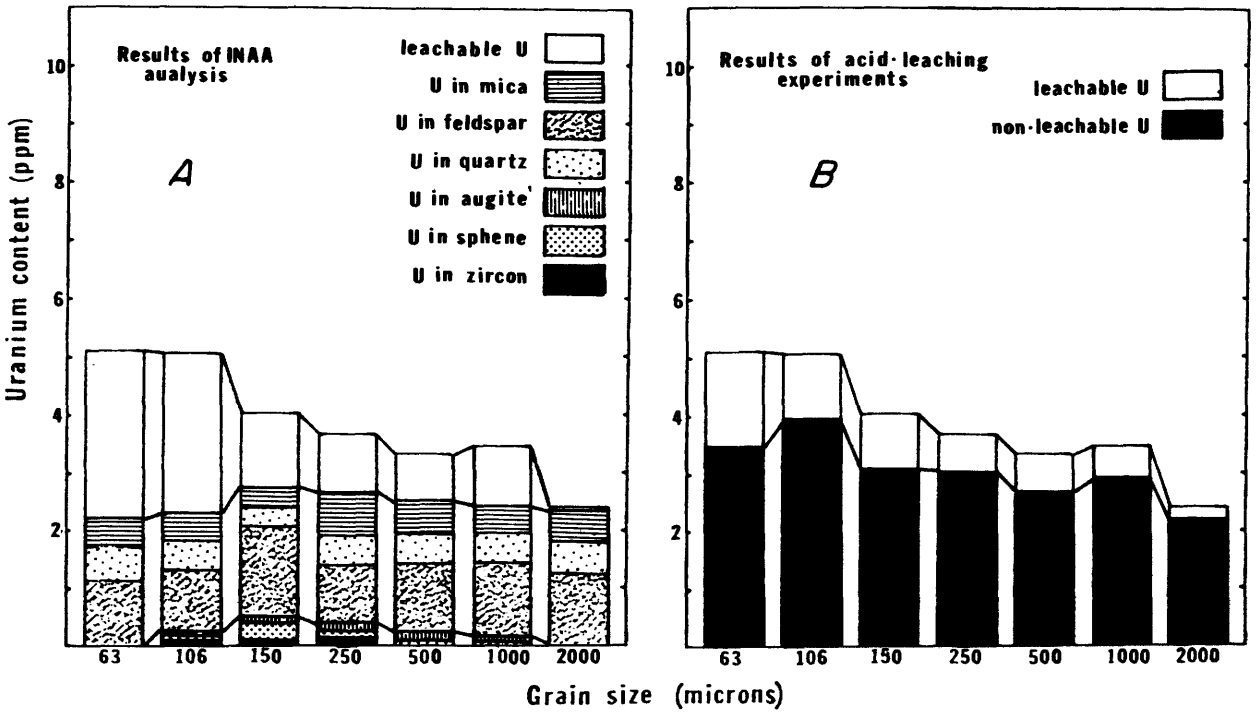

Figure 1.--(A) Distribution of uranium in various size fractions of sediment sample from Walker River Basin (238) as determined by INAA. (B) Distribution of leachable versus non-leachable uranium in sediment sample (238) as determined by acid-leaching experiments.

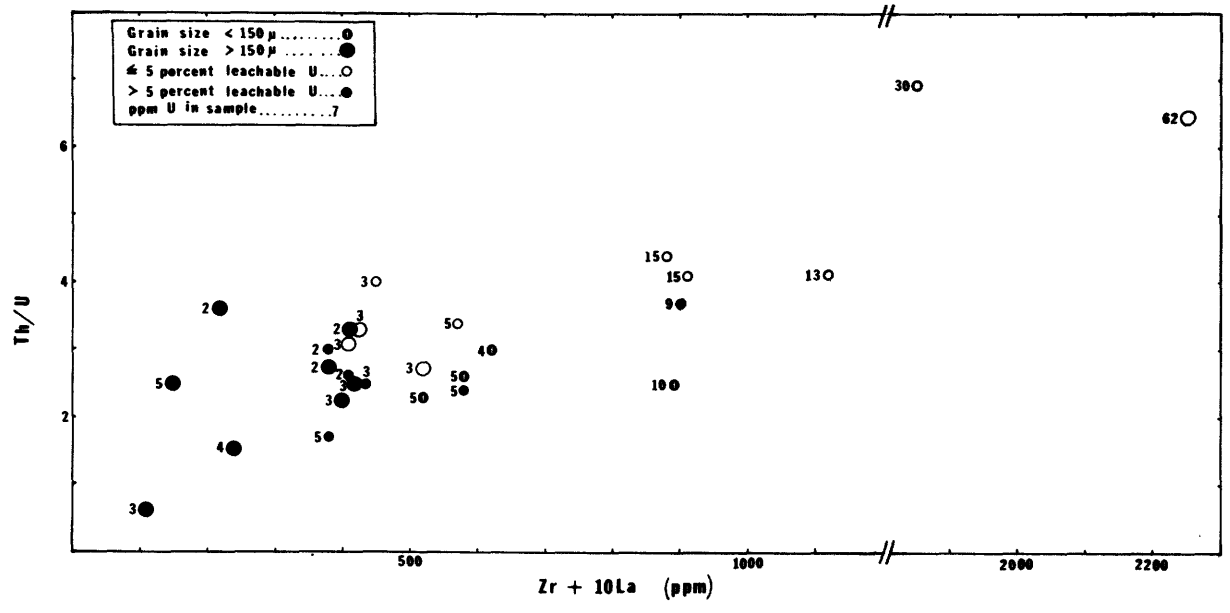

Figure 2.--Plot of Th/U versus Zr + 10 La (ppm) for fine- (small circle) and coarse- (large circle) size fractions of eight sediment samples from Western Nevada Basins.

values. It is suggested that the data derived from multielement INAA can be used to estimate the amount of leachable uranium in a sample without having to conduct costly and time-consuming acid-leaching experiments.

Adams, J. A. S., and Weaver, C. E., 1958, Thorium-to-uranium ratios as indicators of sedimentary processes--Example of concept of geochemical facies: Am. Assoc. Petroleum Geologists Bull., v. 42, no. 2, p. 387-430.

Rogers, J. J. W., and Adams, J. A. S., 1972, Geochemistry of uranium, in Wedepohl, K. H., ed., Handbook of Geochemistry, v. II-3: New York, Springer-Verlag, p. 92-D-1 to 92-D-2.

URANIUM DEPOSITS RELATED TO DEPOSITIONAL ENVIRONMENTS IN THE MORRISON FORMATION (UPPER JURASSIC), HENRY MOUNTAINS MINERAL BELT OF SOUTHERN UTAH

By Fred Peterson, U.S. Geological Survey, Denver, Colo.

Analysis of the depositional framework of the Morrison Formation in south-central Utah (fig. 1) shows that the environments of deposition played a significant role in the formation of uranium deposits in the region. The lower member (Peterson, 1974) and Salt Wash Member of the Morrison comprise a series of fluvial and lacustrine beds that are divided into three fluviolacustrine sequences (fig. 1). The sequences are distinguished from each other in vertical sections by differences in facies, crossbedding dip vectors, and stratification ratios (planar crossbedding/planar crossbedding plus horizontal bedding). The thickness of the sequences in the mineral belt are: lower sequence, 55-90 m; middle sequence, 7-12 m; and upper sequence, 38-87 m.

The lateral distribution of facies within these sequences progressing away from a highland source region, down an alluvial plain, and into a lacustrine area is listed below and shown on figure 1 (time 1). Important exceptions to this distribution occur at or near the uranium deposits, where some of the facies are absent (fig. 1).

Facies A: Chiefly braided-stream deposits consisting of trough-crossbedded, planar-crossbedded, and flat-bedded, gray to brown conglomerate and conglomeratic or pebbly sandstone. Also contains red mudstone and siltstone deposited on flood plains adjacent to the streams.

Facies B: Predominantly meandering-stream deposits consisting of trough-crossbedded gray to brown sandstone and pebbly sandstone containing fining-upward cycles and lateral accretion (point bar) units. Includes red mudstone and siltstone deposited on flood plains flood plains adjacent to the streams.

Facies C: Marginal-lacustrine strata consisting of laminated or locally burrowed light-gray sandstone deposited at or near the shoreline of lakes where silt and clay were washed away by wave-generated currents.

Facies D: Nearshore-lacustrine red beds consisting of laminated and burrowed red mudstone, siltstone, and sandstone deposited in shallow nearshore waters of lakes. Composed of clay, silt, and very fine-grained sand carried in suspension and deposited near the shoreline of lakes that probably had fluctuating shorelines.

Facies E: Offshore-lacustrine beds consisting of dark-gray mudstone containing fine-grained carbonized plant debris. These beds consist of suspended-load sediments deposited in the offshore part of lakes where anaerobic conditions were present in the bottom sediments.

Regional studies indicate that the three sequences were deposited on an extensive alluvial plain or in a relatively small lacustrine area that developed in the Henry structural basin. Sedimentation was chiefly by braided streams that originated in highlands southwest and west of the Henry basin, although meandering streams locally formed on the distal end of the plain where the gradients were low. Lakes formed in a persistent depositional low that formed in the vicinity of the mineral belt whenever the rate of basin subsidence exceeded the rate of sedimentation by fluvial processes. Deposition of most of the fluvial and marginal-lacustrine sandstone beds probably was under oxidizing conditions, as suggested by the associated red beds and the general lack of carbonized plant debris. However, deposition occurred under reducing conditions in the offshore and deeper parts of the lakes where anaerobic processes dominated. The reducing conditions were responsible for preservation of carbonized plant debris incorporated in the bottom muds, and the fluids within the muds were the source of the reductant necessary for the ore-forming process.

The uranium deposits occur as discontinuous tabular bodies up to a meter thick and a hundred or more meters wide

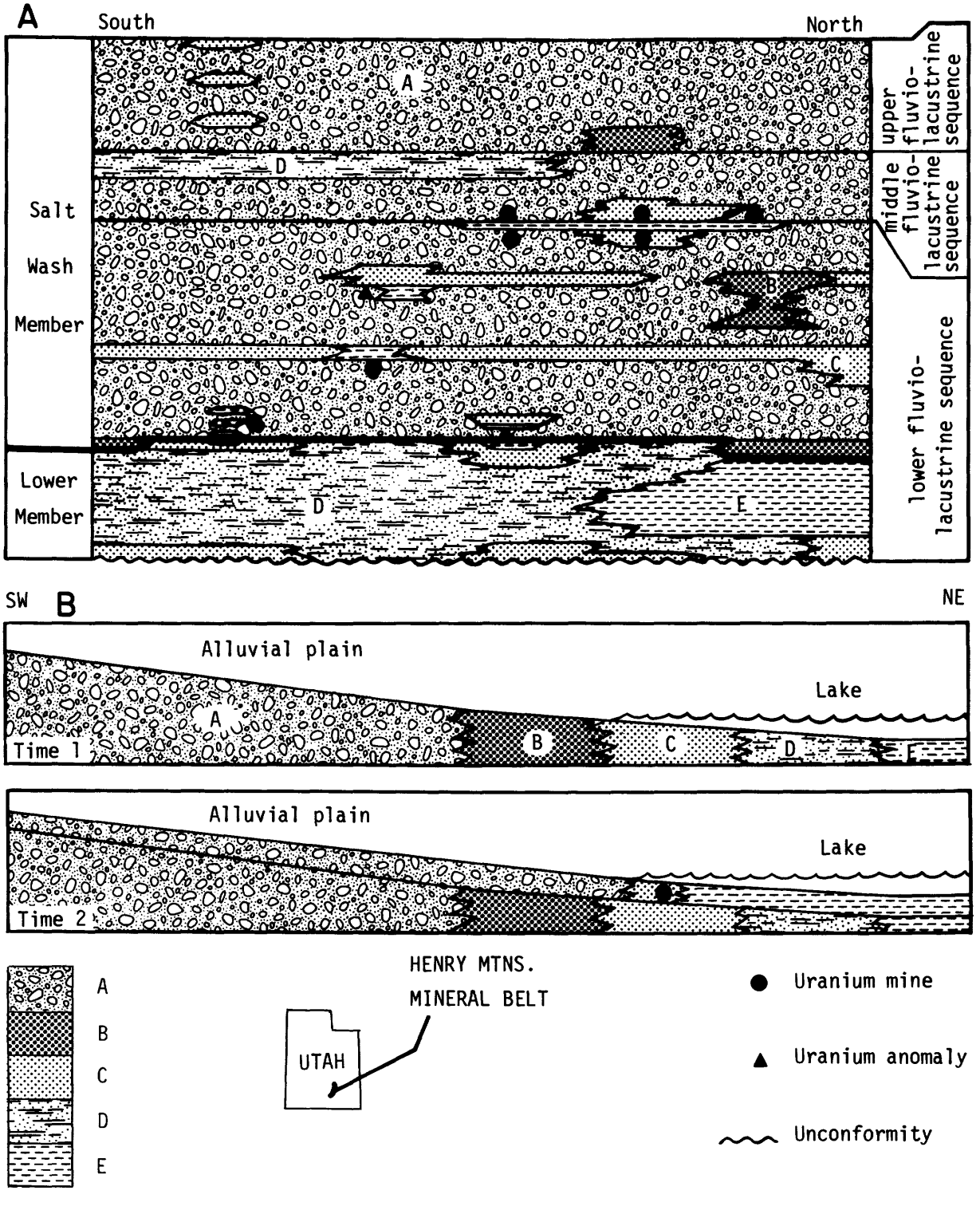

Figure 1.--A, Fluviolacustrine sequences and distribution of facies in the lower member and Salt Wash Member of the Morrison Formation in the Henry Mountains mineral belt. The panel trends at nearly right angles to the general direction of stream flow. Not to scale. B, Distribution of facies in general direction of stream flow in southern Utah. Time 1 shows normal distribution of facies; time 2 shows a later time when facies B and D were not present. Not to scale.

within braided-stream and marginal-lacustrine sandstone beds that are 2-9 m thick. Scattered carbonized plant debris is present in the sandstone at or near the ore deposits but is not preserved elsewhere in the same bed. Near the uranium deposits, thin beds of offshore-lacustrine gray mudstone less than 2 m thick lie directly above, below, or lateral to the sandstone (fig. 1), and thin lenses of the gray mudstone are also present locally within the sandstone.

Proximity of the uranium deposits to offshore-lacustrine gray mudstone in the lower and middle fluviolacustrine sequences indicates that these mudstones played an important role in the mineralization, and this, as well as the association with braided-stream sandstones suggests a model for the mineralization that is related primarily to the depositional environments. The hypothesis presented here is that uranium was transported in solution by oxidized ground water that flowed down the depositional slope of an alluvial plain through sands deposited by fluvial processes. The uranium was precipitated at the distal end of the alluvial plain in braided-stream or marginal-lacustrine sands in places where braided streams emptied directly into lakes, and where meandering-stream sands (facies B) and nearshore-lacustrine red beds (facies D) were not present. Precipitation of the uranium occurred within the sands at the interface between the oxidized uranium-bearing water and reducing fluids that migrated into the sands from the offshore-lacustrine gray muds. Carbonized plant debris in the sandstone at or near the orebodies apparently was preserved by the reducing fluids which migrated into these beds shortly after deposition. Lack of uranium deposits in meandering-stream sandstone beds probably is due to slower flow of ground water through these beds and the scarcity of offshore-lacustrine gray mudstone in proximity to these beds. No uranium deposits have been found in the upper fluviolacustrine sequence, which also contains braided-stream sandstone beds but lacks the offshore-lacustrine gray mudstone. This important difference in the upper fluviolacustrine sequence strengthens the hypothesis that fluids in the gray mudstones in the underlying sequences were necessary for the mineralizing process.

The association of uranium deposits with lacustrine gray mudstone is similar to that described for lacustrine rocks of the Newark basin in Pennsylvania and New Jersey. According to Turner-Peterson (this volume), humic acids and aqueous sulfides were generated in offshore-lacustrine black muds of the Newark basin where anaerobic bottom conditions were present. Pore fluids containing these reducing agents were then expelled by compaction into the adjacent sands at the lake margin where intervening marginal-lacustrine red beds (facies D of this paper) were absent. The black muds could only play a role in the mineralizing process shortly after their deposition, because the reducing agents (humic acids and aqueous sulfides) were only produced within these muds while they were still buried at shallow depths. As applied to the Henry Mountains mineral belt, this explains the geochemical processes involved in generating the reducing fluids in the offshore-lacustrine gray muds. However, in this area the reducing fluids were expelled into braided stream sands as well as marginal-lacustrine sands, in places where either of these lay adjacent to the offshore-lacustrine gray muds.

This depositional model should be useful as an exploration guide to uranium deposits in unexplored subsurface parts of the Henry basin as well as in other regions where closely associated fluvial and lacustrine strata occur.

Peterson, Fred, 1974, Correlation of the Curtis, Summerville, and related units (Upper Jurassic) in south-central Utah and north-central Arizona [abs.]: Geol. Soc. America Abs. with Programs, v. 6, no. 5, p. 466-467.

LOW-LEVEL DETERMINATIONS OF URANIUM AND THORIUM BY X-RAY SPECTROMETRY

By Gerard W. James, Kansas Geological Survey, Lawrence, Kansas 66044

Rapid and accurate low-level determinations of uranium and thorium in geologic samples are essential to large-scale uranium exploration programs. Although X-ray spectrometric techniques have been utilized for the analysis of ore-grade rocks and ore concentrates for over 20 years, most previous work has indicated X-ray methods (1) lack the sensitivity required for low-level analyses of exploration samples, and (2) require the addition of an internal standard for quantitative determinations. As a result, many government laboratories are utilizing automated neutron activation

techniques, and laboratories without access to reactor facilities are utilizing traditional fluorimetric, colorimetric, and counting methods of analysis.

More recent work, however, has demonstrated the rapid and accurate determination of low levels (0 to 100 ppm) of uranium and thorium in geologic samples by wavelength-dispersive X-ray emission spectrometry (James and Hathaway, 1976; James, 1977). This paper summarizes the results of these investigations.

All the data reported in these studies were obtained by utilizing a Philips 1410 vacuum spectrograph with an XRG 3000-watt generator operated at 50 kV and 50 mA. Maximum sensitivities for the determination of uranium and thorium were achieved by employing a molybdenum target X-ray tube in combination with a LiF_{220} analyzing crystal, and measuring the uranium and thorium L_α radiation. Scattered background radiation was measured at 0.901 Å. Sample preparation consisted of directly analyzing rock powders (10-gram samples ground to minus 200 mesh) in 50-mm-diameter sample holders. Analytical count times were 50 seconds at the analyte and background positions. Data reduction involved comparing peak-to-background count-rate ratios of samples to analytical calibration curves, which were determined from the analyses of Ottawa sand samples spiked with a carnotite ore and from U.S. Geological Survey igneous rock standards.

Reproducibility studies indicated no significant errors were associated with the sample preparation (as long as the samples were ground fine enough to be homogeneous) and instrument operation. Hence, the detection limits and precision of the method could be directly estimated on the basis of standard counting errors, which are a function of counting time. For a total analysis time of 5 minutes on a sequential spectrometer (two 50-second measurements at each of the three 2θ positions), the two-sigma (95 percent confidence level) detection limits were 0.8 ppm uranium and 1.0 ppm thorium.

The method was found to be applicable to a broad variety of igneous and sedimentary rock types. For most exploration samples, large variations in SiO_2, Fe_2O_3, $CaCO_3$, and organic material did not have significant influences on the accuracy of the X-ray-predicted concentrations of uranium and thorium. Matrix effects were sufficiently corrected for by the peak-to-background ratio method, which utilizes scattered background radiation as an internal standard. Thus, one analytical calibration curve per element is applicable to all types of sandstones (unaltered, reduced, and oxidized) and most igneous and metamorphic rocks.

The main advantages of X-ray spectrometric techniques over other methods of analysis lie in the simplicity of the sample preparation and the rapidity of the analysis. In addition, X-ray spectrometers are capable of determining low levels of other indicator elements (e.g., selenium) and can be easily adapted for routine quality control applications of ore-grade levels as mined or as recovered in leach solutions.

James, G. W., 1977, Low level determinations of uranium and thorium in geologic samples by X-ray spectrometry: Anal. Chemistry (in press).

James, G. W., and Hathaway, L. R., 1976, Recent advances in analytical methods for determining uranium in natural waters and geological samples, in Exploration for uranium ore deposits: Internat. Atomic Energy Agency, Vienna, p. 311-320.

DETERMINATION OF URANIUM IN SOURCE ROCKS USING RADIUM IN CRYSTAL SPRINGS, GREAT SALT LAKE AREA, UTAH

By J. Karen Felmlee and Robert A. Cadigan
U.S. Geological Survey, Denver, Colo.

The amount of uranium in source rock that would be required to produce the radium in the water of Crystal Springs, north of Brigham City, Utah, has been calculated in order to determine whether the source rock may have a potential for uranium concentrations of economic interest. This study is an outgrowth of reconnaissance sampling of mineral springs in Colorado, Utah, Arizona, and New Mexico in 1975-76 (Cadigan and Felmlee, 1977). The area around the Great Salt Lake in the Basin and Range Province of Utah was revisited in May 1976. Water samples were collected from 11 springs for radium, uranium, and major- and minor-element analysis. Limited data are available (O'Connell and Kaufmann, 1976; Mundorff, 1970) for 4 other springs, making a total of 15 sites. Precipitate samples were collected from 8 of the sites.

Radium in the water has a positive correlation (0.82) with total dissolved solids and with most of the major and minor ions. The three springs having the lowest salinity also have the lowest radium content, less than 1 μμg/l, and one of the briny springs, Crystal Springs, has the most

radium, 220-410 μμg/l. Some springs on faults within 20 km west of the Wasatch Range have moderately high salinity and radium content, 20-140 μμg/l. Others having moderately high salinity, however, have low radium, only 2-5 μμg/l. Such deviations reflect variations in unmeasured parameters, such as uranium content of the source rock, that affect the radium content of the water.

Barium, copper, iron, and manganese in the precipitates are unusually abundant at some localities, notably barium and copper at Stinking Hot Springs and iron and manganese at Utah Hot Springs. These metals are known to be associated with hydrothermal mineral deposits. Many of the mineral springs near the Wasatch Range have moderately high radium contents, but only Stinking and Utah Hot Springs contain high barium or iron. Coprecipitation of radium with barium and iron has produced very radioactive precipitates at these two sites. Although Crystal Springs have no barium- or iron-rich radioactive precipitates, they exceed the other two sites in the radium content of their water. Therefore, it is used in the calculation of uranium in source rocks.

The amount of radium in the water at Crystal Springs exceeds by several hundred times the amount of radium that would be in equilibrium with the amount of uranium in the water. The amount of enrichment, called the radium enrichment factor (REF), can be calculated by using the known equilibrium ratio for radium-226 and uranium-238 and the measured radium and uranium per liter or minute at the spring. The REF at Crystal Springs is 430-440.

The REF in the water depends on the difference in leach between radium and uranium when they are removed from the source and transferred to the spring. Differential leaching, based on differences in response to such parameters as pressure, temperature, oxidation-reduction potential, ionic strength, and mineral phases, leads to disequilibrium within the rocks being leached. If the percentage of leach for the two elements is the same, equilibrium in the rocks is maintained and equilibrium amounts are dissolved in the water. Differential leaching in favor of radium results in an excess of radium in the water and a corresponding depletion at the source. Continued differential leaching eventually leads to extreme disequilibrium in the leached part of the rock. The disequilibrium is actually between radium and its direct parent, thorium-230, which is in relative equilibrium with uranium (O'Connell and Kaufmann, 1976). Therefore, we calculate uranium in the source rocks by assuming that disequilibrium in the rocks is extreme (no equilibrium radium present) and that the only radium available for transport is the amount being produced each minute by thorium-230.

The calculations begin with known measured values at the spring: the concentration of radium in water, and the volume of water flow per minute. Multiplication of these values gives the rate at which the spring is yielding radium. We assumed that the amount of radium available for leaching is the radium being produced each minute. In addition, we assumed that all of the available radium is leached and carried to the surface; in other words, we assumed that the rate of radium yield at the spring is equal to the rate of radium production at the source. The amount of thorium-230 decaying to produce this radium can be calculated by using the half-life equation. The amount of uranium in equilibrium with the thorium-230 can then be determined by using the known equilibrium ratio.

Crystal Springs contain at least 220 μμg/l radium and flows at 6,800 l/min (Mundorff, 1970; Bjorklund and McGreevy, 1974); therefore, the springs yield radium at 1.5×10^6 g/min. By assumption, this rate of yield is equal to the rate of radium production at the source. A production rate of 1.5×10^6 g/min radium is equivalent to the decay rate of 1.5×10^6 g/min thorium-230. The proportion of any amount of thorium-230 (half life 8.0×10^4 years) decaying each minute is 1.7×10^{11}. If 1.5×10^6 g thorium-230 decays each minute, then the amount of thorium-230 present is 9.3×10^4 g. Assuming secular equilibrium (1 g uranium balanced by 1.7×10^5 g thorium-230), the amount of uranium required to maintain the present production of radium at Crystal Springs is at least 5.5×10^9 g, or 5,500 metric tons.

The uranium occurs in either all or part of the total volume of rock involved in the flow of ground water to Crystal Springs. This volume can be estimated by using hydrologic data and geothermal techniques as applied to a flow model in the region of the springs. Regional ground-water flow is from the Wellsville Mountains in the Wasatch Range westward to the lower Bear River valley and the Great Salt Lake. Because the regional flow is westward, saline water in the basin sediments is not likely to flow eastward to contribute any large quantity of water to Crystal Springs. The water at the springs rises along a fault zone at the mountain front and is probably composed mostly of deeply circulating meteoric water that may have come in contact with a cooling magma chamber or with rocks heated by an intrusive igneous complex. Some magmatic water may enter the system at depth, but lack of hydrogen- and oxygen-isotope data makes evaluation of the contribution unfeasible.

The total volume of rock involved in the flow to Crystal Springs is on the order of 10 km^3. The mass of rock, assuming an average density of 2.8 g/cm^3, is thus about 10^{16} g. The length of the volume is 5-10 km, the width is 1-3 km, and the thickness is 1-2 km. The length was measured parallel to the flow direction, or eastward from the springs; the width was measured perpendicular to the flow direction, along the surface-water divide; the thickness was measured by estimating depth of water circulation on the basis of geothermometry (Fournier and Truesdell, 1973, 1974) and geothermal gradient (Bjorklund and McGreevy, 1974).

Whether the uranium is disseminated or concentrated in the source rock is uncertain. If the calculated 5.5×10^9 g uranium were disseminated in 10^{16} g of rock, the content

would be 0.55 ppm, less than the crustal average of 2-4 ppm. Inasmuch as porosity and permeability in the sedimentary-metamorphic terrane of the Wellsville Mountains are controlled mostly by joints and fractures, water flowing through these openings comes in contact with only a small percentage of the total rock. By assuming that the radium is derived from uranium in restricted zones adjacent to fractures and joints, considerably higher potential grades of uranium in the rock can be calculated. The grade would be 0.55 percent if the 5,500 metric tons of uranium were concentrated in 1 percent of a fracture system comprising 1 percent of the volume of rock assumed to be leached by the spring water.

Bjorklund, L. J., and McGreevy, L. J., 1974, Ground-water resources of the lower Bear River drainage basin, Box Elder County, Utah: Utah Dept. Nat. Resources Tech. Pub. 44, 65 p.

Cadigan, R. A., and Felmlee, J. K., 1977, Radioactive springs geochemical data related to uranium exploration: Jour. Explor. Geochemistry (in press).

Fournier, R. O., and Truesdell, A. H., 1973, An empirical Na-K-Ca geothermometer for natural waters: Geochim. et Cosmochim. Acta, v. 37, no. 5, p. 1255-1275.

_____1974, Geochemical indicators of subsurface temperature--part 2, Estimation of temperature and fraction of hot water mixed with cold water: U.S. Geol. Survey Jour. Research, v. 2, no. 3, p. 263-270.

Mundorff, J. C., 1970, Major thermal springs of Utah: Utah Geol. and Mineralog. Survey Water-Resources Bull. 13, 60 p.

O'Connell, M. F., and Kaufmann, R. F., 1976, Radioactivity associated with geothermal waters in the Western United States--Basic data: U.S. Environmental Protection Agency, Office of Radiation Programs, Tech. Note ORP/LV-75-8A, 25 p.

THINNING OF THE FOX HILLS SANDSTONE, CROOK COUNTY, WYOMING--A POSSIBLE GUIDE TO URANIUM MINERALIZATION

By H. W. Dodge, Jr., and C. W. Spencer
U.S. Geological Survey, Denver, Colo.

Uranium mineralization occurs in the Fox Hills Sandstone of Late Cretaceous age in the eastern Powder River Basin, northeastern Wyoming. The Fox Hills is a sequence of marginal marine to estuarine and possibly tidal-flat deposits which were deposited during the eastward regression of the Upper Cretaceous Pierre Sea. The Fox Hills Sandstone consists of an upper and lower unit in the area of mineralization. The lower unit is not known to contain uranium and consists of offshore-marine and transitional-marine shale, siltstone, and fine-grained sandstone that grade upward into submarine-shoreface and tidal-beach sandstones. The upper unit locally is uranium-bearing and is composed largely of organic, thin-bedded claystone, siltstone, and sandstone considered to be deposited in estuarine and possibly tidal-flat environments. The upper unit is interpreted to have been deposited during and following a period of fluvial erosion that cut into the previously deposited lower unit. The upper unit grades into the overlying Lance Formation (Upper Cretaceous) that is composed predominantly of fresh-water delta-plain deposits.

The marine-transitional lower unit of the Fox Hills thins both regionally and locally. There is a regional northward depositional thinning from about 200 m near Lance Creek in central Niobrara County, Wyo., to a thickness of 40-50 m in west-central Crook County, Wyo. This regional thinning is attributed to slightly greater subsidence rates in the south (Niobrara County) with resultant vertical repetition of early Fox Hills paleoenvironments; to the north, less rapid subsidence did not favor a thick accumulation of lower unit sediments. Local erosional thinning of this unit is seen in an isopach map of the lower unit of the Fox Hills, prepared from approximately 100 petroleum test-well electric logs in west-central Crook and northeastern Campbell Counties, Wyo. The pattern of the isopachs shows an erosional thinning of the lower unit superimposed on the regional northward depositional thinning of the formation. The erosional pattern is interpreted to represent an easterly draining dendritic system as much as 20 km wide, 25-30 km long, and as much as 40 m deep.

On the basis of cores and logs from exploratory holes, uranium mineralization is known to be present east of and associated with this easterly draining dendritic system. Interpretation of these cores shows mineralization in estuarine and associated sediments of the upper unit. It is believed that low-density plant matter was carried into estuaries and associated environments by high-energy fluvial systems. Upon reaching the low-energy drowned valleys, the

organic matter was dropped out of suspension. This organic material was a focal point for later uranium mineralization.

If these observations hold for this area they may also be true for other areas, leading to the proposition that regional thinning of regressive sandstones, coupled with evidence of fluvial-estuarine erosion and deposition, constitute a possible guide to the location of uranium mineralization.

Though the exact time of mineralization is not known, many alternatives could be offered for the uranium source and time of emplacement; however, on the basis of present data we interpret the following sequence of events for the area of mineralization:

1. Deposition of Upper Cretaceous marine shales of the Pierre Shale.
2. Shallowing of marine waters (regressive cycle).
3. Deposition of transitional and marginal-marine sediments (lower unit of Fox Hills Sandstone).
4. Development of a fluvial-estuarine system.
5. Deposition of locally organic-rich thin-bedded claystone, siltstone, and sandstone in estuarine and associated environments (upper unit).
6. Deposition of overlying fluvial and delta-plain deposits (Lance Formation).
7. Deposition of Tertiary Fort Union and Wasatch Formations.
8. Erosion and truncation of westward-dipping Fox Hills and younger formations.
9. Deposition of uranium-rich semipermeable White River Formation (Oligocene).
10. Uplift and ground-water leaching of uranium coupled with hydrodynamic flow into westward-dipping highly permeable lower unit of the Fox Hills.
11. Reduction and precipitation of uranium minerals in the adjacent organic-rich upper unit of the Fox Hills.

URANIUM EXPLORATION USING HELIUM DETECTION--A CASE STUDY

By G. M. Reimer, U.S. Geological Survey,
Denver, Colo.

In order to provide a case study of the application of helium-detection methods to uranium exploration, a roll-type uranium deposit in Weld County, Colo., was investigated by both water and soil-gas sampling. The general geologic setting of the Weld County uranium deposit is discussed by Reade (1976). The deposit is low grade, near the surface, and below the ground-water table, which is about 10 m below the surface. Eighteen water samples and 200 soil-gas samples, collected in the vicinity of the uranium deposit, were analyzed for helium using the mobile helium detector developed by the U.S. Geological Survey (Reimer, 1976). This instrument consists of a small mass spectrometer installed in place of the rear seat for a four-door pickup truck. The inlet system of the spectrometer was modified slightly to accommodate the sample collecting scheme used for both water and soil gas. This mobile laboratory has the capability to analyze samples within a few minutes at the field location, and the results of the analyses can be used immediately to guide the direction of exploration.

Subsurface water samples were collected wherever a source was available, such as domestic- or stock-supply wells. Eighteen samples were collected from an 80-km^2 area. The shallow stock-supply wells, ranging from 3-10 m deep, showed low helium values. Domestic wells, about 25 m deep, that were on the down-gradient side of ground-water flow relative to the uranium deposit, had higher helium concentrations than those on the up-gradient side. All helium concentrations in the water samples analyzed in this Weld County study were anomalously high when compared to atmospheric-equilibrated values. The high values are consistent with the magnitude of anomalies found to be associated with other uranium deposits by Dyck (1976) and Pogorski, Quirt, and Blascheck (1976). Because the ground-water anomaly can be detected over a large area, helium detection using ground water may be an extremely valuable regional reconnaissance technique. Maintaining sampling control is difficult when collecting water, turbulence and mixing with air are the largest problems encountered. Those actions scrub the dissolved gases from the water and are, in fact, employed in the technique used to remove the gas from the sample for our analysis. Consequently, a certain degree of qualitative evaluation must be used in the interpretation of the analytical results. Shallow wells and turbulent water generally have low helium concentrations.

The soil-gas investigations incorporated two basic sampling patterns: (1) to obtain information on the regional helium distribution, sample spacing was on 3.2- and 1.6-km centers; (2) in the immediate vicinity of the uranium deposit, sample spacing was on about 320-m centers. The range of helium values in the regional soil-gas study was distinctly greater than that of the values taken near the uranium deposit. This difference in range suggests that the background helium concentration changes regionally and widely

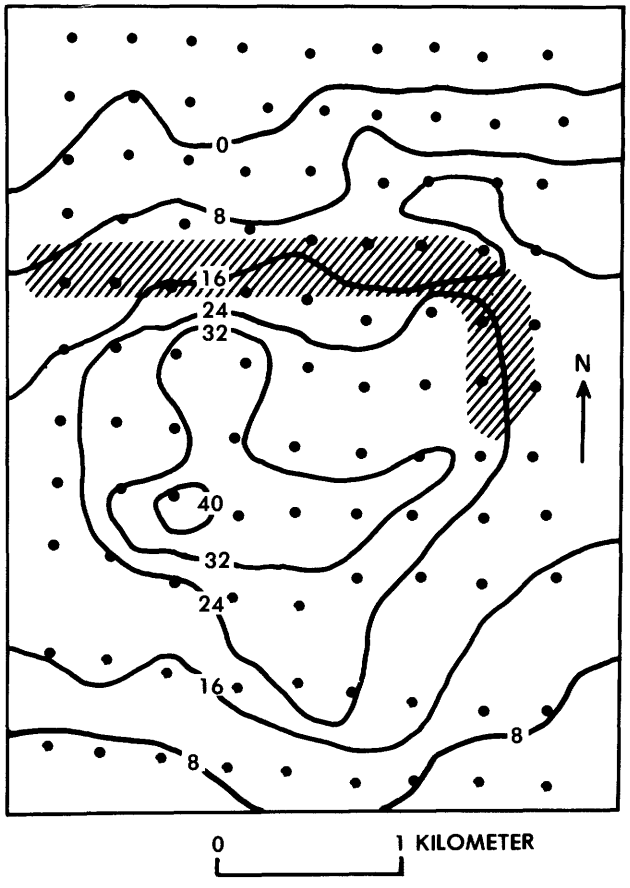

Figure 1.--Contour map of helium in soil gas in the vicinity of the Weld County, Colo., roll-type uranium deposit. Contour interval is 8 ppm. The base value for the atmosphere is 5,239 ppb. The highest anomaly is displaced about 1.5 km from the roll front (cross-hatched area). Ground-water flow is presently to the southwest. Sample locations are shown by dots.

spaced soil-gas sampling does not provide much useful information, a direct contrast to the water-sampling results. The closely spaced soil-gas sampling over the uranium deposit produced a more consistent pattern. Parts of this survey were repeated on three separate occasions over a three-month period to allow us to consider the effects of the temporal variations in soil-gas helium content that have been observed in other studies (Reimer and others, 1976). These replicate surveys demonstrated the reproducibility of the pattern of the anomaly. The raw data indicated a density of higher helium values roughly centered about 2 km from the uranium roll front in the direction of ground-water flow. A very simple statistical averaging technique was used to enhance the plotted data. The value of any one sample point is influenced by the average of all the neighboring sample values, weighted by their relative distances from the central point. This statistical approach resulted in a contour map (fig. 1) that minimizes the effects of spurious values that may be the result of localized structural or other controls. The map summarizes the soil-gas data and demonstrates an important point, that the center of the anomaly may not correspond to the location of the ore deposit. In the Weld County study, ground-water flow is probably a factor controlling the displaced location of the anomaly.

The positive results of the preliminary studies indicate that helium detection in both water and soil-gas samples can make a significant contribution to an integrated geochemical and geophysical exploration program.

Dyck, Willy, 1976, The use of helium in mineral exploration: Jour. Geochem. Explor., v. 5, no. 1, p. 3-20.

Pogorski, L. A., Quirt, G. S., and Blascheck, J. A., 1976, Helium surveys--A new exploration tool for locating uranium deposits: Toronto, Ontario, Chem. Proj. Ltd., Tech. Paper CPL-6/76, 27 p.

Reade, H. L., Jr., 1976, Grover uranium deposit--a case history of uranium exploration in the Denver Basin, Colorado: Mtn. Geologist, v. 13, no. 1, p. 21-31.

Reimer, G. M., 1976, Design and assembly of a portable helium detector for evaluation as a uranium exploration instrument: U.S. Geol. Survey Open-File Rept. 76-398, 18 p.

Reimer, G. M., and Otton, J. K., 1976, Helium in soil gas and well water in the vicinity of a uranium deposit, Weld County, Colorado: U.S. Geol. Survey Open-File Rept. 76-699, 10 p.

Reimer, G. M., Roberts, A. A., and Denton, E. H., 1976, Diurnal effects on the helium concentration in soil-gas and near-surface atmosphere: U.S. Geol. Survey Open-File Rept. 76-715, 9 p.

GEOCHEMICAL INTERPRETATION OF ORE ZONATION AT THE RIFLE VANADIUM MINE, COLORADO

By Dennis J. LaPoint and Gergeley Markos
Department of Geological Sciences
University of Colorado
Boulder, Colorado 80309

The Rifle vanadium deposits are located along East Rifle Creek about 13 miles northeast of Rifle, Colo., on the southern flank of the White River Plateau. Fischer (1960) described the deposit and suggested that uranium-vanadium-lead-selenium-chromium mineralization occurred at an S-shaped interface between two fluids (fig. 1), but he recognized no evidence to suggest the source of mineralizing solutions or the elements they contained.

The compositions reported in table 1 for vanadium clay minerals are based on analyses by Foster (1959), and the compositions of chromium clay minerals are assumed to be analogous to those of vanadium because of the similarity in site occupancy in the clay mineral structure. Thermodynamic calculations are computed according to the method described by Markos (1977); Gibbs free energies of clay minerals are calculated using the method described by Tardy and Garrels (1974), and the Gibbs free energy for galena-clausthalite solid solution is estimated for Pb ($S_{0.5}$ $Se_{0.5}$) from data published by Coleman (1959).

Although we are discussing the mixing of two fluids, one of which is warm and saline, calculations are based on a temperature of 25°C, and the activity of water was set at one with no corrections for salinity, temperature, or pressure. It should also be noted that no attempt was made to calculate concentrations, which may have values significantly different from activities in saline waters. Changes of two orders of magnitude in the assumed activities do not alter the interpretations.

At the zone of fluid interaction, ore minerals precipitated due to three causes: (1) cooling of the brine,

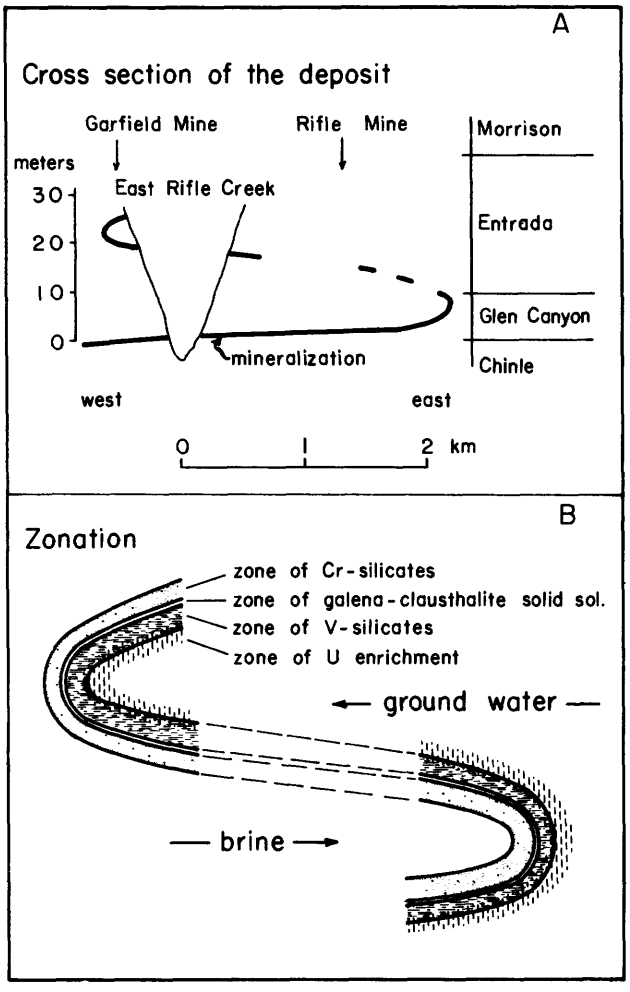

Figure 1.--(A) Cross section of the Rifle vanadium deposit in Jurassic and Triassic rocks. Modified from Fischer (1960). (B) Idealized representation of metal zonation and directions of water movement.

(2) dilution of the brine, and (3) the availability of ions in amounts sufficient to form the observed minerals. The first two causes can only be evaluated indirectly at this time. As the brine cooled and mixed with the ground water, chloride complexes became unstable and the water was oversaturated in elements carried as complexes.

Vanadium, as roscoelite, is the major ore mineral in the Rifle deposit. In the formation of roscoelite, if vanadium is carried as V^{+4}, it can be reduced to V^{+3} in the mica structure. Calculations show V^{+5}, which can be carried in oxidizing ground water, will not be reduced to V^{+3} to form mica. Likewise, Cr^{+3} is required to form mariposite, the dominant mineral of the chromium zone. Mariposite forms

Table 1.--*Gibbs free energies of formation (calculated for this paper) and composition of minerals*

Minerals	ΔG_f^o kcal/mole (25°C, 1 atm)
A. Vanadium minerals	
V-mica-montmorillonite mixed layer mineral $(Al_{0.57}V^{4+}_{0.82}Fe^{2+}_{0.2}Mg_{0.25})(Si_{3.17}Al_{0.83})O_{10}(OH)_2K_{0.95}$	-1241.16
Roscoelite $(Al_{1.13}V^{3+}_{0.72}Fe^{2+}_{0.1}Mg_{0.05})(Si_{3.25}Al_{0.75})O_{10}(OH)_2K_{0.8}H_{0.1}$	-1271.255
Montroseite VO(OH)	-163.5
B. Chromium minerals	
Volkhonskoite $(Al_{0.8}Cr^{3+}_{0.6}Fe^{2+}_{0.4}Mg_{0.4})(Si_{3.2}Al_{0.8})O_{10}(OH)_2K_{0.6}Ca_{0.1}Mg_{0.1}$	-1267.39
Mariposite $(Al_{1.13}Cr^{3+}_{0.72}Fe^{2+}_{0.1}Mg_{0.05})(Si_{3.25}Al_{0.75})O_{10}(OH)_2K_{0.8}H_{0.1}$	-1263.767
C. Lead mineral	
Galena-clausthalite solid solution $Pb(S_{0.5}Se_{0.5})$	-23.95
D. other	
Illite $(Al_{1.85}Fe^{2+}_{0.1}Mg_{0.05})(Si_{3.25}Al_{0.75})O_{10}(OH)_2K_{0.8}H_{0.1}$	-1313.015

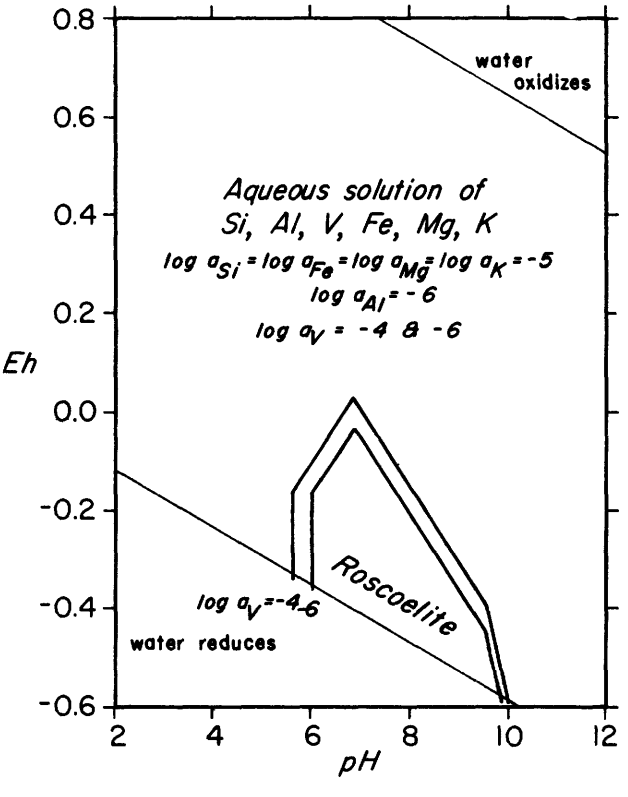

Figure 2.--The Eh-pH field for the formation of roscoelite from solution. An increase in the activity of vanadium expands the field for roscoelite. A low oxidation potential and neutral to alkaline pH is required to form roscoelite from solution.

easily over a broad range of Eh-pH conditions which roscoelite has a narrow stability field (fig. 2).

The equilibrium ratio of chromium to vanadium for coexisting mariposite and roscoelite is strongly pH dependent (fig. 3). The zonation of chromium and vanadium micas is therefore probably due to exhaustion of chromium in solution or to a rapid and pronounced decrease of pH. Both minerals are similar in composition and structure to illite, but the presence of chromium or vanadium prevents the precipitation of illite at pH values greater than six and eight, respectively.

In the vanadium zone, the relative stability between montroseite and roscoelite is controlled by pH and the activities of silica and aluminum. At low pH, unreasonably high amounts of silica are needed to form vanadium mica. Calculations indicate that vanadium montmorillonite is not formed from solution, but instead it is secondary, post-depositional transformation of roscoelite at a pH below 6.5 to 7.1. Both chromium mica and montmorillonite minerals are likely to form from solution; however, the chromium mica is preferred.

The small amounts of uranium present in the orebody make the determination of its mineralogy difficult (Fischer, 1960). A study of potential source rocks and ore fluids suggest the uranium was carried in ground water as a carbonate complex. The absence of discrete uranium minerals may indicate that the uranium is adsorbed onto the vanadium clay minerals and calcite cement.

Galena-clausthalite solid solution forms when the sulfur activity and Eh are both relatively low in solution, and the solution is alkaline (Tischendorf and Ungethüm, 1963). Selenium, entering a reducing environment with lead and sulfur available,will readily precipitate in a narrow zone. This suggests that the galena-clausthalite zone represents the actual interface between the two solutions.

One of the fluids was a typical bicarbonate ground water that had a low temperature, slightly alkaline pH, and a high oxidation potential. Of the ore-forming elements, selenium and uranium may have been carried in this type of water. The overlying Morrison Formation of Jurassic age is proposed as the source of the water and these ore-forming elements. The second fluid was a warm, chloride brine which may have been derived from sediments of the Central Colorado Basin of late Paleozoic age. In the brine, major ions of importance were chloride, sodium, potassium, and magnesium. Iron, lead, chromium, and vanadium were also transported in this brine. Sulfur could have been transported in either fluid. Chemical calculations support the hypothesis that two fluids of very different composition interacted to cause the Rifle deposit.

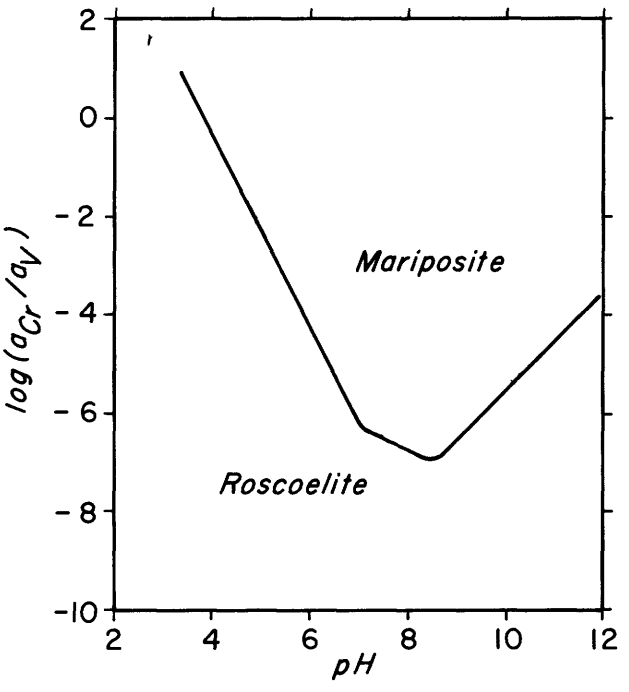

Figure 3.--A comparison of equilibrium activities of vanadium and chromium in the formation of mica minerals as a function of pH. At pH 3.9 the activities of vandium and chromium are equal. At pH 7, mariposite will form even if the activity of chromium is as little as one millionth of the activity of vanadium.

Coleman, R. G., 1959, The natural occurrence of galena-clausthalite solid solution series: Am. Mineralogist, v. 44.

Fischer, R. P., 1960, Vanadium-uranium deposits of the Rifle Creek area, Garfield County, Colorado: U.S. Geol. Survey Bull. 1101, 52 p.

Foster, H. D., 1959, Chemical study of the mineralized clays: U.S. Geol. Survey Prof. Paper 320, p. 121-132.

Markos, G., 1977, Geochemical alteration of plagioclase and biotite in glacial and periglacial deposits: Univ. Colo. Ph.D. thesis.

Tardy, Y., and Garrels, R. M., 1974, A method of estimating Gibbs energies of formation of layer silicates: Geochim. et Cosmochim. Acta, v. 38, p. 1106-1116.

Tischendorf, G., and Ungethüm, H., 1963, Uber die bildungsbedingungen von clausthalit-galenit und bemerkungen zur selenverteilung im galenit in abhängigkeit vom redoxpotential und vom pH-wert: Chemie Erde, v. 23, p. 279-311.

ASSAY FOR URANIUM AND MEASUREMENT OF DISEQUILIBRIUM BY MEANS OF HIGH-RESOLUTION GAMMA-RAY BOREHOLE SONDES

By Allan B. Tanner, Robert M. Moxham, and Frank E. Senftle
U.S. Geological Survey, Reston, Va. 22092

In-hole assay has been done by measurement of gamma radiation since the early days of uranium exploration. Because detectors used are most sensitive to the radioactivity of nuclides far down the decay chain of the uranium and thorium series, radioactive disequilibrium or significant concentrations of thorium result in assay erors that can be significant.

Gamma-ray detectors made of germanium have been in laboratory use for a decade. They are capable of resolving most of the numerous natural X-rays and gamma rays, and in principle they can measure uranium directly, without regard to the state of radioactive equilibrium. There has been some reluctance to use these high-resolution detectors in the field because they are expensive, require sophisticated electronics and data reduction, and must be cooled to liquid-nitrogen temperature for operation. The germanium detector has been adapted to the borehole environment by substituting melting propane (85 K) for boiling nitrogen (77 K) as the coolant, thus enabling the detector sonde to be sealed for operation underwater. In the 1975 Uranium and Thorium Research and Resources Conference, we reported the design of such a sonde and some laboratory borehole measurements made with it; we report here the results of field measurements made using it and an earlier sonde in boreholes in a uranium deposit near Pawnee, Bee County, Tex. The two sondes are intended for different uses: one houses a high-purity, or "intrinsic," germanium disc about 5 mm thick and 500 mm^2 in area, and is best suited to measurement of radiations in the range of the X-rays of the heavy elements and low-energy gamma rays; the other houses a lithium-compensated, or "Ge(Li)," germanium cylinder with a volume of 45 cm^3, and is suited to measurements of gamma rays of higher energy than the X-rays.

Because far fewer gamma rays per unit time are received from any one radioactive species than from all species combined, spectrometry requires longer counting periods than total counting to achieve the same statistical accuracy. Routine, top-to-bottom logging of a particular gamma-ray energy at a feasible speed of only a few meters per hour is unacceptably slow. For delimiting zones worth investigating by high-resolution spectrometry, we recorded total counts received during successive 10-second periods while the sonde moved continuously at about 1 m per minute. The resulting log is comparable in definition and statistical quality to the conventional scintillation log.

Having used rapid, total-count, continuous-motion logging to find the zones of greatest activity, we shifted to 10-minute accumulations of spectra in a pulse-height analyzer. The data were transferred to magnetic cassettes during movement of the sonde from one station to the next. Data reduction by the minicomputer takes about 5 minutes and could be done during the station if desired.

Assay for uranium was tried using the 63.3-keV gamma ray of ^{234}Th and the 1001.4-keV gamma ray of ^{234m}Pa. The short half lives of these isotopes (24.1 days and 1.175 minutes, respectively) imply that they reach equilibrium in a few months after deposition of the parent ^{238}U and that they should be reliable measures of the concentration of the parent in solid deposits. Although nearly 10 times as many 63.3-keV as 1001.4-keV gamma rays are emitted from a given sample, the 1001.4-keV gamma rays reach the detector from greater distances in the wall rock of a borehole, and the detector used is more efficient; consequently, the counting rates from the two gamma rays are nearly equal. The same general pattern of ^{238}U distribution is inferred from logs of the 63.3-keV and the 1001.4-keV gamma rays, but they show significant differences in detail. We believe that the differences are due less to instrumental error than to the approximately fivefold difference in mass effectively sampled by the two detectors.

Calibration was done by comparing the intensity of the 1001.4-keV gamma radiation at a location in the borehole with that from a core sample from the same location and, in turn, with that from standard samples. The result was 9 percent lower than the result of fluorimetric analysis of the split of core closest to the same location. The combined sampling and analytical errors of the fluorimetric analysis may exceed the 9 percent difference.

The sensitivity of the method is estimated at about 80 ppm U_3O_8 when the 1001.4-keV gamma ray is measured for a counting period of 10 minutes. We base the estimate on the concentration at which our data reduction program just rejects the 1001.4-keV peak when a one-standard-deviation test is imposed.

High-resolution gamma-ray spectrometry is unique because it offers an in situ method of determining the state of equilibrium in the ^{238}U and ^{235}U series by simultaneous measurements using a single detector. Of the six isotopes or groups capable of independent behavior over geologically important periods of time, five can be evaluated

unambiguously by at least one gamma ray; the remaining one, ^{226}Ra, can be evaluated if a correction is made for ^{235}U.

We investigated four boreholes alined approximately in the direction of the dip. The borehole most updip penetrated a thin upper ore zone and both "limbs" of a lower-ore-zone roll. The next hole penetrated a 3-m-thick upper ore zone and a 5-m-thick lower ore zone. The lower ore zone in this second hole contained the highest grade ore found in any of the four holes. The two holes farther downdip encountered progressively lower grades of ore in both ore zones. Spectra were taken in all ore zones of the first two holes and in the lower ore zone of the last two holes.

The ^{222}Rn group, as measured by ^{214}Bi, is present in excess of equilibrium at the inner boundaries of the roll limbs in the first hole, at both boundaries of both ore zones in the second hole, and at both boundaries of mineralization in the two holes downdip. At each location, the ^{222}Rn group is deficient to some extent between the ore zones. The results for ^{226}Ra are not consistent enough to apportion the causes of the uneven ^{222}Rn group distribution between radium migration and radon migration.

An intermediate decay product, ^{230}Th, in the ^{238}U series, is relatively deficient in the middle of the lower ore zone in the hole penetrating the ore of highest grade, but is in relative excess toward the upper and lower boundaries of that zone. On the basis of preliminary determination of the relative intensities of the 63.3-keV ^{234}Th and 67.7-keV ^{230}Th gamma rays in borehole geometry, we infer that ^{230}Th is present in threefold or greater excess at the two locations. If this is true, ^{234}U--and almost certainly ^{238}U of commensurately higher concentration--must have been dispersing from those locations for about the last 80,000 years, a time span comparable to the half life of

The ^{231}Pa group of the ^{235}U series, controlled by the 34,300-year half life of ^{231}Pa, is also apparently present in excess of equilibrium toward the lower boundary of the main ore zone, as is the ^{230}Th. However, an excess of the ^{231}Pa group was not found near the upper boundary of this zone. Such a difference in the relative proportions of ^{230}Th and the ^{231}Pa group could arise if leaching of the uranium isotopes from the upper part of the main ore zone had started earlier or progressed faster than in the lower zone.

REFINEMENT OF THE THERMODYNAMIC PROPERTIES OF URANIUM MINERALS AND DISSOLVED SPECIES, WITH APPLICATION TO THE CHEMISTRY OF GROUND WATERS IN SANDSTONE-TYPE URANIUM DEPOSITS

By Donald Langmuir[1] and Kenneth Applin[2]
Department of Geosciences
The Pennsylvania State University
University Park, Pa. 16802

Hostetler and Garrels (1962) examined the solubility of four uranium minerals dissolving to form seven uranium-bearing species in water. In our study, thermodynamic data have been collected and critically evaluated for a total of 25 minerals and 42 dissolved species of uranium. This expanded, updated listing permits a far more detailed appraisal of the low-temperature aqueous geochemistry of uranium than before possible. The data show that complexing of uranyl (UO_2^{2+}) and uranous (U^{4+}) ions is the rule in natural waters, and is more important than generally realized. The existence and stability of these complexes indicates that the mobility of uranium in water may be enhanced under a wide variety of conditions. The study also shows that the solubility of uraninite (and coffinite) is about 8 to 10 orders of magnitude less than was indicated by Hostetler and Garrels. This suggests that, for a given Eh and pH, precipitation of these minerals can occur from ground waters far more dilute in uranium than usually assumed.

Table 1 lists the thermochemical data for uranium minerals and aqueous species at 25°C and 1 atmosphere total pressure. The data have been computed using values for non-uranium species listed in Wagman and others (1968, 1969, 1971, and 1976) and Parker and others (1971); they are considered internally consistent, with the exception of $\Delta G_f°$ for H_2PO_4, which should be -270.17 kcal/mol. The thermochemical values for U^{4+}, UO_2^{2+} ions, and for uraninite, $UO_{2.67}$ (1/3 U_3O_8), and γ-UO_3 are the only ones accepted as given by their sources. Thermodynamic properties of all other solutes and solids have been computed or estimated from

[1]Professor of Geochemistry.
[2]Graduate Research Assistant.

TABLE 1.--*Thermochemical data for uranium minerals and aqueous species at 25°C and 1 atm total pressure*

[Parentheses on entropy (S°) values indicate uncertainty greater than ±5 cal/mol deg. Enthalpies (ΔH_f°) calculated from these uncertain values are also enclosed in parentheses]

Mineral or Aqueous Species	ΔH_f° (Kcal/mol)	ΔG_f° (Kcal/mol)	S° (cal/mol deg)	Source
U^{4+}	-141.3	-126.9	-99	Fuger and Oetling, 1976.
UOH^{3+}	-197.9	-182.7	-46	Baes and Mesmer, 1976.
$U(OH)_2^{2+}$	-259.7	-236.7	-16.5	Do.
$U(OH)_3^+$	(-322.9)	-289.0	(3)	Do.
$U(OH)_4^\circ$	(-387.3)	-339.6	(12)	Do.
$U(OH)_5^-$	(-451.4)	-388.5	(17)	Do.
$U_2(OH)_5^{3+}$	----	-529.4	----	Do.
UO_2(c) uraninite	-259.3	-246.6	18.41	V. B. Parker, oral commun., 1977.
UO_2(am)	----	-233.7	----	
$UO_{2.67}$(c)	-284.8	-268.5	22.51	V. B. Parker, oral commun., 1977.
$USiO_4$(c) coffinite	-478	-452.0	28.4	
$USiO_4$(am)	----	-439.2	----	
UF^{3+}	-216.3	-205.8	-46	Ahrland and others, 1973.
UF_2^{2+}	-292.7	-279.6	-15	Do.
UF_3^+	-371.6	-352.0	3	Do.
UF_4°	-453.3	-424.5	12	Do.
UF_5^-	-532.5	-493.3	17	Do.
UF_6^{2-}	-613.2	-563.1	20	Do.
UCl^{3+}	-168.3	-157.1	-46	Naumov and others, 1974
USO_4^{2-}	(-341.5)	-309.9	(-20)	Ahrland and others, 1973.
$U(SO_4)_2^\circ$	(-554.6)	-491.1	(10)	Do.
$UHPO_4^{2+}$	(-439.1)	-403.6	(-15)	Moskvin, Essen, and Bukhtiyarova, 1967.
$U(HPO_4)_2^\circ$	(-750.2)	-677.6	(15)	Do.
$U(HPO_4)_3^{2-}$	(-1065)	-949.7	(25)	Do.
$U(HPO_4)_4^{4-}$	(-1389)	-1221	(5)	Do.
$U(HPO_4)_2 \cdot 4H_2O$(c)	-1029	-910.9	85	Do.
$CaU(PO_4)_2 \cdot 2H_2O$(c) ningyoite	-1016	-933.4	70	Muto, 1965.
UO_2^{2+}	-243.5	-227.7	-23.2	Fuger and Oetling, 1976.
UO_2OH^+	-299.0	-277.5	13.3	Nikitin and others, 1972.
$UO_2(OH)_2^\circ$	-361.6	-324.3	16.1	Do.
$UO_2(OH)_3^-$	(-418.6)	-365.6	(19)	Naumov and others, 1974.
$UO_2(OH)_4^{2-}$	(-471.7)	-402.9	(22)	Do.
$(UO_2)_2(OH)_2^{2+}$	-610.3	-561.0	5.5	Nikitin and others, 1972.
$(UO_2)_3(OH)_5^+$	-1047	-945.2	26.7	Baes and Mesmer, 1976.
γ-UO_3(c)	-292.5	-273.9	22.97	Fuger and Oetling, 1976; V. B. Parker, oral commun., 1977.
UO_3(am) gummite	-288.8	-270.2	23.1	Nikitin and others, 1972; Fuger and Oetling, 1976.
β-$UO_2(OH)_2$(c)	-365.8	-332.7	29.9	Nikitin and others, 1972.
$UO_2(OH)_2 \cdot H_2O$(c) schoepite	-435.7	-389.6	41.9	Do.
UO_2CO_3(c) Rutherfordine	-404.7	-373.3	32.0	Sergeyeva and others, 1972.
$UO_2CO_3^\circ$	-404.2	-367.3	12.1	Do.
$UO_2(CO_3)_2^{2-}$	-563.3	-502.8	39.1	Do.
$UO_2(CO_3)_3^{4-}$	(-737.8)	-635.4	(4.4)	Do.
UO_2F^+	-323.1	-301.1	-4.5	Naumov and others, 1974; Ahrland and others, 1973.
$UO_2F_2^\circ$	-403.8	-373.7	8.3	Do.
$UO_2F_3^-$	-486.0	-446.4	16.5	Do.
$UO_2F_4^{2-}$	-567.4	-516.5	18.2	Do.
UO_2Cl^+	-282.2	-259.4	-4.5	Naumov and others, 1974.
$UO_2SO_4^\circ$	-455.8	-409.4	10.8	Lietzke and Stoughton, 1960.
$UO_2(SO_4)_2^{2-}$	-672.2	-589.4	25.4	Do.
$(UO_2)_3(PO_4)_2$(c)	-1328	-1237	92	Chukhlantsev and Alyamovskaya, 1961.
UO_2HPO_4(c)	-548.3	-504.7	38	Sillen and Martell, 1964.
$UO_2HPO_4^\circ$	(-550.9)	-499.5	(12)	Moskvin, Shelyakina, and Perminov, 1967.
$UO_2(HPO_4)_2^{2-}$	(-865.9)	-773.7	(30)	Do.
$UO_2H_2PO_4^+$	(-552.5)	-502.0	(15)	Marcus, 1958.
$UO_2(H_2PO_4)_2^\circ$	(-870.6)	-775.5	(20)	Do.
$UO_2(H_2PO_4)_3^-$	(-1188)	-1048	(25)	Do.
$H_2(UO_2)_2(PO_4)_2$(c) H-autunite	-1098	-1011	76	Muto and others, 1968.
$Na_2(UO_2)_2(PO_4)_2$(c) Na-autunite	-1216	-1136	91	Do.
$K_2(UO_2)_2(PO_4)_2$(c) K-autunite	-1229	-1147	94	Vesely and others, 1965.
$(NH_4)_2(UO_2)_2(PO_4)_2$(c) uramphite	----	-1051	----	Chukhlantsev and Stepanov, 1956; Karpov, 1961.
$Mg(UO_2)_2(PO_4)_2$(c) saléeite	-1194	-1116	83	Muto and others, 1968.
$Ca(UO_2)_2(PO_4)_2$(c) autunite	-1219	-1141	85	Do.
$Sr(UO_2)_2(PO_4)_2$(c) Sr-autunite	-1220	-1142	88	Do.
$Ba(UO_2)_2(PO_4)_2$(c) uranocircite	-1206	-1168	89	Do.
$FE(UO_2)_2(PO_4)_2$(c) bassetite	-1101	-1024	86	Do.
$Cu(UO_2)_2(PO_4)_2$(c) torbernite	-1050	-972.8	86	Do.
$Pb(UO_2)_2(PO_4)_2$(c) przhevalskite	-1071	-993.4	91	Do.
$K_2(UO_2)_2(VO_4)_2 \cdot 3H_2O$(c) carnotite	-1385	-1267	134	Hostetler and Garrels, 1962.

published empirical results (chiefly stability constants) consistent with the tabulated properties of U^{4+} and UO_2^{2+} ions. Entropies of many aqueous species have been estimated. Entropies of coffinite and all the phosphate minerals have been estimated (probably to within ±5 cal/mol deg) using approaches described by Naumov and others (1974). Detailed explanation of the sources, methods of calculation and estimation of the data, and application of the data to uranium geochemistry will be presented in a future report.

The relative importance of different uranium complexes as a function of pH was assessed at 25°C and $P_{CO_2}=10^{2.0}$ or $10^{2.5}$ atm for some typical total ligand concentrations in ground water (F=0.2 or 0.3 ppm; Cl=10 ppm; SO_4=100 ppm; and PO_4=0.1 ppm). In the following discussion, complexes are termed "important" if they exceed 10 percent of the total concentration or uranous or uranyl species. A species is "predominant" if it comprises more than half the total of uranous or uranyl species. For uranous ion, calculations showed that the fluoride complexes are predominant at pH's below 3-4, and that hydroxyl complexes are predominant at higher pH's. Uranyl ion formed important complexes with

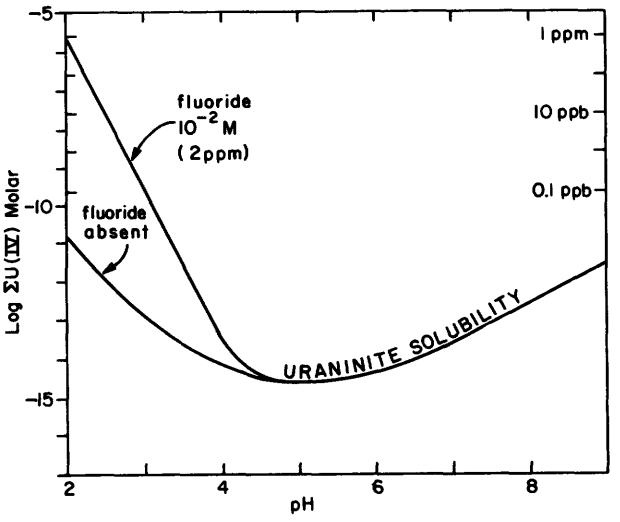

Figure 2.--Increase in uraninite solubility caused by uranous fluoride complexing at 25°C.

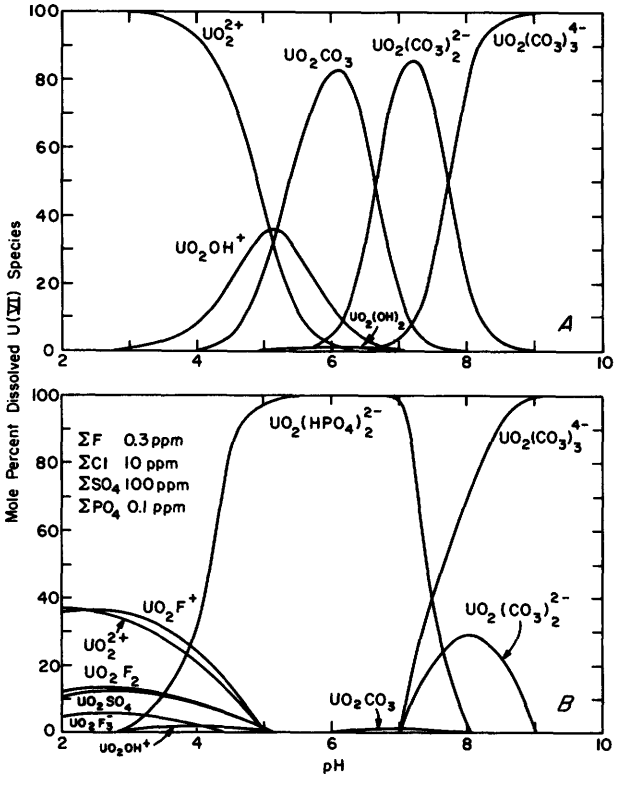

Figure 1.--Mole percent dissolved uranium vs pH for some uranyl complexes, at 25°C with $P_{CO_2}=10^{-2}$ (A), and $P_{CO_2}=10^{-2.5}$ (B).

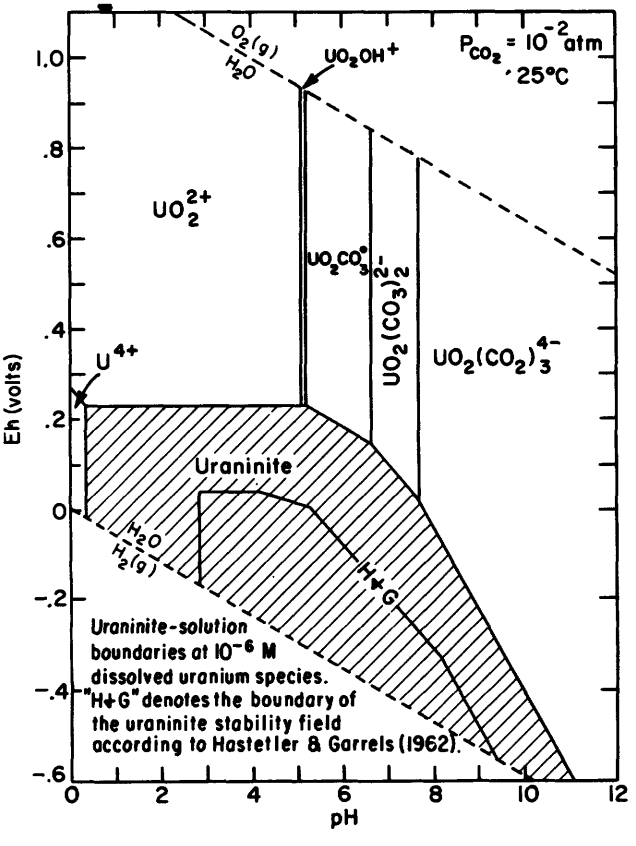

Figure 3.--The increased field of stability of uraninite indicated by our data (patterned area) compared with that indicated by data from Hostetler and Garrels (1962) (enclosed by line marked "H and G").

fluoride and sulfate at pH's below 4.5-5.5. The fluoride complexes predominated at pH's below about 4. The complex $UO_2(HPO_4)_2^{2}$ was surprisingly stable, and was the predominant uranyl species between about pH 4.5 and 7.5. In the absence of phosphate, uranyl carbonate complexes predominated at all pH's above 4.5, but in the presence of $UO_2(HPO_4)_2^{2}$ they only predominated above pH 7.5.

Figure 1 illustrates relations among some uranyl complexes. The increase in uraninite solubility caused by uranous fluoride complexing is shown on figure 2. The Eh-pH diagram on figure 3 compares the greater stability of uraninite indicated by our data to its stability computed using free-energy data listed in Hostetler and Garrels (1962).

Ahrland, S., Liljenzin, J. O., and Rydberg, J., 1973, Solution chemistry [of the actinides], in Comprehensive inorganic chemistry, v. 5, Actinides, Master Index: New York, Pergamon Press, p. 465-635.

Baes, C. F., Jr., and Mesmer, R. E., 1976, The hydrolysis of cations: New York, John Wiley & Sons, 489 p.

Chukhlantsev, V. G., and Alyamovskaya, K. V., 1961, Solubility product of uranyl, beryllium and cerium phosphates: Vyssh. Ucheb. Zavedeniy Izv. Khimiia i Khimicheskaia Tekhnologiia, v. 4, p. 359-363.

Chukhlantsev, V. G., and Stepanov, S. I., 1956, Solubility of uranyl and thorium phosphates: Zhur. Neorganicheskoi Khimii, v. 1, p. 478-484.

Fuger, J., and Oetling, F. L., 1976, The chemical thermodynamics of actinide elements and compounds--Part 2, The actinide aqueous ions: Vienna, Internat. Atomic Energy Agency, p. 16-20.

Hostetler, P. B., and Garrels, R. M., 1962, Transportation and precipitation of uranium and vanadium at low temperatures, with special reference to sandstone-type uranium deposits: Econ. Geology, v. 57, no. 2, p. 137-167.

Karpov, V. I., 1961, Solubility of neutral uranyl phosphate: Zhur. Neorganicheskoi Khimii, v. 6, p. 531-533.

Lietzke, M. H., and Stoughton, R. W., 1960, The solubility of silver sulfate in electrolyte solutions--VII, Solubility in uranyl sulfate solutions: Jour. Phys. Chemistry, v. 64, p. 816-820.

Marcus, Y., 1958, Anion exchange of metal complexes--the uranyl phosphate system: United Nations Internat. Conf. Peaceful Uses Atomic Energy, 2d., Proc., v. 3, p. 465-471.

Moskvin, A. I., Essen, L. N., and Bukhtiyarova, T. N., 1967, Complexing of tetravalent thorium and uranium in phosphate solutions: Zhur. Neorganicheskoi Khimii, v. 12, p. 3390-3392.

Moskvin, A. I., Shelyakina, A. M., and Periminov, P. S., 1967, Solubility product of uranyl phosphate--composition and dissociation constants of uranyl phosphate complexes: Zhur. Neorganicheskoi Khimii, v. 12, p. 3319-3325.

Muto, T., 1965, Thermochemical stability of ningyoite: Mineralog. Jour., v. 4, no. 4, p. 245-274.

Muto, T., Hirono, S., and Kurata, H., 1968, Some aspects of fixation of uranium from natural waters: Japan Atomic Energy Research Inst. Report NSJ Transl. No. 91, from Mining Geology, 1965, v. 15, p. 287-298.

Naumov, G. B., Ryzhenko, B. N., and Khodakovsky, I. L., 1974, Handbook of thermodynamic data: Natl. Tech. Inf. Service, U.S. Dept. of Commerce, Springfield, Va., 328 p.

Nikitin, A. A., Sergeeva, Z. I., Khodakovsky, I. L., and Naumov, G. B., 1972, Uranyl hydrolysis in a hydrothermal region: Geokhimiya, no. 3, p. 297-307.

Parker, V. B., Wagman, D. D., and Evans, W. H., 1971, Selected values of chemical thermodynamic properties: U.S. Natl. Bur. Standards Tech. Note 270-6, 119 p.

Sergeyeva, E. I., Nikitin, A. A., Khodakovsky, I. L., and Naumov, G. B., 1972, Experimental investigation of equilibria in the system UO_3-CO_2-H_2O in 25-200°C temperature interval: Geochemistry Internat., v. 9, p. 900-910.

Sillen, L. G., and Martell, A. E., 1964, Stability constants of metal-ion complexes: Spec. Pub. No. 17, The Chemical Society, Burlington House, London, 754 p.

Vesely, V., Pekarek, V., and Abbrent, M., 1965, Uranyl phosphates--IV, Sorption of some four-valent cations on ammonium uranyl phosphate: Jour. Inorganic Nuclear Chemistry, v. 27, p. 1419-1425.

Wagman, D. D., Evans, W. H., Parker, V. B., and Schumm, R. H., 1976, Chemical thermodynamic properties of compounds of sodium, potassium, and rubidium: U.S. Natl. Bur. Standards Interim Rept. 76-1034, 73 p.

Wagman, D. D., Evans, W. H., Parker, V. B., Halow, I., Bailey, S. M., and Schumm, R. H., 1968, Selected values of chemical thermodynamic properties: U.S. Natl. Bur. Standards Tech. Note 270-3, 264 p.

_____1969, Selected values of chemical thermodynamic properties: U.S. Natl. Bur. Standards Tech. Note. 279-4, 141 p.

Wagman, D. D., Evans, W. H., Parker, V. B., Halow, I., Bailey, S. M., Schumm, R. H., and Churney, K. L., 1971, Selected values of chemical thermodynamic properties: U.S. Natl. Bur. Standards Tech. Note 270-5, 49 p.

URANIUM POTENTIAL OF SEDIMENTARY AND IGNEOUS ROCKS IN WESTERN AND SOUTHWESTERN OKLAHOMA

By Al-Shaieb, Zuhair and John W. Shelton
Department of Geology
Oklahoma State University
Stillwater, Okla.

Uranium anomalies in western and southwestern Oklahoma are present in Permian terrigenous clastic rocks and Cambrian igneous rocks. Uranium anomalies are known to occur in siltstones of the Doxey Formation of western Oklahoma (Al-Shaieb and others, 1977), in the Post Oak Conglomerate near the Wichita Mountains, and in dikes within the igneous complex of the Wichita Mountains.

A carnotite-tyuyamunite-bearing zone is localized in the lower part of the Upper Permian Doxey Formation, which crops out in Custer, Washita, Beckham, and Rogers Mills Counties. Outcrops of the Doxey are along both flanks of the Anadarko basin and near its center.

The Doxey Formation (160-190 ft thick) is characterized by alternating siltstones, mudstones, and shale. The host rock is composed of highly resistive, well stratified, pale-reddish-brown sandy siltstone beds, 15-150 cm thick. Subangular to angular quartz and feldspar grains are cemented by secondary gypsum and calcite. Ripple marks and small-scale crossbedding are major sedimentary structures. The Doxey Formation and the upper part of the underlying Upper Permian Cloud Chief Formation were deposited in tidal-flat environments. Many of these beds have been leached to a grayish-green or white color. They are fractured, and many fractures are filled with secondary gypsum and calcite. Lovett (1961) proposed that these gypsum-filled fractures formed as the result of post-depositional precipitation either by circulating ground water or by a sulfate-rich solution squeezed from an evaporite mash during lithification of the Cloud Chief Formation. Uranium occurs as spotty encrustations along bedding planes, as filling of small fractures, and as part of the cement in siltstones. The mineralization appears to be spatially related to grayish-green siltstone and also to the secondary gypsum disseminated in siltstones and filling fractures.

Factor analysis on several ground water samples shows a strong positive relationship between uranium, calcium, magnesium, sulfate, and total dissolved salts and a relatively weak negative relationship between uranium and HCO_3. Figure 1 shows that the $[UO_2(CO_3)_2\ 2\ H_2O]^2$ is the complexing agent in these waters. If the activities of carbonate species become low, the activity of the uranyl ion becomes high (Dall'Aglio and others, 1974). Evaporation would increase the activities of specific ion species until the solubility products of carnotite and tyuyamunite are reached, resulting in precipitation of both.

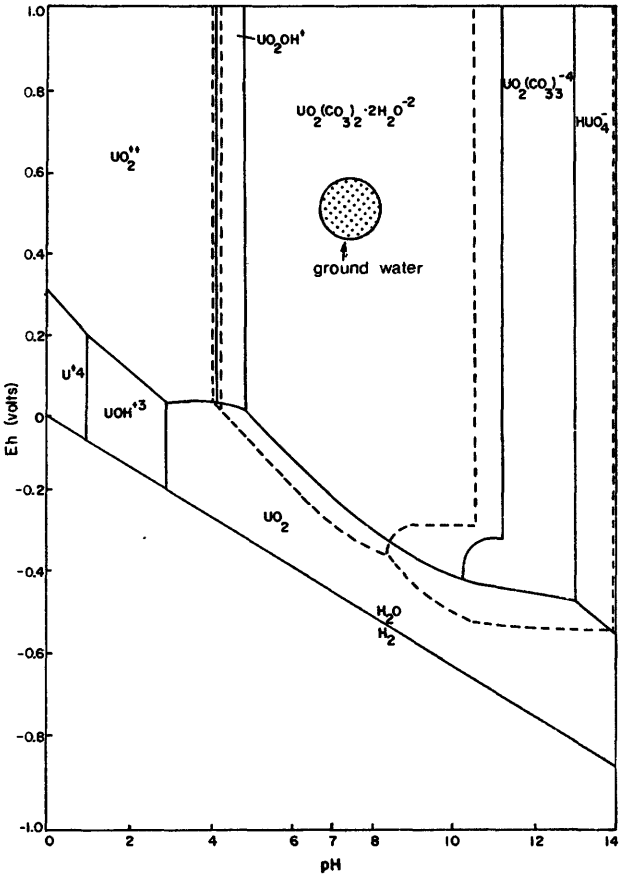

Figure 1.--Eh-pH of ground water in some Permian rocks of western Oklahoma on aqueous equilibrium diagram of the $U-O_2-H_2O-CO_2$ system with total $CO_2=10^{-3}M$. Dashed lines show boundaries for system with total $CO_2=10^{-2}M$. Modified from Hostetler and Garrels (1962).

The Post Oak Conglomerate represents the uppermost or Permian unit of a thick section of Pennsylvanian and Permian arkosic and carbonate detritus derived from the Wichita uplift. The Oklahoma Geological Survey considers it equivalent to the Hennessey Shale (Havens, 1977).

The Post Oak was divided by Chase (1954) into four phases, consisting of granite conglomerate, rhyolite conglomerate, limestone conglomerate, and granite-gabbro conglomerate with zeolite-opal cement. The first two of these comprise the greatest volume of the Post Oak. Granite conglomerate is present in several isolated patches north of the eastern part of the Wichita Mountain and as a larger more continuous belt to the south.

The conglomerate near the mountains consists of cobbles and boulders, commonly exceeding 30 cm in diameter, in a matrix of sandstone which displays many abrupt lateral and vertical changes in grain size. Medium-scale crossbedding, truncation, and cut-and-fill are the dominant sedimentary structures. In the outcrop belt south of the mountains, the size and percentage of cobbles and boulders decrease southward, as the amount of red and green shales and siltstones increases. Within 9 km of the mountains the Post Oak consists of lenticular fluvial sandstones and flood plain siltstones and claystones. The depositional environment is inferred to change southward from alluvial piedmont to alluvial plain.

Sandstones of the Post Oak are lithic arkoses and feldspathic litharenites, with angular grains and moderate to very poor sorting. Quartz, microperthite, and granitic rock fragments are the dominant constituents. Detrital iron oxides are present, and plagioclase and biotite are found in trace amounts. Zircon is generally present, along with rare sphene and allanite. Cementation history in the Post Oak is complex. Diagenetic clay, the earliest cement, is generally kaolinite, but mixed-layer illite-montmorillonite is also present. The clay was followed, in succession, by limonite and hematite, carbonate, and another generation of illitic clay. Barite is a rare cement. Commonly the sequence is not completely represented in any one sandstone.

The Post Oak shows low uranium contents ranging from 2 to 8 ppm, and averaging 2.3 ppm. The highest uranium values are found in sandstones which are characterized by a matrix of silt and clay, and which occur immediately south of granite outcrops. It is suggested, therefore, that uranium within most of the Post Oak has been flushed from the ground waters which are responsible for the complex cementation. Uranium was retained only in those rocks which possessed a relatively impermeable clay matrix.

Uranium anomalies are present also in a coarse-grained, arkosic, channel sandstone 20 km south of the granitic rocks of the Wichita Mountains. The sequence, which is 3 m thick, consists of thin beds of sandstone, less than a meter thick, and interbedded yellow-red and green shale. The sandstone consists primarily of quartz, microperthite, and granophyric rock fragments cemented by iron oxides and sparry calcite. Apatite and zircon occur in minor quantities. The average uranium content of several samples is 60 ppm. However, no uranium minerals were identified.

Riebeckite-aegirine pegmatite dikes, genetically related to the peralkaline Cambrian Quanah Granite, contain 40 to 100 ppm uranium. A typical example of these dikes is located on the western edge of the U.S. Wildlife Refuge in the Wichita Mountains. This dike is north-trending and is essentially vertical (Anderson, 1955). It consists of an aplitic core with a xenomorphic, granular texture which grades outward into a coarsely crystalline phase, which in turn grades into the host rock. A pronounced banding is due to preferred orientation of black riebeckite and (or) green aegirine crystals and light-colored feldspars and to gradational texture. The dike is composed mainly of quartz, microperthite, orthoclase, albite, riebeckite, aegirine, and small quantities of hornblende. Two distinct generations of albite were observed: an early stage associated with K-feldspars and a later hydrothermal stage. Presumably hydrothermal, microcrystalline quartz, usually in the form of veins, cuts across primary minerals. An outstanding feature is the abundance of the alkaline-rich riebeckite and aegirine, which represent overlapping periods of crystallization. Much of the aegirine has undergone corrosion and resorption. Zircon is relatively abundant (up to 10 percent); it evidently was an early crystallization product. Iron oxides occur both as primary and secondary minerals.

Fission tracks show that the uranium is associated with both aegirine-riebeckite and refractory minerals such as zircon and allanite. It was not determined whether uranium occurs as submicroscopic mineral inclusions in Na-rich minerals, or if it is fixed in their lattice structures. It is proposed that uranium in these dikes is related to a late uranium-rich hydrothermal stage which followed an early magmatic phase.

Al-Shaieb, Zuhair, Olmsted, R. W., Shelton, J. W., May, R. T., Owens, R. T., and Hanson, R. E., 1977, Uranium potential of Permian and Pennsylvanian sandstones in Oklahoma: Am. Assoc. Petroleum Geologists Bull., v. 61, p. 360-375.

Anderson, K. E., 1955, Pegmatites and miarolitic cavities of the Wichita Mountains, Oklahoma: Univ. Oklahoma M.S. thesis, 66 p.

Chase, W. W., 1954, Geologic note on Permian conglomerate around Wichita Mountains, Oklahoma: Am. Assoc. Petroleum Geologists Bull., v. 38, p. 2028-2035.

Dall'Aglio, M., Gragnani, R., and Locardi, E., 1974, Geochemical factors controlling the formation of secondary minerals of uranium, in Nininger, R. D. (chairman), Formation of uranium ore deposits: Internat. Atomic Energy Agency, Proc. Ser., no. STI/PUB/374, p. 33-48.

Havens, J. S., 1977, Reconnaissance of the water resources of the Lawton quadrangle, southwestern Oklahoma: Oklahoma Geol. Survey Hydrologic Atlas 6 (in preparation).

Hostetler, P. B., and Garrels, R. M., 1962, Transportation of uranium and vanadium at low temperature, with reference to sandstone-type uranium deposits: Econ. Geology, v. 57, no. 2, p. 139-167.

Lovett, F. F., 1961, Areal geology of the Quartermaster area, Rogers Mills and Ellis Counties, Oklahoma: Univ. Oklahoma M.S. thesis, 81 p.

NEW AND RECENT RESULTS FROM THE CANADIAN URANIUM RECONNAISSANCE PROGRAM

By A. G. Darnley
Geological Survey of Canada
601 Booth St.
Ottawa, Ont. K1A 0E8, Canada

The Geological Survey of Canada (G.S.C.), which is a Branch of the Canadian Federal Department of Energy, Mines and Resources, was involved in developing new methods of exploration either specifically for uranium or with relevance to uranium throughout the 1960's when exploration for this element was at a low ebb. The principal methods developed were ground and airborne gamma-ray spectrometry, and various forms of regional geochemistry. These methods progressed from modest small-scale experiments to extensive test surveys conducted in several different areas known to contain uranium. This demonstrated the general suitability of the methods for rapid and efficient coverage of large regions. The operational experience made it possible to prepare detailed specifications of a common national standard for the execution of the work by several contractors.

Although exploration for uranium in Canada has been pursued by industry many times over the last 30 years, and most accessible parts of the country have been examined, there has been no systematic record to indicate the thoroughness with which any nonmining area has been searched. It can be safely assumed that while some areas have been explored to the limits of present-day capability, other areas have been very inadequately examined. Unfortunately, for the majority of exploration areas the thoroughness of past work is not clearly known, because of inadequate records. In these circumstances it is prudent for a national program to start from first principles, and assume that previous work has been conducted with methods less sensitive than those now available. By covering all areas, including those containing known mineralization, it is possible for a national program to use the response over known areas as the basis for interpreting results from the same methods over poorly known areas.

The first aim of the Uranium Reconnaissance Program is to ensure that all regions in Canada where the crust contains an above normal amount of uranium are known and adequately delineated. Evidence from G.S.C. studies in Canada and published information from elsewhere shows that the dimensions of these areas of above average uranium content are sufficiently large to be recognizable with widely spaced sampling intervals. A small but important aspect of the Uranium Reconnaissance Program is the progressive provision of facilities for the standardization and calibration of exploration measurements. Past exploration work has entailed measurements of a qualitative or semi-quantitative type, at best, and this has prevented the compilation and comparison of results obtained in different places in different times. The Geological Survey of Canada is encouraging the adoption by the exploration fraternity of the recommendations recently published by the International Atomic Energy Agency (Technical Report No. 174) relating to radiometric standards and calibration, and is providing the physical facilities to enable this to be done. Facilities for airborne and ground radiometric equipment are available and those for borehole equipment are under construction.

Over the last 10 years there has been an international evolution of ideas concerning the genesis of uranium ore deposits. These ideas, which to a considerable extent originated in France, came about partly from restudy of well known deposits, but also from the study of recently discovered deposits in Australia, West Africa, and Canada. These studies emphasized the importance of surface weathering processes in moving and concentrating uranium, and the strong tendency of uranium deposits to be found in proximity to ancient major unconformities. These unconformities represent long periods of time during which rocks were subjected to weathering. The studies also suggested that one of the most favorable places to look for uranium deposits formed by these processes is in the vicinity of older rocks containing an above normal amount of

uranium. With such a working hypothesis an exploration program which seeks to delineate those areas of the country containing above normal amounts of uranium is likely to be successful in two ways. Firstly, those areas of above normal uranium content may themselves contain localities with a concentration sufficient to be economically interesting. Secondly, uranium derived from such areas may be concentrated in related younger rocks. The Canadian Uranium Reconnaissance Program rests upon the concept that most uranium deposits are geologically related to and occur in or near regions of the crust containing higher than average amounts of uranium.

One important factor which contributed to the design of the Uranium Reconnaissance Program was the success achieved by the combined Federal-Provincial Aeromagnetic Program initiated in 1960. This program served two purposes: It was an aid to geological mapping especially in areas of poor bedrock exposure, and at the same time it clearly delineated the extent of base-metal-bearing greenstone belts and iron formations across the Canadian Shield.

The uranium program primarily depends upon airborne gamma-ray spectrometry and regional geochemistry, but other methods are not excluded if these serve the objectives of the program. The objectives are (1) to provide the mineral industry with high quality reconnaissance data to indicate those areas of Canada where there is the greatest possibility of finding new uranium deposits, and (2) to provide government with systematic and nationally consistent data to serve as a base for uranium resource appraisal. The program is expected to continue at least until 1985. Airborne gamma-ray spectrometry is primarily undertaken over relatively flat areas where there is some rock outcrop and generally thin overburden. High sensitivity equipment is being employed with a line spacing for reconnaissance purposes of 5 km; but in areas which are remote and may not be reached by the main program for a number of years, some advance reconnaissance work is being done from time to time at wider spacing in order to assign priorities for later, more detailed work. Airborne spectrometry is being used principally over the Shield, but also over other parts of the country where the topography does not prevent effective coverage by fixed-wing aircraft. In 1976 for example, the hilly area of New Brunswick surrounding the central Carboniferous basin was flown.

Regional geochemistry is the only method being used at present in mountainous areas, but it is also being used in parts of the country with extensive overburden and in areas considered particularly favorable for uranium occurrence. Because the agreement with the Provinces permits them to require searches for other elements besides uranium, in some districts geochemistry has priority in order to fulfill this commitment. Obviously gamma-ray spectrometry is of prime interest only for radioactive elements, whereas geochemistry has more general applicability. Eleven elements plus loss on ignition are normally measured. The list varies according to region, but it typically includes zinc, copper, silver, cobalt, nickel, lead, mercury, molybdenum, arsenic, iron, and manganese. Regional geochemistry is based upon stream-sediment, lake-sediment or bedrock analyses, and sample spacing is normally in the range of one sample per 12.5 km^2. Water sampling is carried out wherever possible as part of the regional sampling program. This technique has a unique application to the analysis of subsurface waters to detect the presence of uraniferous material in otherwise unexposed horizons.

The results from the program are published as rapidly as they can be compiled, and are made available simultaneously by the Federal and Provincial authorities. There is a potential problem with the large amount of data required in the course of the program. The 1:250,000 map sheets of the National Topographic System (N.T.S.) are used as the basic blocks for the program. For each map sheet there are normally 12 geochemical and 9 geophysical parameters. Up to the end of 1976, standard airborne reconnaissance data had been published for 36 of the 1:250,000 N.T.S. map sheets, and standard geochemical data for 24 map sheets. In addition, a preliminary airborne reconnaissance had been made over a million square kilometers in the District of Keewatin, and individual flight lines extended over other portions of the Shield. In 1977, radiometric and (or) geochemical data will be released for 56 additional map sheets. Most of the work to date has been carried out in the western half of the Shield north and west of Lake Superior.

One of the conditions of the program is that steps are taken to monitor the usefulness of the results. This entails ascertaining the extent to which results lead to the discovery of uranium, and also whether improvements in technique are possible. In part this is done by feedback from the exploration industry, although the comments received are an incomplete record of events and opinion and sometimes indicate the data are not being used in the most efficient manner. For this reason the G.S.C. is undertaking a limited number of followup investigations on selected anomalies in several areas in order to provide an in-house assessment of the reconnaissance program. These investigations are undertaken with the agreement of companies or individuals holding the mineral rights. In general, work is only undertaken subject to agreement that the results of these investigations can be published within a reasonable period of time, so that everyone may benefit.

INTERPRETATION OF URANIUM CONTENT OF GROUND WATER IN WEST-CENTRAL KANSAS

By L. R. Hathaway
Kansas Geological Survey
Lawrence, Kansas

The uranium content of ground water collected from 239 pumping irrigation wells during the summers of 1974 and 1975 has been determined by X-ray fluorescence (Hathaway and James, 1975; 1976). Ground water from these wells is derived from (1) the Ogallala Formation (Tertiary), (2) undifferentiated Tertiary (Ogallala) and Quaternary sequences, and (3) Quaternary alluvial sediments along the Arkansas River in the west-central Kansas study area, which covers parts of eight counties. The bedrock formations from north to south (Pierre Shale to Dakota Sandstone) increase in age from Late to Early Cretaceous. The water table slopes regionally from west to east, and the water varies from an alkaline earth-bicarbonate type to an alkaline earth-sulfate type.

Previous determinations of the uranium content of ground water from the study area suggested an anomalously high regional background level (Scott and Baker, 1962, p. 47). In the current study a uranium concentration range of 2-172 ppb, with a mean of 14 ppb, was found. The areal distribution of waters with uranium levels above 20 ppb appears closely related to a north-south-trending topographic depression (Scott-Finney depression and Scott Basin) that is also reflected in bedrock contours, and to portions of the Arkansas River valley. These areas also contain saline soils and shallow water tables, and usually exhibit sulfate-type ground water and higher total dissolved solids content. In the Scott Basin area the higher total dissolved solids level in the ground water appears to be related to leaching of soluble salts from the soils in the basin area (Hathaway and others, 1975). Water from the sandy areas south of the Arkansas River exhibits low uranium levels.

Several major chemical species and the total dissolved solids in the ground water show a positive correlation with uranium (table 1), which suggests the higher uranium values observed may result from an increased salt loading of soils and ground water in areas of shallow water tables. Correction for common correlation with total dissolved solids is found to reduce greatly the number of variables exhibiting a significant correlation with uranium (SiO_2, F, Sr, and Mg). A comparison of uranium content with total dissolved solids suggests that water from the Scott Basin, some of the upland drainage areas, and the northern half of the Scott-Finney depression exhibit a higher uranium-to-total-dissolved-solids ratio than water from the southern half of the depression and the alluvium of the Arkansas River valley. This comparison also suggests that waters having two different compositions, both with relatively high uranium contents, exist in the study area. The relatively high uranium content of ground water from this area suggests that a regional anomaly exists for the aquifer and related systems in the Ogallala. Such an anamoly may result from leaching and dissolution of volcanic ash that contains about 6 ppm uranium (James, 1977) and is found in the Ogallala Formation (Swineford and others, 1955).

Table 1.--Correlations of several chemical species and total dissolved solids with uranium at the 95 percent significance level (>0.115)

Variable	Correlation coefficient
SiO_2	0.138
HCO_3	0.376
F	0.249
SO_4	0.366
Cl	0.343
Ca	0.317
Mg	0.392
Na	0.376
K	0.378
Sr	0.384
Total Dissolved Solids	0.372

The significance of uranium anomalies in ground waters from similar settings needs to be interpreted carefully in view of the overall water chemistry and aerial variables such as soil associations, surface and bedrock topography, depth to water, and nature of the surface of the water table.

Hathaway, L. R., and James, G. W., 1975, Use of chelating ion-exchange resin in the determination of uranium in ground water by X-ray fluorescence: Anal. Chemistry, v. 47, no. 12, p. 2035-2037.

_____1976, Preconcentration of uranium in natural waters for X-ray fluorescence analysis: Advances in X-ray Analysis, v. 20 (in press).

Hathaway, L. R., Magnuson, L. M., Carr, B. L., Galle, O. K., and Waugh, T. C., 1975, Chemical quality of irrigation waters in west-central Kansas: Kansas Geol. Survey Chem. Quality Ser. 2, 46 p.

James, G. W., 1977, Uranium and thorium in volcanic ash deposits of Kansas--Implications for uranium exploration in the central Great Plains: Kansas Geol. Survey Bull. 111, pt. 4 (in press).

Scott, R. C., and Baker, F. B., 1962, Data on uranium and radium in ground water in the United States 1954 to 1957: U.S. Geol. Survey Prof. Paper 426, 115 p.

Swineford, A., Frye, J. C., and Leonard, A. B., 1955, Petrography of the Late Tertiary volcanic ash falls in the central Great Plains: Jour. Sed. Petrology, v. 25, no. 4, p. 243-261.

GEOCHEMICAL PROSPECTING AT THE LADWIG URANIUM MINE, NEAR GOLDEN, COLORADO

By C. S. Ferris and Norman Bennett
Consultants
11427 W. 57th Ave.
Arvada, Colo. 80004

The Ladwig uranium mine is located approximately 4.8 km northwest of Golden in the Colorado Front Range. The geologic setting is similar to that of the Schwartzwalder uranium mine 6.4 km further north, although there are some important differences. Country rock consists of gneisses and schists of the 1.8- to 2.0-b.y.-old Idaho Springs Formation, and a pegmatite, the 1.4-b.y.-old Silver Plume Granite.

Rocks at the Ladwig mine consist principally of east-northeast-striking, steeply dipping garnet-biotite-quartz gneiss, biotite-quartz gneiss, biotitic schist, calc-silicate gneisses, minor pyroxenite, quartzite, and granite pegmatite. The mine is within the northwest-trending Hurricane Hill breccia reef fault zone, and the fault system goes through the mine area, but no fault has yet been mapped within 600 m. The principal vein in the mine strikes northwest and is roughly at the contact of pegmatite and garnet-biotite-quartz gneiss.

The original Ladwig mine was operated in 1955-56 by Denver-Golden Corp. Near its contact with garnet-biotite-quartz gneiss, highly fractured pegmatite was mineralized with pitchblende, gummite, and autunite at and near the surface. This was open-pit mined and nearly all the rock was shipped for milling. A shaft was sunk approximately 22.5 m from the floor of the pit; more ore was discovered, and was mined from a vein dipping 30° northeast near the bottom of the shaft. In 1967, Kerr-McGee Corp. undertook a radiometric and soil geochemical survey of the property that found additional anomalies. Angled core holes were drilled to explore the strongest geochemical anomaly, and to test veins in the vicinity of the shaft. The strongest geochemical anomaly was found to represent a nearly vertical vein of pitchblende extending to a depth of at least 180 m. However, for various reasons, Kerr-McGee did not explore further. In 1969, Reserve Oil and Minerals Corp. acquired the property and drove a 900-m adit westward to the pitchblende vein discovered by Kerr-McGee. Exploratory mining and drilling has been conducted intermittently since then. This paper relates known pitchblende veins to some of the radiometric and geochemical anomalies found 10 years ago.

Initially a square 1,000 feet (305 m) on each side, centered on the old Ladwig shaft, was sampled for radioactivity and soil molybdenum content on a 25-foot (7.6-m) grid. The central grid was surrounded by a zone 500 feet (152 m) wide, in which samples were taken at 100-foot (30.5-m) intervals. Anomalies in parts of this zone led to further sampling at 25-foot intervals. Care was taken to avoid contaminated areas.

Radiometry was conducted with an Eberline PRM-4 scintillometer with a 50.8-mm crystal. A check station was monitored twice a day for changes in background value. The contour lines in figure 1 represent relative values and not multiples of background value. The lowest value shown is considerably higher than background.

Soil samples were analyzed for molybdenum, a known associate of pitchblende in Front Range vein uranium deposits. Molybdenum, more stable than uranium in the

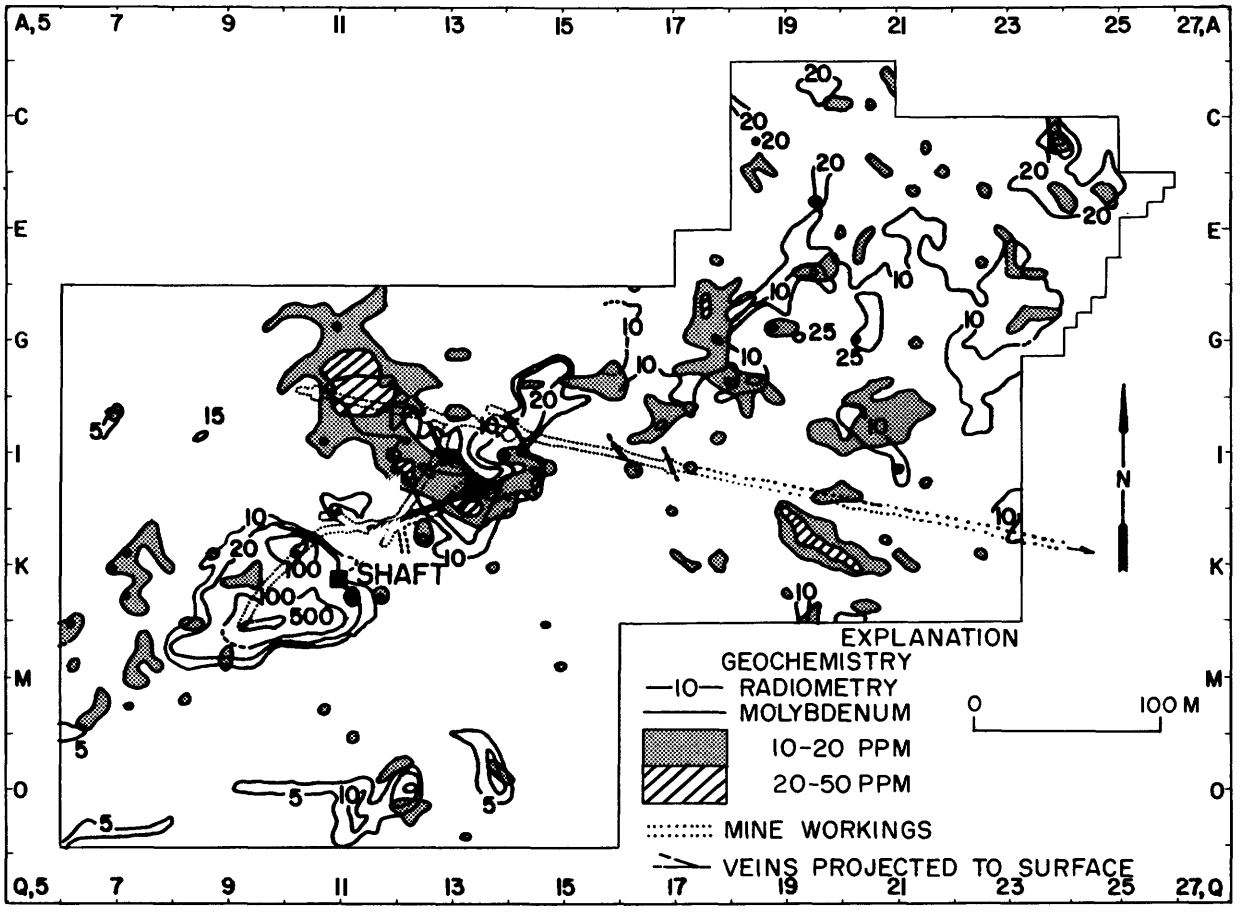

Figure 1

weathering environment, should indicate the existence of uranium veins at depth. Background values of molybdenum are 2 ppm. Values of 10 ppm or more were considered anomalous.

There is some degree of correlation between radioactivity and molybdenum in some areas, such as the two small southern anomalies, the strong NW-SE anomaly, and several small anomalies northeast of the strong one (fig. 1). However, some molybdenum anomalies, such as the northwest part of the strong anomaly and the smaller NW-SE anomaly in the eastern part of the area, show no significant radioactivity. Conversely, anomalous radioactivity without corresponding molybdenum extends northeasterly from the main anomaly and also forms a large zone westward from the shaft. The presence of molybdenum without radioactivity may be assumed to mean that soil cover retains or acquires molybdenum more easily than it retains or acquires the radioactive daughters of uranium. However, radioactivity without molybdenum may mean contamination of the surface without migration of contaminating molybdenum. Contamination of part of the area west of the shaft is likely.

Trenching of molybdenum anomalies showed that most are related to narrow radioactive veins. Most veins are nearly vertical and strike northwest, although some strike northeast and some dip at less than 45°. Drilling of one northwest-trending vein confirmed that the vein was mineralized.

Mine workings, anomalies, and the principal veins discovered are shown on figure 1. Of the northwesterly veins, only the westernmost one was extensively explored. Drilling from within the mine indicates it may have a vertical extent of 600 m. The easternmost vein contains ore where intersected by other structures but is otherwise indistinct and weakly mineralized. It was found underground and has not been traced to the surface. In addition to steep veins there are a number of so-called "flat" veins, which dip generally less than 45 north to northeast.

The strongest soil molybdenum anomaly corresponds to

the westernmost northwest vein. Drilling has shown that the vein extends farther southeast than the surface anomaly. The northwestern part of the anomaly has not been explored at depth, but trenching indicates continuation of the structure. The other northwest veins do not provide sharp molybdenum anomalies at the surface, although there is a weak anomaly for one, and there is autunite in a trench between vertical extensions of two of them. The cause of the strong molybdenum anomaly trending northwest on the east side of the area is not known.

Northeast-dipping "flat" veins, normally less than a foot in width, have been found at depth and in some trenches. Anomalies relating to these veins do not, of course, signify structures that may be projected vertically.

In conclusion, where uranium is suspected within a Colorado Front Range area with dimensions of several hundred meters, detailed soil sampling for molybdenum is a valuable supplement to radioactivity in locating pitchblende veins. At the Ladwig property the principal vein, not found by the original prospectors, showed a molybdenum geochemical expression more prominent than the radiometric expression.

HYDROGEOCHEMISTRY OF URANIUM IN THE WALKER RIVER BASIN, CALIFORNIA AND NEVADA[1]

By D. L. Leach and L. V. Benson
Lawrence Livermore Laboratory
University of California
Livermore, Calif.

The Lawrence Livermore Laboratory is conducting a hydrogeochemical and stream sediment reconnaissance (HSSR) in seven western states as part of the National Uranium Resource Evaluation (NURE) program sponsored by the U.S. Energy Research and Development Administration. The objective of the NURE-HSSR program is to complete a systematic survey of the nation's surface water, ground water, and stream sediment for the purpose of evaluating the uranium resources of the United States. Orientation studies were conducted in the Basin and Range province, including the Walker River Basin in California and Nevada, to aid in the design of the NURE-HSSP survey for this environment. The specific objectives of this report are to (1) describe the geochemical transport system which governs the distribution of uranium in water in this environment, (2) evaluate the different water types (tributary, river, spring, well, and lake) as mediums for detecting uranium anomalies, (3) describe the possible temporal changes in uranium concentration, and (4) evaluate the possible effects of mining and agricultural activities on the hydrogeochemistry of uranium.

The Walker River Basin, with an area of approximately 11,000 km^2, lies along the western margin of the Basin and Range province. East Walker River and West Walker River head in the Sierra Nevada Mountains of California, flow through several small valleys, and merge to form the Walker River which terminates in Walker Lake. The entire drainage area forms a closed basin with no outlet to the sea.

Granitic, metavolcanic, and metasedimentary rocks of Mesozoic age are the basement rocks of the Walker Basin. Over much of the region they are buried by thick accumulations of Cenozoic sedimentary and volcanic rocks. Most of the exposed basement consists of quartz monzonite or granodiorite. A small number of uraniferous deposits and prospects are present along the East Walker River. Uraninite, kasolite, and various secondary uranium minerals occur in three closely related settings: (1) quartz veins in granitic rocks containing silver, lead, copper, and iron sulfides; (2) altered granitic rocks adjacent to quartz veins; and (3) fault gouge zones. In addition, the Yerington porphyry copper deposit is located below the confluence of the East and West Walker Rivers.

Snow, tributaries, rivers, springs, wells, and lakes were sampled and analyzed for a spectrum of elements by neutron activation and other techniques. The rivers were sampled twice: in June during the high-runoff season, and in August during the low-flow regime. Each sampling was accomplished within a single day so that the chemistry of the system was "fixed" with respect to time.

Snow samples reveal the composition of the aqueous phase prior to its introduction into the surface and

[1]This work was performed under the auspices of the U.S. Energy Research and Development Administration, under contract No. W-7405-Eng-48.

subsurface hydrologic systems. Of 26 snow samples collected from different sites in the east-central Sierra Nevada, 10 were analyzed for uranium. Only one sample contained detectable uranium, indicating the insignificance of the flux of uranium via precipitation.

With the onset of spring, snowmelt is released to the tributary system. Along this segment of the transport path, the acidic fluid (pH ~5.6) reacts chemically with exposed granite, granodiorite, and felsic volcanics, thereby releasing uranium. In the Sierran headwater region, concentration of uranium was found to be less than 2 ppb and often only a few tenths of a ppb. In tributaries north of the Sierran headwater region, concentrations in excess of 2 ppb are common, and some are as high as 58 ppb, suggesting the presence of a uranium anomaly. Some of the snowmelt and tributary discharge recharges the subsurface ground-water system, a portion of which later emerges in springs. The distribution of uranium in springs is similar to the distribution found in tributaries. The concentration is typically less than 0.5 ppb, and is often below detectability in the Sierran headwaters. An area of springs rich in uranium with concentrations as great as 124 ppb is found in the center of the basin, about 35 km northeast of the anomalous area indicated by the tributaries.

The East Walker River flows for about 75 km through the area of uranium occurrences with only a minor increase in uranium concentration. For the high-flow condition in June, the concentration increased from 1.3 ppb upstream to 1.9 ppb downstream; and the August samples showed an increase from 1.5 to 1.9 ppb. The concentration of uranium increases gradually, as does the concentration of chloride and sodium through this region. River discharge measurements show that the river loses water in this region during low flow, whereas very little water is lost during high flow. In addition, the flow is apparently maintained at a high level during the normal low-level period in August by release from the Bridgeport Reservoir. Any anomalous uranium ground water that may be entering the East Walker River is apparently insignificant compared to the flux of low-uranium Bridgeport water. From the base of the Sierras to the convergence with the East Walker River, the uranium concentration in the West Walker River shows a similar increase with distance of transport. For the June samples, the increase is from 1.8 ppb to 6.4 ppb, and for the August samples, from 0.9 ppb to 6.2 ppb. However, the increase in uranium concentration is more irregular than that observed for the East Fork, and seems to be affected by areas under irrigation. Below the confluence with the East Fork, the Walker River flows through Mason Valley, which contains the Yerington porphyry copper mine on the west and large areas of irrigable agricultural lands on the east side of the river. Through this region, the uranium and most other dissolved components show a gradual increase in concentration towards Walker Lake. For uranium, the June increase is from 3.7 ppb to 6.3 ppb, and the August increase is from 6.7 to 15 ppb. These increases in uranium concentration with transport distance can largely be accounted for by evaporative concentration of river water through irrigation procedures. Mass flux calculation show that chloride mass decreased by 10 percent through this region whereas uranium has a 25 percent increase in mass over the same distance. Assuming that chloride is as mobile as uranium, there is a net increase in uranium relative to chloride of nearly 35 percent, which cannot be explained by simple evaporation through irrigation procedures. Calculations on the amount of fertilizer used in Mason Valley requires that unreasonable amounts of fertilizer be added to the system to account for the large increase in uranium. Another potential source for uranium in the area is the Yerington copper deposit. However, the addition of uranium to the river system begins far upstream from the Yerington mine. The increase in uranium relative to chloride through the region may be due to selective leaching of uranium from soil and gravels by irrigation water, or in the lower reaches of the Walker Basin, to leaching of uranium-rich sediments from Pleistocene Lake Lahontan.

These data show that uranium is conserved and increased in the river system, and that its mobility in that system is as high as chloride and sodium. Uranium does not appear to be appreciably absorbed by the stream sediments, and actually may be released from sediments by the leaching action of irrigation water. Agricultural irrigation significantly affects the uranium chemistry of the river system, particularly during the low-flow regime in August when irrigation is at maximum. In addition, the river data do not indicate the presence of known uranium deposits. The chemistry of the river is dominated by either high flow of low-uranium tributary water or low flow of high-uranium agricultural water.

The mass transport system terminates at Walker Lake. Concentrations of most elements in the lake are considerably enhanced since Walker Lake functions as a large evaporating pan. The concentration of uranium is 130 ppb, which is high compared to other large surface bodies of water, and represents a total uranium mass of about 460,000 kg. The high concentration of uranium in Walker Lake can be attributed to the stability of the uranium-bicarbonate complex in the high-bicarbonate complex in the high-bicarbonate lake water. However, mass balance calculations on Walker Lake show that the uranium present in the lake water represents approximately 5 percent of the total uranium flux since the last playa stage some 5,000 years ago. The remaining uranium has been removed by a downward flux of uranium into the sediments. This flux is driven by the absorption of uranium within the reducing sediments of Walker Lake.

The data presented provide some insight into the mass transport of uranium within a closed hydrologic basin.

Uranium is an extremely mobile component in the stream waters and does not appear to be effectively removed by interaction with the sediments. In terms of geochemical reconnaissance, tributary water is effective in indicating surficial uranium sources, whereas spring water is effective in locating buried deposits. Streams within the basin may not be effective in locating uranium anomalies, particularly if they receive little ground-water input and are modified by reservoirs and irrigation procedures.

URANIUM AND THORIUM DISTRIBUTION IN CONTINENTAL TERTIARY ROCKS OF THE COOK INLET BASIN AND SOME ADJACENT AREAS, ALASKA

By Kendell A. Dickinson, U.S. Geological Survey, Denver, Colo.

The distribution of uranium in potential host rocks may indicate whether the uranium was leached from potential source rocks and concentrated in the host rocks in the Cook Inlet area, including the Susitna lowlands and the lower end of the Matanuska valley. Suitable uranium source rocks in the form of granite and tuff are present in the surrounding area, and a large thickness of continental sedimentary rocks containing carbonaceous material is found in the basin. The important question is whether or not uranium has been leached from the potential source rocks and concentrated in the potential host rocks. One approach to this problem, although not a proven technique, is to determine the present

Table 1.--Sources of samples for uranium and thorium analysis

Stratigraphic unit	Area	Age	Rock description in area of sampling
Sterling Formation.	McNeil Canyon, Ninilchik beach and Southern Kenai Peninsula.	Pliocene-Miocene.	Sandstone, reddish-brown and gray; gray mudstone and shale; and coal. Fluvial sequence.
Beluga Formation.	Homer bluff, Southern Kenai Peninsula.	Miocene.	Sandstone, gray and reddish-brown, fine- to medium-grained, some calcitic cement; gray shale and mudstone, and coal. Fluvial sequence.
Tyonek Formation.	Capps Glacier and Chuitna River, 20-30 km northwest of Tyonek.	Miocene-Oligocene.	Sandstone, light-brown, fine- to coarse-grained, conglomeratic; gray mudstone and coal. Fluvial sequences.
West Foreland Formation.	Beluga River, 17 km north of Tyonek.	Eocene.	Siltstone and shale, gray, hard, micaceous.
Kenai Group undifferentiated.	Near Houston and Petersville.	Pliocene-Oligocene.	Sandstone, brownish-gray, fine-grained, hard and soft; and shale, gray, hard, micaceous.
Chickaloon Formation.	Premier coal mine, Glenn Highway, and Chickaloon River.	Paleocene.	Sandstone and conglomerate, gray and light-brown, soft and hard, arkosic: shale and mudstone, gray and brown; and coal.

distribution of uranium in the potential host rock to see if it has been mobilized by dissolution, transported, and redeposited. An advantage of this approach is that it provides background data that will aid in the recognition of areas affected by uranium mineralization.

A total of 57 samples of potential host rock were collected from various localities in the Cook Inlet area (table 1). Thorium and uranium were determined in these samples by the delayed-neutron method in the analytical laboratories of the U.S. Geological Survey at Lakewood, Colo. One measure of the precision of the data is the coefficient of variation for the counting statistics, which averaged 19 percent for thorium determinations and 4.5 percent for uranium determinations.

The Cook Inlet basin is a structural fault-bounded basin in southern Alaska between the Alaska Range to the west and the Chugach Mountains and Kenai Mountains to the east. It is about 300 km long and 100 km wide. More than half of the area is submerged in Cook Inlet, which opens into the Gulf of Alaska to the southeast and the Shelikof Strait to the southwest. The Cook Inlet basin contains about 7,925 m of continental sedimentary rocks that compose the Tertiary Kenai Group and West Foreland Formation. Calderwood and Fackler (1972) have divided the Kenai Group, in ascending order, into the West Foreland Formation, Hemlock Conglomerate, Tyonek, Beluga, and Sterling Formations (table 1). Later Magoon, Adkison, and Egbert (1976) removed the West Foreland from the Kenai; and their usage will be followed in this report. The Susitna lowlands, which are separated from the Cook Inlet basin by the Castle Mountain fault, may be a northern extension of the basin.

The Matanuska valley is a fault-bounded basin between the Talkeetna Mountains to the north and the Chugach Mountains to the south. The valley, which connects to the Cook Inlet basin along its northeast margin, contains about 2,135 m of Tertiary continental sedimentary rocks. These rocks are divided into three formations, in ascending order, the Chickaloon, Wishbone, and Tsadaka (table 1; Magoon and others, 1976).

The thorium and uranium contents found in continental sedimentary rocks in the Cook Inlet area are remarkably uniform (table 2). The uranium content averaged about 2.4 ppm and the range was from about 0.5 to 4.3 ppm. The thorium:uranium ratio averaged about 2.3, low compared to the general terrestrial ratio of 3-4, and low compared to many oxidized nonmarine sedimentary rocks that characteristically have ratios of more than 7 (Adams and Weaver, 1958). Shale, siltstone, and mudstone samples contain about 1 ppm more uranium than sandstone samples. This difference may have resulted from slightly more leaching of uranium from porous sandstone or adsorption by the clay, but it could also have resulted from depositional segregation of heavy uranium-bearing minerals into placer deposits. Reddish-brown sandstone, which presumably was subjected to oxidation, has nearly the same uranium content as gray sandstone, indicating that the oxidation was insufficient to leach uranium from the sandstone.

Table 2.--Distribution of uranium and thorium in continental Tertiary rocks of the Cook Inlet basin, Susitna basin, and the southern part of the Matanuska Valley as shown by average values and ratios.

[Numbers in parentheses are number of samples averaged.]

	Thorium (ppm)	Uranium (ppm)	Uranium: thorium ratio
All samples	5.59 (57)	2.38 (66)	2.30 (57)
Sterling Formation	5.27 (15)	2.13 (21)	2.19 (15)
Beluga Formation	5.22 (20)	2.24 (22)	2.38 (20)
Tyonek Formation	6.14 (2)	4.00 (2)	1.51 (2)
West Foreland Formation	8.95 (2)	2.97 (2)	3.01 (2)
Kenai Group undifferentiated	4.69 (4)	1.97 (4)	2.37 (4)
Chickaloon Formation	6.68 (7)	2.85 (7)	2.22 (7)
Reddish-brown sandstone	4.16 (17)	2.01 (17)	2.12 (17)
Gray sandstone	4.34 (18)	1.99 (18)	2.18 (18)
Mudstone, siltstone, and shale	6.84 (21)	2.88 (21)	2.42 (21)

The low uniform uranium content and the low thorium:uranium ratio found in Tertiary sedimentary rocks of the Cook Inlet area may indicate that geochemical conditions have not been favorable for the formation of epigenetic uranium deposits in these rocks, but it is important to note that the samples collected and analyzed for this report may not adequately represent the large amount of potential host rocks. Not known yet, for instance, are the geochemical conditions that existed in the subsurface, especially around petroleum accumulations. Hayes, Harms, and Wilson (1976) reported rocks in the Sterling Formation that contain montmorillonite and some from which volcanic glass has been dissolved. None of these samples were evaluated in this report.

Adams, J. A. S., and Weaver, C. E., 1958, Thorium-to-uranium ratios as indicators of sedimentary processes--example of concept of geochemical facies: Am. Assoc. Petroleum Geologists Bull., v. 42, no. 2, p. 387-430.

Calderwood, K. W., and Fackler, W. C., 1972, Proposed stratigraphic nomenclature for Kenai Group, Cook Inlet basin, Alaska: Am. Assoc. Petroleum Geologists Bull., v. 56, no. 4, p. 739-754.

Hayes, J. B., Harms, J. C., and Wilson, T., Jr., 1976, Contrasts between braided and meandering stream deposits, Beluga and Sterling Formations (Tertiary), Cook Inlet, Alaska, in T. P. Miller, ed., Recent and ancient sedimentary environments in Alaska: Proc. Alaska Geol. Soc. Symposium, Anchorage, 1975, Proc., p. J-1-J-27.

Magoon, L. B., Adkison, W. L., and Egbert, R. M., 1976, Map showing geology, wildcat wells, Tertiary plant fossil localities, K-Ar age dates, and petroleum operations, Cook Inlet area, Alaska: U.S. Geol. Survey Misc. Inv. Map I-1019, scale 1:250,000.

A ^{252}Cf-BASED BOREHOLE LOGGING SYSTEM FOR IN-SITU ASSAYING OF URANIUM ORE

By D. K. Steinman, D. G. Costello, C. S. Pepper, W. E. Gober, D. B. Breuner, J. S. M. Wilson, J. C. Young, and Joseph John
IRT Corporation, San Diego, Calif. 92138

IRT Corporation, under contract with the U.S. Energy Research and Development Administration (ERDA), has constructed a prototype of a second-generation, ^{252}Cf-based direct uranium measurement system for borehole logging. Preliminary tests of this system have been conducted in the laboratory and in the field. The technical feasibility of using ^{252}Cf sources for borehole logging of uranium was first demonstrated by Kerr-McGee Corporation several years ago. The ERDA-sponsored program at IRT has been directed at building and testing a practical hardware system using ^{252}Cf. It is anticipated that the first commercial system could be available by June 1978.

Thermal neutron fission is used to uniquely identify any uranium present in the rock around a borehole. Uranium-235 undergoes fission upon capture of a thermal neutron. The fission products emit radiations such as beta rays, gamma rays, and neutrons during their decay to stable isotopes. Of these, the neutrons represent the most interference-free means of of uranium identification because the natural background sources of neutrons are very weak.

Californium-252 is a practical neutron source for assays, and has the desirable engineering features of small size and steady, maintenance-free output. It requires no power and generates negligible internal heat. Neutrons from the ^{252}Cf source induce fission of the uranium in the rock around the borehole, and delayed neutrons from the ^{235}U fission are detected in the sonde to indicate the presence and concentration of uranium in the rock. This method, called delayed neutron activation analysis (DNAA), is sensitive because there is no background source of neutrons to mask the delayed neutrons from fission. The method is also selective, because the thermal neutrons can only induce nuclear fission in ^{235}U.

The logging system consists of a sonde which contains the formation measurement subsystems, the sonde-support, the source-storage cask which provides the biological shielding, and the mechanism for transferring the ^{252}Cf source between the cask and the sonde. In addition, there is the logging truck containing the power supply, the logging winch, the teletype and plotter, and the electronic equipment used to control the sonde and to acquire, analyze, and display the data from the sonde. The sonde has a diameter of 5.7 cm, and it contains the measurement subsystem from which the delayed neutron signal, the monitor detector signals, and the natural gamma-ray signals are detected and conditioned for use by the uphole electronic units. Low-voltage dc power is supplied to the sonde through two conductors in the 4HO logging cable. Signals and commands between the detectors in the sonde and the electronic units in the truck are sent through the other two conductors in the cable. The surface electronic units receive, process, and display the detector signals, and the system control unit, an LSI-11 minicomputer, is able to reduce the data and display it in a form useful for uranium exploration or mine planning.

In keeping with the overall program goal of developing a practical, sensitive, economic, and safe uranium logging system, the following factors were considered: (1) acceptability to the uranium industry, (2) logistics of logging and maintenance, (3) sensitivity and precision of measurement, (4) cost of acquisition and operation, and (5) safety of operation.

To make the system acceptable to the uranium industry, it was thought that its operation should represent as little change as possible from current logging practice. In addition, the intensity of the ^{252}Cf neutron source had to be minimal. A new activation technique permitted reduction

of the source size to a tenth of that used by Kerr-McGee with a net gain in sensitivity. All necessary information is obtained in a single pass through a borehole. The DNAA log is made with the sonde going upwards at 1.5 m/min. Logistically, a single vehicle with a GVW rating of 10,000 pounds can transport the system, including the biological shield for the source. One technician can operate the system, with the aid of the system control unit. The system has sensitivity to 100 ppm U_3O_8; the neutron counts detected are equal to 9.1 per percent U_3O_8 per μg ^{252}Cf. With a source loading of 330 μg, a neutron count of 3,000 counts is obtained in 1 percent ore. The background counting rate is negligible, so sensitivity to less than 100 ppm U_3O_8 is statistically useful. In addition to statistical precision, the system also includes a neutron flux monitor which measures the effects of the surrounding rock on the source neutrons and uses the resulting signals to correlate effects on the DNAA signal. The monitor signals are themselves useful as a lithology log. For safety, the design of the system minimizes both the exposure of the operator to the source and the possibility of losing control of the source. A mechanism on the sonde permits retrieval of the source if the sonde becomes stuck in the borehole. The source is shielded and kept in a guiding channel during all loading and unloading operations to help prevent accidental loss. For each hole logged, the operator is exposed to an amount of radiation that is less than 3 percent of the weekly maximum permitted by Federal law. Cost projections show that the system can be used for 45¢ to 72¢ per foot ($1.48 to $2.36 per meter).

Field tests in 21 boreholes in the three major uranium-producing districts of the country show the system performs satisfactorily in temperatures from 0° to >32°C, in both cased and uncased holes, and with ore grades from less than 100 ppm to more than 1.5 percent U_3O_8. At many of the measured holes, core assays were available for comparison. Field tests also showed the system could be set up in less than 10 minutes and stored back on the truck in less than 7 minutes.

ANOMALOUS URANIUM IN THE WATERS OF THE RIO OJO CALIENTE, NEW MEXICO

By K. J. Wenrich-Verbeek, U.S. Geological Survey, Denver, Colo.

A high U value (15 μg/ℓ) found in water of the Rio Ojo Caliente, La Madera, Rio Arriba County, N. Mex., during a regional sampling technique study in August 1975 by the author, was further investigated in May 1976 to determine whether stream waters could be effectively used to trace the source of an anomaly. The associated stream sediments, sampled in 1975, contain only an average U content, 3-6 ppm (variation among replicate samples) and would not have been useful for isolating an anomalous area in a reconnaissance program (Wenrich-Verbeek, 1977).

Although uranium in the pegmatites was first reported in 1930, pegmatite deposits in the Petaca-Ojo Caliente area of northern New Mexico have been sources of commercial mica since the 17th century (Jahns, 1946). The rocks in the Petaca-Ojo Caliente area are predominantly Precambrian quartzites and quartz-mica schists with lesser amounts of Precambrian amphibole schists, meta-rhyolites, and a medium-grained granite. These units are transected by pegmatite bodies and quartz veins containing sparsely disseminated crystals of U minerals, notably samarskite. No Paleozoic or Mesozoic rocks are exposed in the area above La Madera although the Tertiary Carson Conglomerate of Just (1937), and Tertiary and Quaternary Santa Fe Formation are present. Quaternary basalts cap many of the mesas and Quaternary alluvium has been deposited to form flat valley bottoms along some stretches of the Tusas and Vallecitos rivers.

Numerous thermal springs occur in this region of New Mexico. Some of them have been studied by Summers (1976, p. 24-28) who reported limited Rn-222 determinations, but no U. Although the Rn in the hot springs of the Ojo Caliente area ranges from 820 to 9,400 pC/ℓ, no insight into the uranium content can be gained from these data because of the different solubility of radium, the direct parent of radon; uranium concentrations are frequently low in springs of high radium content.

A detailed study of the tributaries to the Rio Ojo Caliente above La Madera was conducted during a moderate discharge period, May 1976, so that small tributaries would contain water. The U.S. Geological Survey gaging station at La Madera was resampled, and due to the increased discharge, from 15 to 109 cfs, the water showed an expected decrease in

uranium concentrations from 15 to 3.3 μg/ℓ. This example of changing uranium concentration with discharge emphasizes a major problem in water sampling, that is, maintenance of a constant discharge during the sampling of an entire study area. This problem is minimized if the uranium concentration is normalized by the similarly decreased conductivity (100xU/conductivity); under these conditions the uranium content of the Rio Ojo Caliente remains anomalous (greater than two standard deviations above the mean) with respect to other normalized values from its drainage basin. This particular anomaly is sufficiently large that even without normalizing the values the source of the uranium anomaly can readily be traced (fig. 1). Cañada de la Cueva, a small tributary to the Ojo Caliente, was found to contain 40 μg/ℓ whereas other tributaries contain <3 μg/ℓU. The source of the anomaly appears to be a hot spring

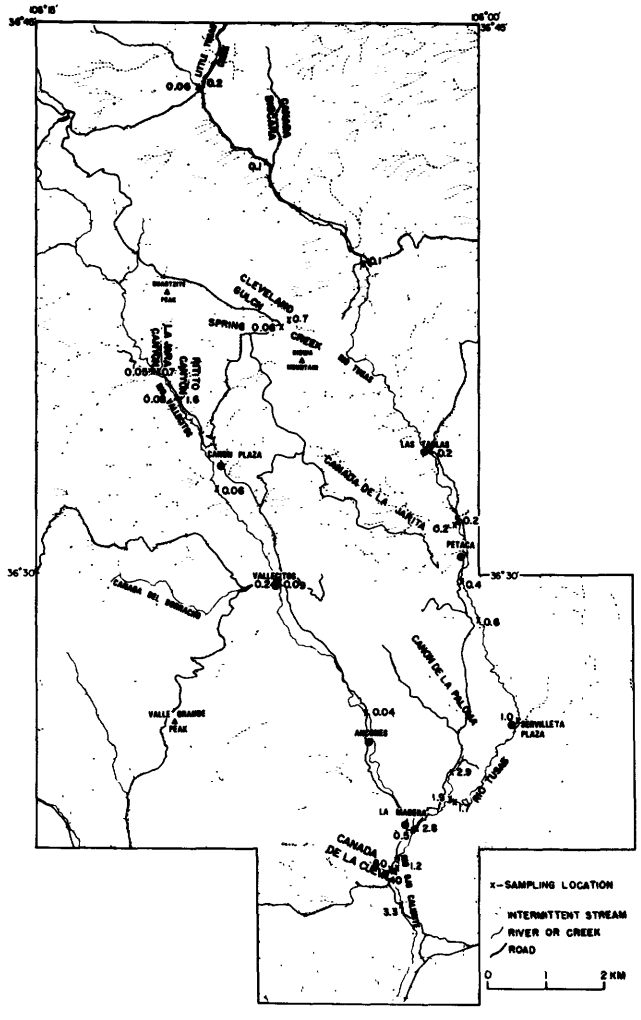

Figure 1

containing 60 μg/ℓU that discharges into Cañada de la Cueva; this is an unusually high value for hot springs, among the highest reported in the United States (J. K. Felmlee, oral commun., 1977).

From figure 1 it can be seen that other sites in the area have uranium values comparable with the Rio Ojo Caliente at the U.S. Geological Survey gaging station. Yet, when the values are normalized, only the Rio Tusas above the junction with Rio Vallecitos (1.04), the Rio Ojo Caliente at the gaging station (1.40), Cañada de la Cueva (1.63), and the hot spring on Cañada de la Cueva (3.80) are anomalous with respect to all other localities (<0.80). From these results it appears that the Rio Tusas above the junction with the Rio Vallecitos should also be studied in more detail. Between 1975 and 1976 the Rio Ojo Caliente at the U.S. Geological Survey gaging station ranged from 2.10 to 1.40 normalized uranium. Thus, uranium values at this site, when normalized, maintain a constant relation to drainage-basin background values regardless of variation in discharge.

Correlations between uranium and other parameters are listed in table 1 for two groups of data: (1) all sample sites and (2) all sites except the hot spring and Cañada de la Cueva, both containing uranium concentrations an order of magnitude greater than the other samples. Correlation coefficients of group 2 when compared with group 1 give a suggestion as to elements which may be present in the source rock contributing uranium to the ground water that feeds the hot spring at La Madera.

Table 1.--*Correlation coefficients between U and other parameters measured in water from the Rio Ojo Caliente Drainage basin, N. Mex.*

[r = Correlation coefficient; n = Number of samples; ** Significant at the 99 percent confidence limit; * Significant at the 95 percent confidence limit]

Parameter	All 29 sites			27 sites--omitting anomalous U sites		
	r	n	Sign.	r	n	Sign.
Water Temperature	0.67	29	**	0.56	27	**
Conductivity	0.73	29	**	0.58	27	**
pH	-0.31	21		0.38	19	
Alkalinity	0.81	29	**	0.64	27	**
Hardneas	0.96	28	**	0.75	26	**
Ca	0.94	26	**	0.76	24	**
Mg	0.97	28	**	0.64	26	**
Na	0.44	28	*	0.48	26	*
K	0.94	28	**	0.66	26	**
F	0.08	29		0.53	27	**
As	0.96	25	**	0.57	23	**
Ba	-0.11	29		0.12	27	
B	0.87	17	**	0.54	16	*
Cu	0.58	27	**	0.25	26	
Fe	-0.15	29		-0.30	27	
Pb	0.63	25	**	0.82	18	**
Mn	-0.18	25		-0.18	25	
Mo	0.59	9		0.59	9	
Ni	0.40	15		0.34	23	
Sr	0.92	29	**	0.70	27	**
V	0.59	25	**	0.59	23	**
Zn	0.07	25		0.39	23	
Al	-0.06	29		-0.20	27	
Li	0.29	25		0.48	23	*
Ti	0.12	25		-0.24	23	
Hg	0.06	25		-0.34	23	
Eh	0.24	25		0.10	27	

Uranium in the waters of the Rio Ojo Caliente drainage basin is most closely related to the alkalies and alkaline earths; calcium, magnesium, sodium, potassium, alkalinity, conductivity, and hardness all show significant correlations with uranium. R-mode factor analysis places them in the same factor group with uranium. This result is expected, particularly for calcium which, in these samples, is related to the CO_3^2 anion that has a large influence on the solubility of uranium. Due to this association of uranium with the alkalies and alkaline earths, normalization of the uranium content by conductivity, which is controlled by the concentration of the major ions, should be effective in minimizing the effects of evaporation and dilution on the uranium content of surface waters.

The elements arsenic and boron show much higher correlation coefficients for the sample group including the high-uranium sites, although both have significant correlations without the high-uranium sites. This suggests that arsenic and boron are very high in the uranium source rock and (or) show solubilities similar to uranium. Previous studies (Wenrich-Verbeek, 1977a) have shown that arsenic and boron frequently correlate with uranium in water, so their solubilities are possibly very similar; their very high correlation coefficients, 0.96 and 0.87 respectively, suggest also that they are high in the uranium source rock. The nonsignificant correlation of uranium with other metals may be as much, if not more, a function of differences in the other metals' soluble complexes and solubility constants from those of uranium as they are a function of the metals' occurrence, or lack of it, in the source rock.

Only a few anomalous values occur among the other elements and these are distributed primarily within two areas: (1) the hot spring and Cañada de la Cueva contain anomalous concentrations of Ca, Mg, Na, K, As, B, and Sr, and (2) Cañon de la Paloma contains anomalies of Na, Li, B, F, and Mo. The association of Mo with F, Li, B, and Na also occurs to the northeast of Ojo Caliente in the molybdenite deposit of Questa, N. Mex. Perhaps the Cañon de la Paloma Mo anomaly should be studied further. The pegmatite at the Paloma Canyon mica prospect is albitized and contains fluorite perhaps contributing to the F and Na anomaly.

Conclusions: A uranium anomaly found in the waters of the Rio Ojo Caliente has been traced upstream along Cañada de la Cueva to a hot spring. Hence surface-water sampling has been shown to be an effective geochemical technique for tracing a stream stream-water uranium anomaly back to a ground-water source for the uranium and consequently has value as a tool for locating buried deposits. Normalizing uranium concentrations with conductivity proved extremely useful in negating the effect of a change in stream discharge from 15 to 109 cfs.

Although the Petaca-Ojo Caliente area has long been known for its samarskite occurrences in pegmatites, the uranium anomaly traced to the hot spring in Cañada de la Cueva suggests the possibility that a uranium occurrence, perhaps a concentration from the uranium-bearing pegmatites up the drainage, is present in the Tertiary-Quaternary sediments, or possibly deeper in the Precambrian, beneath the surface near La Madera, N. Mex. Additional sampling of the ground water and numerous springs, particularly those springs linearly alined along Cañada de la Cueva from the anomalous hot spring, should prove valuable in delineating the anomalous area.

Jahns, R. H., 1946, Mica deposits of the Petaca district, Rio Arriba County, New Mexico, with brief descriptions of the Ojo Caliente district, Rio Arriba County, and the Elk Mountain district, San Miguel County: New Mexico Bur. Mines and Mineral Resources Bull. 25, 289 p.

Just, Evan, 1937, Geology and economic features of the pegmatites of Taos and Rio Arriba Counties, New Mexico: New Mexico School of Mines Bull. 13, 73 p.

Summers, W. K., 1976, Catalog of thermal waters in New Mexico: New Mexico Bur. Mines and Mineral Resources Hydrol. Rept. no. 4, 80 p.

Wenrich-Verbeek, K. J., 1977a, Uranium and coexisting element behavior in surface waters and associated sediments with varied sampling techniques for uranium exploration: Jour. Geochem. Explor. (in press).

_____1977b, The effectiveness of stream-sediment sampling along the Rio Ojo Caliente, New Mexico, in Energy Resource and Development Administration Symposium on Hydrogeochemical and stream-sediment reconnaissance for uranium in the United States, Proc. (in press).

★U.S. Government Printing Office: 1977-777-102/12